CT 5050 - Additional MSc Thesis
Executed at Sogreah Consulting

Wave modelling in the Bay of the River Seine

Échirolles, France; April 2010

Joost van Wiechen
1213431; Delft University of Technology

Index

Abstract

The Bay of the River Seine is situated in the north-west of France, in front of the coasts of Normandy. Beginning in 2001, in the Port 2000 project, a large extension of the port of Le Havre has been carried out. Due to the newly constructed port, bathymetry and dimensions at the northern bank in the head of the River Seine have changed drastically. These changes will influence the climate and propagation of waves in the head of the River Seine.

Studying the behaviour of waves in the near-shore is important, both to gain knowledge in the processes that play a role, as well as to control and update numerical models for wave propagation. In this research, measurements taken by different buoys, placed in the Bay of the River Seine, have been evaluated and the data have been used as input and validation for the construction of a (numerical) SWAN model. Also the differences between SWAN in generation 2 and 3 have been investigated.

It is pointed out that results for the calculation of significant wave height give more accurate results in SWAN generation 3, than in generation 2. For both generations, the calculations for mean wave period by SWAN are largely underestimated.

The calculations of significant wave height for the deeper parts (in this research called off-shore) of the Bay give accurate results, they coincide well with the measurements. The modelling of waves by SWAN in the head of the River Seine is however not good; It is concluded that the bathymetry near-shore is too complicated for SWAN and also that too much processes play a role, for proper calculations by SWAN.

Somewhat more thorough research on one of those processes that play a role, refraction over an access channel in shallow water, shows that SWAN does model this process well, even if total reflection occurs.

1 Introduction

1.1 The Bay of the River Seine

The Bay of the River Seine is situated in the north west of France, at the coasts of Normandy in the English Channel. Its surface area measures roughly 5000 km^2 ; 100 km in east-western direction, 50 km in north-south direction.

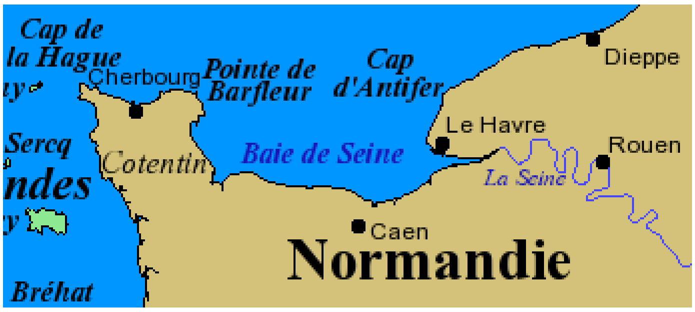

Figure 1: Bay of the River Seine.

Towards the northeast, the Bay of the River Seine is connected by the Strait of Dover to the North Sea. Following the English Channel to the southwest the Bay is connected to the Atlantic Ocean.

In the southeast of the Bay, at the city of Le Havre, the River Seine flows into the Bay. The River Seine can be navigated by ocean-going vessels up to the city of Rouen (120 km of river track).

1.2 The port of Le Havre

The port of Le Havre is situated south of the city of Le Havre, at the mouth on the northern bank of the River Seine. It is the second largest port in France (after Marseille) and the fifth largest port of Northern Europe, with a handle of 80.5 million tonnes in 2008. The port of Le Havre is the leading French port for container traffic with nearly 2.5 million TEU in 2008, which is more than 63% of all container handling in French ports. Also 40% of all crude oil entering France passes par Le Havre.


Figure 2: The port of Le Havre before Port 2000.

1.3 Port 2000

In 1999 approval was given for the start of a series of extensions of the port of Le Havre; Port 2000. The actual works in the first phase of the plan started in 2001 and consisted of a growth in container handling capacity.

In this first phase, which was finalised in march 2006, 1.4 kilometres of quays for four ship handling berths were constructed, making it possible to receive the worlds' largest container ships in Le Havre.

In the second phase of Port 2000 another 2100 metres of quays will be constructed, the works on it started in the summer of 2007 and are foreseen to be finished in 2010. The complete project (3 phases) will consist of 4.2 kilometres of quays and twelve mooring places for container vessels.

Figure 3: The port of Le Havre. On the left the old port, in the middle Port 2000, on the right the River Seine.

Because the newly constructed terminals of Port 2000 were planned in the territory of the Estuary of the Seine, which is a first order natural site (classified as a natural reserve since 1997), there had to dealt with the Natura 2000 - and Special Protection Area (SPA) laws of the European Union.

Therefore a meander of approximately fifteen hectares has been widened to improve the water circulation and to create new salt marshes. Also an artificial island of five hectares at low tide was fitted with 260.000 cubic metres of stones and sand, protected by riprap. In total, the port of Le Havre has spent 46 million euros on the first phase of Port 2000 to preserve the natural heritage of the area.

2 Research Topic

2.1 Research Questions

Due to the newly constructed Port 2000 bathymetry and dimensions at the northern bank in the head of the River Seine have changed. These changes will influence the climate and propagation of waves in the head of the River Seine.

During the years 2006-2008 measurements by different buoys, placed both off-shore in the Bay of the River Seine, as well as in the head of the Estuary, have been carried out. These buoys have been collecting data on waves. Wind data, over the same period, are provided for two off-shore locations in the Bay of the River Seine by the principle of hindcasting.

With the hindcasted wind data it is possible to construct a (numerical) SWAN model. SWAN will produce wave data, which on their hand can than be validated by the available wave data from the buoys.

The SWAN program has being kept on developing over the years, resulting now in a third generation wave model. The program offers the possibility to be ran in one of the three generations. It is of interest to have a look at the differences in output delivered by the second and third generation of SWAN.

The above described, results in the following three research questions:

For the program SWAN:

- Are there, for non-stationary two-dimensional runs on the Bay of the River Seine, differences visible between results following from SWAN having run in second and third generation?

For the entrance of the new container terminal (Port 2000):

- How does the newly dredged access channel towards Port 2000 modify the wave transformation in the northern part of the mouth of the River Seine? And what kinds of wave disturbances happen at the entrance of the new Port 2000?
- Is SWAN, with the new bathymetry for the entrance channel and breakwaters of Port 2000, able to give results for the wave climate that match with the measured climate by the different buoys?

2.2 Hypothesis

- SWAN being run in third generation includes white capping and quadruplet wave-wave interactions. In this research, for the generation 3 runs, also triad wave-wave interactions are switched on. SWAN in second generation only takes white-capping into account (if run in default). Since the two mentioned wave-wave interactions do play a role in actual life, it can be expected that SWAN in generation 3 gives more accurate results.

However, since a run in SWAN generation 2 is less complicated, the convergence for generation 2 will probably be quicker, resulting in less computational time but still reasonable results.

- Phase one of the Port 2000 project includes a large quay south of the old port. The breakwater built to protect the moored vessels inside that new part of the port, will definitely influence the wave climate and tidal current: Waves will break and be diffracted by this breakwater.
  The second change in the bathymetry of the head of the River Seine includes a large entrance channel from the newly constructed quays, towards the old parts of the port, to the open sea. Waves propagating in the Bay of the River Seine that meet this channel (coming from areas with only small depths), will be diverged away from the coast, due to the effect of refraction.

- With the knowledge of previous research on SWAN, it must be possible for SWAN, especially when being run in third generation, to give matching results with the measured data by the buoys.
  However it is also known by previous research that, where SWAN provides good results for the significant wave height, in general predictions for the mean wave period are underestimated.

3 Input and validation data

3.1 Wind and wave data from buoys

After the construction of the first phase of Port 2000, three buoys were installed in the head of the Estuary of the River Seine. Two buoys were installed at the head of the breakwaters of the newly constructed docks: One at the northern head (Musoir Nord) and one at the southern head (Musoir Sud). Buoy LH17 is situated in the new entrance channel, south of the head of the breakwater of the old docks. Buoy LHA is situated off-shore in the Bay of the River Seine (see figures 4 and 5).

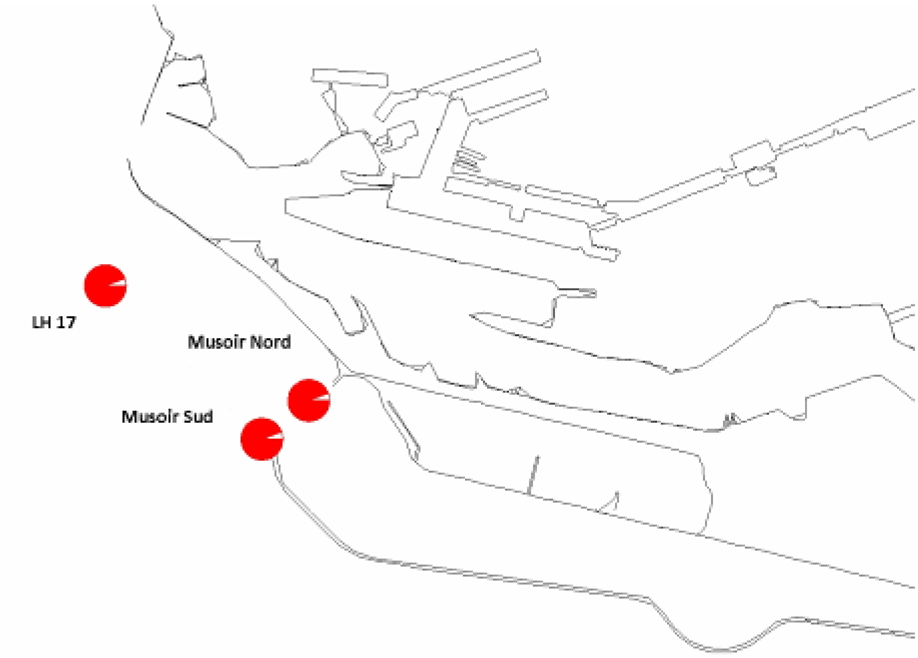

Figure 4: Position of buoys LH17, Musoir Nord and Musoir Sud in the head of the River Seine.

The four buoys, Musoir Nord, Musoir Sud, LH17 and LHA, only provide data on wave height and period. Data on wind (force and direction) and wave direction are not given by these four buoys. The cover of period of available data, by all four buoys, runs from June 2007 till September 2008.

Wind (force and direction) and wave direction data are available at two off-shore points in the Bay of the River Seine: D-Day and Antifer (see figure 5). The datasets for D-Day and LHA were made available by hindcasting in the Previmer project by the SHOM (Service Hydrographique et Océanographique de la Marine).

According to Magne *et al.* (2010; in submitting) hindcasted data are produced by the integration of a numerical model over a historical period where no or not enough observations have assimilated. In the Previmer project offshore hindcasts have been proven to be very accurate, with errors between nine and fifteen percent against in situ three-hourly averaged values of significant wave height and mean wave period. In coastal areas, errors are however typically larger, often exceeding twenty percent. The multi-wave forecasting system developed by the SHOM combines several relatively coarse models and high resolution coastal zooms.

Figure 5: Position of the buoys LHA, D-Day and Antifer in the Bay of the River Seine.

Name:	Latitude:	Longitude:	Type:	Wave parameters:	Wave direction:	Wind data:
Musoir Nord	49°28'02" N	0°06'31" E	Real time	Yes	No	No
Musoir Sud	49°27'55" N	0°06'20" E	Real time	Yes	No	No
LH17	49°28'20" N	0°5'18" E	Real time	Yes	No	No
LHA	49°31'39" N	0°9'48" W	Real time	Yes	No	No
D-Day	49°30' N	0°45' W	Hind cast	Yes	Yes	Yes
Antifer	49°39' N	0°7'48" W	Hind cast	Yes	Yes	Yes

Table 1: Position, type of buoy and measured data for the buoys used in the Bay of the River Seine

3.2 Tidal data

Tidal data were delivered by the GMPH (Grand Port Maritime du Havre) and consisted of two large datasets, one giving the tide at buoy ‘Le Havre’, the other at buoy ‘Balise A’. In original form the datasets gave the tidal level every five minutes, however to save on computational time, it was decided to work with tidal data with an interval of one hour. Since both buoys are located very near to each other, no difference in tidal range is visible between them.

Name:	Latitude:	Longitude:	Original delta t:	Used delta t:
Le Havre	49°29'14" N	0°05'28" E	5 min	1 hour
Balise A	49°25'43" N	0°06'48" E	5 min	1 hour

Table 2: Position and both measured as used time interval for the buoys providing tidal data

3.3 Selection of storm events

With the data from buoy LH17 nine highest storm events were selected (threshold of 1,50 metres). These same nine storms were also found in the datasets of buoys LHA, Antifer and D-Day, and were used as a start for the 2-D modelling cases (off-shore and with the new bathymetry) in SWAN.

It was decided for both 2-D parts (the off-shore and near-shore part) to only look at pure wind-sea generated waves in the Bay of the River Seine. From the nine original storms, only five met this criterion (wind direction during the storm event between 180 and 270 degrees and no visible influence of swell).

Storm case:	Begin date event:	End date event:
Case 1	06/01/2008 12h00	09/01/2008 12h00
Case 2	09/03/2008 12h00	13/03/2008 12h00
Case 3	05/12/2007 00h00	08/12/2007 12h00
Case 4	30/11/2007 00h00	05/12/2007 00h00
Case 5	17/01/2008 00h00	21/01/2008 00h00

Table 3: Selected storm events.

Appendix B gives the different (wave) parameters (significant wave height, wind velocity, wind direction, peak- and mean wave direction, mean wave period, peak wave period and tide) in graphical form for each of the five cases.

4 Modelling

4.1 Test modelling (1D and 2D)

The research was started with some simple arbitrary 1D and 2D, in order to see how SWAN handles certain settings and bathymetries. Hereunder the input and objective of the cases is given, results follow in Chapter 5.1.

Test Case 1a	
Dimension:	1D
Generation:	GEN 2
Forcing:	wind (270 degrees)
Bathymetry:	A260N
Test:	How does the system react to wind only? A260N gives a fetch of 60 kilometres. Results for Tm_{02} and H_{sign} will be used as input for case 2a. Run is in GEN 2, to be compared with 1b.

Test Case 1b	
Dimension:	1D
Generation:	GEN 3
Forcing:	wind (270 degrees)
Bathymetry:	A260N
Test:	How does the system react to wind only? Same as case 1a. Also Tm_{02} and H_{sign} will be used as input for case 2b. Run is in GEN 3, to be compared with 1a.

Test Case 2a	
Dimension:	1D
Generation:	GEN 2
Forcing:	swell (270 degrees)
Bathymetry:	A260N
Test:	How does the system react to swell only? Fetch of 60 kilometres, Hsign and Tm02 from case 1a. Run is in GEN 2, to be compared with Case 2b.

Test Case 2b	
Dimension:	1D
Generation:	GEN 3
Forcing:	swell (270 degrees)
Bathymetry:	A260N
Test:	How does the system react to swell only? Fetch of 60 kilometres, Hsign and Tm02 from case 1b. Run is in GEN 3, to be compared with Case 2b.

Test Case 3	
Dimension:	2D
Generation:	GEN 2
Forcing:	swell (270 degrees) and a longshore current
Bathymetry:	60*60 km, from 20 m depth to 0 m depth at the coast
Test:	How do waves in SWAN, induced by swell at -20 m depth, react to a longshore current near the coast?

Test Case 4	
Dimension:	2D
Generation:	GEN 2
Forcing:	swell (270 degr.) and an estuarine current
Bathymetry:	60*60 km, from 20 m depth 0 m depth at the coast
Test:	How do waves in SWAN, induced by swell at -20 m depth, react to an estuarine current near the coast? Added tide is 5 metres.

Test Case 5	
Dimension:	2D
Generation:	GEN 2
Forcing:	swell (337.5 degr.)
Bathymetry:	60*6 km from 20m depth to 0m, + channel (-15m) in NS direction.
Test:	Incoming waves from north-west direction meet at smaller depths, under an angle, the channel. How does SWAN handle the refraction that should take place?

Test Case 6	
Dimension:	2D
Generation:	GEN 2
Forcing:	swell (270 degrees)
Bathymetry:	60*6 km + wall over limited length in NS direction
Test:	Straight incoming waves from the west, meet a wall with zero transmission. How does SWAN handle breaking of waves against a wall and how does it handle with diffraction behind the wall? This case was also used as a test how to work with a nested run.

Test Case 7	
Dimension:	2D
Generation:	GEN 2
Forcing:	swell (270 degr.)
Bathymetry:	60*6 km + walls at north and south boundary.
Test:	Following from cases 3, 4 and 6: With waves coming straight from the west, dissipation of energy and ‘direction’ takes place at the northern and southern boundary. Is it possible, with the use of two walls at those boundaries, to model a flume, without loss of energy and ‘direction’?

Bathymetry A 260 N is the bathymetry in the Bay of the River Seine over a length of 60 kilometres. It is the bathymetry following from a line under an angle of 260 degrees towards point A (see fig X.XX). The last 20 kilometres of bathymetry towards A follow from a given bathymetry, the deepest 40 kilometres is taken constant at -25.30 metres.

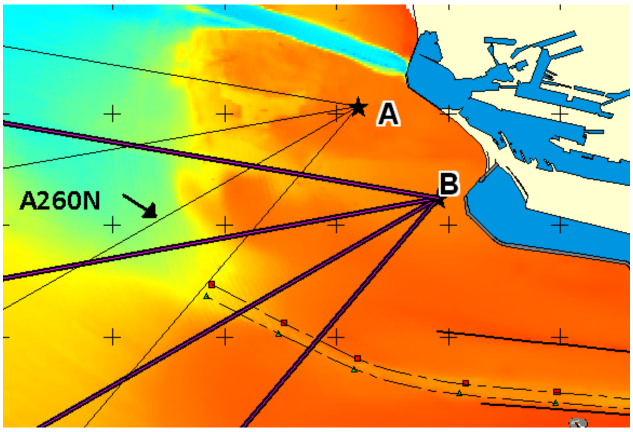

Figure 6: Position of bathymetry A260N

In all the cases the bathymetry is taken as a line (1D) or square (2D) running from 270 degrees west to 90 degrees east.

4.2 2-D modelling (off-shore)

Within the five storm cases, selected from the wind and wave data (3.3 - Selection of storm events), for each storm the peak event(s) is/are chosen, resulting in a begin- and end date of the simulation that will be carried out by SWAN:

Storm case:	Begin date event:	End date event:	Begin date simulation:	End date simulation:
Case 1	06/01/2008; 12h00	09/01/2008; 12h00	07/01/2008; 00h00	07/01/2008; 12h00
Case 2	09/03/2008; 12h00	13/03/2008; 12h00	10/03/2008; 00h00	11/03/2008; 12h00
Case 3	05/12/2007; 00h00	08/12/2007; 12h00	06/12/2007; 06h00	07/12/2007; 12h00
Case 4	30/11/2007; 00h00	05/12/2007; 00h00	30/11/2007; 12h00	01/12/2007; 12h00
Case 5	17/01/2008; 00h00	21/01/2008; 00h00	18/01/2008; 12h00	19/01/2008; 12h00

Table 4: Selected periods for measured and computed cases

For each case a simulation was made in both SWAN generation 2 as 3. All runs were carried out as non-stationary runs with a maximum of five iterations per time step (delta t = one hour).

The computational grid size was chosen 1000 by 1000 metres, resulting in a grid of 136 meshes in x-direction (eastwards) and 67 meshes in y-direction (northwards), the total surface covered by the grid is 136 * 67 km.

The spectral directions of the model covered the whole circle of 360 degrees, with a step size of 2.5 degrees, resulting in 144 meshes in the theta-space. Concerning the frequencies in the calculation; 0.05 Hz was chosen as lowest discrete frequency, 0.8 Hz as highest frequency and a total number of frequencies of 31.

The grid size for the bottom profile of the Bay of the River Seine and the hourly changing water levels (tide) followed the computational grid size and was chosen 1000 by 1000 metres, also resulting in 136 meshes eastwards and 67 meshes northwards.

The wind forcing on the system was covered by the wind data following from Antifer and D-Day. A simple one by one grid was created (136 km eastwards, 67 km northwards) to read in the wind data: At the west the wind data from buoy D-Day, data from buoy Antifer at the east. No other boundary forcing was added to the system and the system started from rest.

For the runs in SWAN generation 2, the parameters bottom friction, triad wave-wave interactions and quadruplet wave-wave interactions were switched off, white-capping was activated. All other physical variables had default values. The runs in SWAN generation 3 included both wave-wave interactions (triad and quadruplet) and white-capping. Bottom friction was switched off. All other physical variables also had default values (linear wind growth by Cavaleri and Melanotte-Rizzoli (1981), exponential wind growth by Komen *et al.* (1984)).

Some trial and error runs have been carried out to come to the above described settings, cases one and two in generation 2 have here fore been used. Trial and error took place on the following settings:

- Maximum number of iterations per time step; runs with one, three and five iterations per time step showed that in order to get accurate enough results, five iterations per time step were required. Five iterations is a maximum value, if the required accuracy of 98 percent was already achieved in an earlier iteration, computations for the next time step would begin. Computations with even more iterations would mean more computational time and was not in favour.
- Grid size; runs on 500*500, 1000*1000 and 2000*2000 metres showed that runs with a grid size of 1000*1000 metres gave the best results for the ratio of computational time to accuracy.
- Computational scheme; One computation was carried out with the BSBT (Backward in Space, Backward in Time) scheme, results were however not satisfying and chosen was to work with the default S&L scheme.
- Bottom friction; One run including bottom friction was also carried out. Results for buoy LHA showed no remarkable differences with runs where the bottom friction was switched off.

For Case 1, both in second and third generation, after some first trial runs, it was found that the wind force, which followed from the hindcasting at D-Day and Antifer, was too small. For the final run of Case 1, 20 % of actual wind force was added as input to the system.

Appendix A gives all the above described in tabular form.

4.3 2-D modelling (new bathymetry)

The same five storm cases as used for the off-shore modelling were chosen for the near-shore modelling with the new bathymetry. Since the modelling of case 1 only covered a period of 12 hours, which is a bit short, it was chosen to elongate its period of modelling with 12 hours to January 8th, 2008 00h00. Table 5 gives begin - and end dates for the modelling of the five cases.

Storm case:	Begin date event:	End date event:	Begin date simulation:	End date simulation:
Case 1	06/01/2008; 12h00	09/01/2008; 12h00	07/01/2008; 00h00	08/01/2008; 00h00
Case 2	09/03/2008; 12h00	13/03/2008; 12h00	10/03/2008; 00h00	11/03/2008; 12h00
Case 3	05/12/2007; 00h00	08/12/2007; 12h00	06/12/2007; 06h00	07/12/2007; 12h00
Case 4	30/11/2007; 00h00	05/12/2007; 00h00	30/11/2007; 12h00	01/12/2007; 12h00
Case 5	17/01/2008; 00h00	21/01/2008; 00h00	18/01/2008; 12h00	19/01/2008; 12h00

Table 5: Selected periods for measured and computed results for the near-shore modelling cases.

In order to come to good results for the complex near-shore bathymetry, use was made of the method of nesting (SWAN user manual, 2009). The idea of nesting is to first compute the waves on a coarse grid for a larger region and then on a finer grid for a smaller region. The computation on the fine grid uses boundary conditions that are generated by the computation on the coarse grid. Nesting can be repeated on ever decreasing scales using the same type of coordinates for the coarse computations and the nested computations, boundaries should always be rectangular.

Finally a double nested run was carried out for each storm case (see figure 7). The coarse grid run, which covered the whole Bay of the River Seine, was carried out on a grid of 1000 by 1000 metres, resulting (as for the case of the off-shore modelling) in a grid of 136 meshes in x-direction (eastwards) and 67 meshes in y-direction (northwards). The first nesting was done on a grid of 100 by 100 metres, sixteen kilometres long to the east, thirteen to the north. The base of this grid is placed 103 kilometres eastwards and 14 kilometres northwards from the base of the original coarse grid. This resulted in a grid with 160 meshes in x-direction and 130 in y-direction. A second nesting was than carried out in order to properly model the complex bathymetry around the access channel towards the new port. This nested run had a grid size of 20 by 20 metres, 5.5 kilometres long in both northern as eastern direction. The base of this grid was chosen 111 kilometres eastwards and 18.5 kilometres northwards of the base of the original coarse grid base (1000 by 1000 metres). With this 20 by 20 metres grid size it gave 275 meshes in both x - and y - direction.

The calculations by SWAN were carried out in generation 3, the comparison of results following from the simulations made off-shore in both generation 2 and 3 showed more accurate results for the modelling of significant wave height for generation 3 (see chapter 5.2 – 2D modelling off-shore). For the near-shore modelling, as for the 2-D modelling off-shore, all runs (including the nested) were carried out as non-stationary with a maximum of five iterations per time step (delta t = one hour), together with a required accuracy of 98 percent. This means that, with the double nested runs taken into account, for a grid point within the finest grid, up to fifteen iterations could have been carried out.

As for the off-shore modelling, the spectral directions of the model covered the whole circle of 360 degrees, with a step size of 2.5 degrees, resulting in 144 meshes in the theta-space. Concerning the frequencies in the calculations; 0.05 Hz was chosen as lowest discrete frequency, 0.8 Hz as highest frequency and a total number of frequencies of 31.

The grid size for the bottom profile of the Bay of the River Seine followed the computational grid. The coarse grid run was done with a bottom profile of 1000 by 1000 metres, for the first nested run the bathymetry was taken with a mesh size of 100 by 100 metres. Finally the second nested run was carried out with a bathymetry of mesh size 20 by 20 metres, which was also the smallest mesh size available. The hourly changing water levels to model the tide followed from the data of buoys Le Havre and Balise A, and were added to each point of the bathymetry in both the coarse grid run as in the two nested ones.

The wind forcing was covered by the wind data from Antifer and D-Day. A simple one by one grid was created (136 km eastwards, 67 km northwards) to read in the wind data for the coarse grid: At the west the wind data from buoy D-Day, data from buoy Antifer at the east. For the nested runs the same was done, however on a smaller one by one grid. The values for the wind force and direction at the boundaries of these smaller grids were calculated by simple interpolation. For the coarse grid run no other boundary forcing was added to the system. For the two nested runs the boundary forcing and initial conditions (besides the wind) followed from the previous courser run. In that coarser run SWAN created a file consisting of boundary data, which was than read in at the next run on the finer grid.

The runs in generation 3 included triad wave-wave interactions, quadruplet wave-wave interactions and white-capping. Bottom friction was switched off. All other physical variables had default values (linear wind growth by Cavaleri and Melanotte-Rizzoli (1981) and exponential wind growth by Komen *et al.* (1984)).

For Case 1 again 20 percent of wind was added as input to the system. All above described can be found in tabular form in Appendix B.

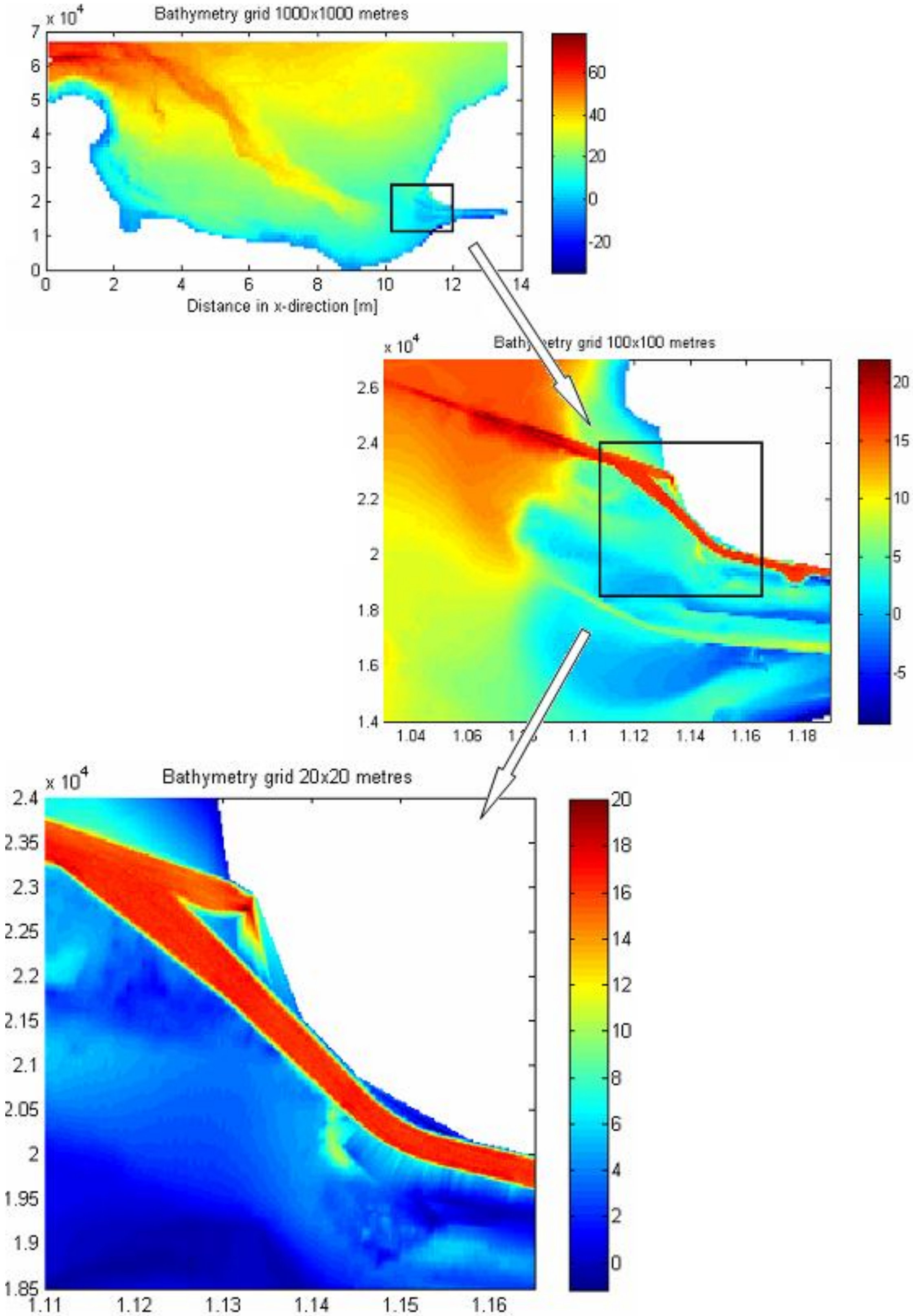

Figure 7: Grids used for the nesting.

5 Results

5.1 1-D modelling

The test cases produced almost all output as expected by theory; however test cases 3 and 7 gave some striking results, which ask for some explanation. In 5.1.1 the results of the seven test cases will be discussed in short, 5.1.2 will handle the results from cases 3 and 7.

5.1.1 Results test cases

Test 1a and 1b looked at the reaction of a 1-D modelling case with input by wind only. Test 1a was ran in SWAN generation 2, test 1b in generation 3. Results are as expected: waves develop over the fetch and towards the coast depth-induced breaking occurs. The basis of the little differences in results for wave height and - period in generation 2 and 3 will be explained in chapter 5.2.

Test 2a and 2b looked at swell over the same bathymetry as in test 1. Results were satisfying, also here little differences were visible between SWAN in generation 2 and 3.

In test 3 a 2-D model was ran in SWAN generation 2. At the western boundary it was induced by swell. The waves approached the coast over a length of 60 kilometres, the last five they met a longshore current. Both a run with a longshore current to the north as to the south has been carried out. Due to the interaction of the current and the waves, it was expected that waves would become steeper and eventually would break more than when waves just reach the coast without being imposed to a longshore current. However this is not the case, see 5.1.2.

Test 4 is comparable to test 3, however this time not a longshore, but an estuarine current was imposed over the last 5 kilometres. The depth near the coast was chosen deeper (five metres), in order to make it waves able to reach the current without too much breaking. Results are as expected, when the waves meet the opposing current, they increase and eventually break, both depth-induced as by steepness.

Test 5 was carried out to see how SWAN handles refraction of waves over a navigation channel. This test was carried out with the thoughts on the new bathymetry in the head of the Estuary of the Seine, which includes a newly dredged navigation channel. The test was satisfying; waves did refract away from the coast, however in the middle of the bathymetry, left from the channel, some unsatisfying results were gained.

In figure 7 it can be seen that the swell-waves are coming in from the north-west. When they meet the channel they turn away from the coast (which is on the right hand side). However what happens at the third, fourth and fifth ‘line’ is not according to nature: waves turn away to the deeper waters. A possible explanation can be that the model was constructed too simple, only with a rough bathymetry and swell coming from the north-west. It was chosen not to investigate this behaviour further, since the objective of the test, the occurrence of refraction, was reached.

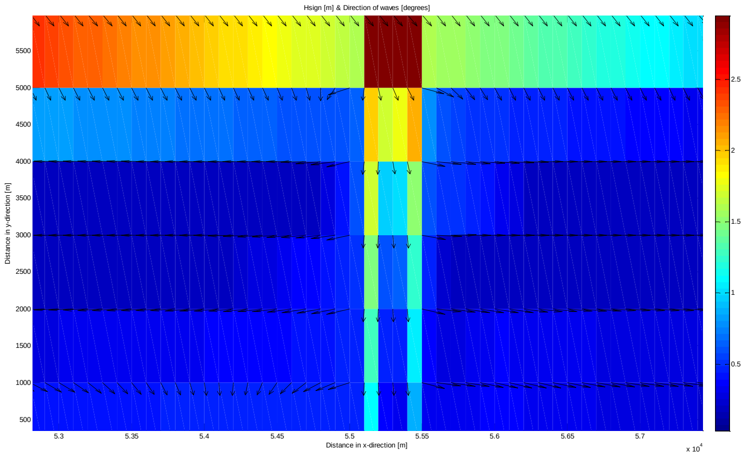

Figure 8: Refraction over the navigation channel.

Test 6 looked at straight incoming waves that meet a wall with zero transmission. Objective was to see whether the waves would break on the wall and if diffraction would take place behind it. Swan produced output results that showed both phenomena.

Test 7 is discussed hereunder.

5.1.2 Test cases 3 and 7

Test 3 gave unsatisfying results for waves produced by off-shore swell, meeting a longshore current in front of the coast. Two runs have been carried out: The first run of the 2D model consisted of swell at the western boundary with a longshore current towards the north; the second run had the longshore current towards the south. Comparing both runs it seemed impossible to proper model a longshore current, since the influence of the current, which as a maximum value was set to1.5 metres per second, showed to be only very little to nothing. It was decided not to look further into the problem due to lack of time.

Test case 7 originated from observations in the results of test cases 3 till 6. At the northern and southern boundaries dissipation of energy and 'direction' took place. In order to avoid this at both 'dissipation-sides' walls were modelled, resulting in the modelling of a flume. However results were not satisfying, coming to the conclusion that it is impossible to model a flume with the help of SWAN.

5.2 2-D modelling (off-shore)

For the off-shore modelling ten runs in SWAN have been carried out; each of the five cases has been run in both second and third generation. 5.2.1 Will handle the variance density spectra to explain differences in runs for generation 2 and 3. In 5.2.2 the validation of the SWAN model for buoy LHA and points D-Day and Antifer is carried out. The behaviour of the mean wave period, both measured as computed, showed three remarkable phenomena, 5.2.3 is used to explain them. Finally, in 5.2.4, extra attention is given to the results of case 2.

5.2.1 SWAN spectra for generation 2 and 3

As already explained in 4.2, SWAN generation 2 did not take the triad wave-wave interactions and quadruplet wave-wave interactions into account. The runs for SWAN in third generation included the two phenomena.

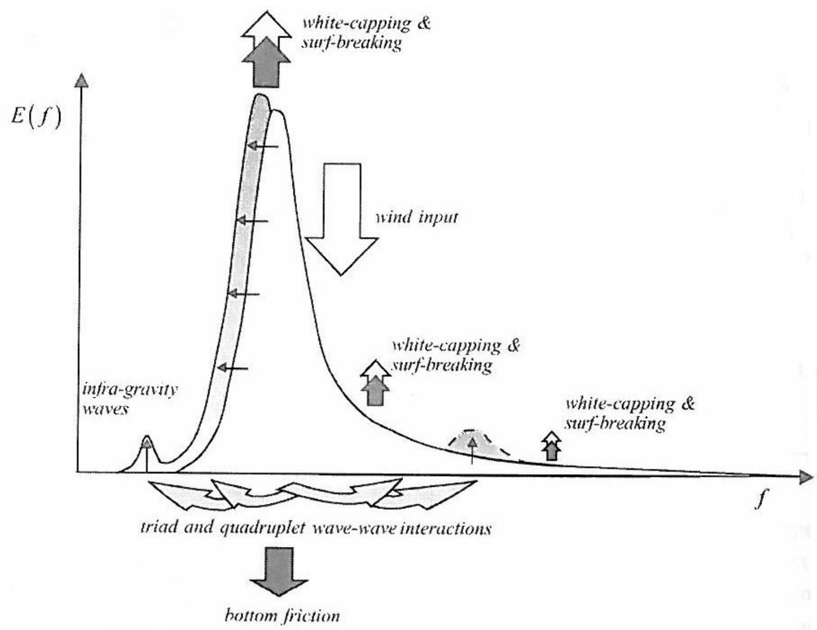

Figure 9: Influence of physcial processes on the energy density spectrum

According to theory of waves in coastal waters (Holthuijsen 2007), the transfer of wind energy to the waves occurs mostly at near the peak of the spectrum and at the mid-range frequencies. The corresponding energy gain at these frequencies is removed by wave-wave interactions (triad and quadruplet) to lower and higher frequencies and by white-capping. At the higher frequencies most of the energy that is received from the mid-range frequencies is dissipated both by white-capping and surf-breaking (higher frequencies are barely affected by bottom friction), but it is not quite clear what happens additionally. Near the outer edge of the surf zone, the transfer of energy from the spectral peak to its second harmonic by triad wave-wave interactions is so strong that a secondary high-frequency peak is created, but, deeper inside the surf-zone, it disappears. At the lower frequencies (below the peak frequency) the energy that is received from the mid-range frequencies is absorbed just below the peak frequency by the quadruplet wave-wave interactions, resulting in a downshifting of the peak frequency.

Plots of the variance density spectra for the five storm cases, comparing generation two and three, show, for generation 3, the behaviour of the above described. In figure 9 the variance density spectra for cases 1 and 2 at buoy LHA during the peak of the storm are made dimensionless by dividing the original variance density per frequency by the total variance density. According to the theory, energy is shifted from the peak and midrange frequencies towards higher and lower frequencies by the quadruplet and triad wave-wave interactions. At the higher frequencies most of this received energy is dissipated by white-capping and surf-breaking. The remaining energy at the higher frequencies results in the wider spectrum towards the higher frequencies. Just below the peak frequency the energy received from the mid-range frequencies is absorbed by the quadruplet wave-wave interactions, resulting in the clearly visible downshifting.

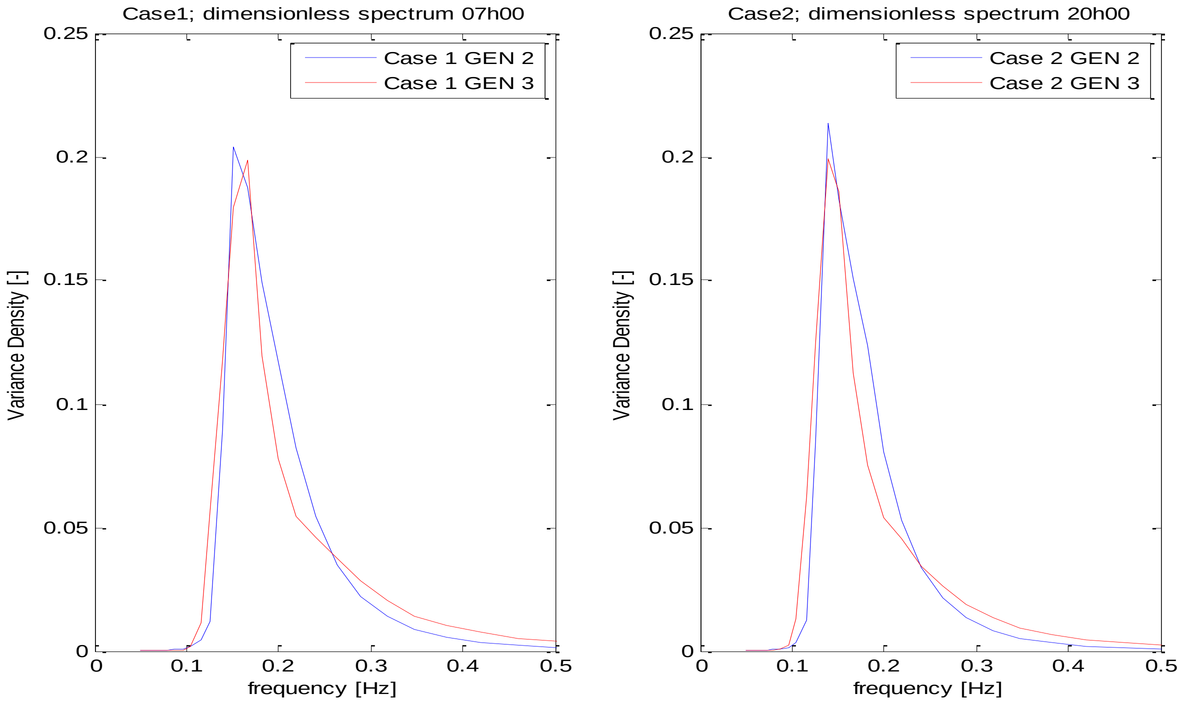

Figure 10: Dimensionless variance density spectra for case 1 and case 2.

The theory also mentions the possibility for a second high-frequency peak due to triad wave-wave interactions. In this case this second peak is not present, since buoy LHA is situated in the still deeper parts of the Bay of the River Seine.

In figure 10 the variance density spectrum with absolute values is given. The peak frequency in generation 3 has a higher value than when ran in generation 2. This can be explained by the difference in calculation of the linear- and exponential wind growth terms in SWAN generation 2 and 3.

The total input by wind is calculated in SWAN (both generation 2 and 3) as:

$$S_{in} = A + BE \qquad (5.1)$$

With A being the linear wind growth term and BE the exponential wind growth term (in which E is the spectral density).

For the linear wind growth, generation 2 makes use of the modified Cavaleri and Melanotte-Rizzoli formula (1981):

$$A = \frac{188}{2\pi}\frac{\pi}{g^2} C_{drag}^2 \left(\frac{\rho_a}{\rho_w}\right)^2 \left(U_{10} \max[0, \cos(\theta - \theta_w)]^4\right) \qquad (5.2)$$

with:

$$C_{drag} = 0.0012$$

Generation 3 uses the unmodified Cavaleri and Melanotte-Rizzoli formula (1981) for the linear wind growth:

$$A = \frac{1.5 * 10^{-3}}{g^2 2\pi} [U_* \cos(\theta - \theta_w)]^4 * G \qquad (5.3)$$

with:

$$U_*^2 = C_{drag} U_{10}^2 \qquad (5.4)$$

in which:

$$C_{drag} = 1.2875 * 10^{-3} \qquad \text{for } U_{10} < 7.5 \text{ m/s}$$

$$C_{drag} = (0.8 + 0.065 U_{10}) * 10^{-3} \qquad \text{for } U_{10} \geq 7.5 \text{ m/s}$$

In which G is a cut-off function to avoid growth at frequencies lower than the Pierson-Moskowitz frequency (Tolman 1992).

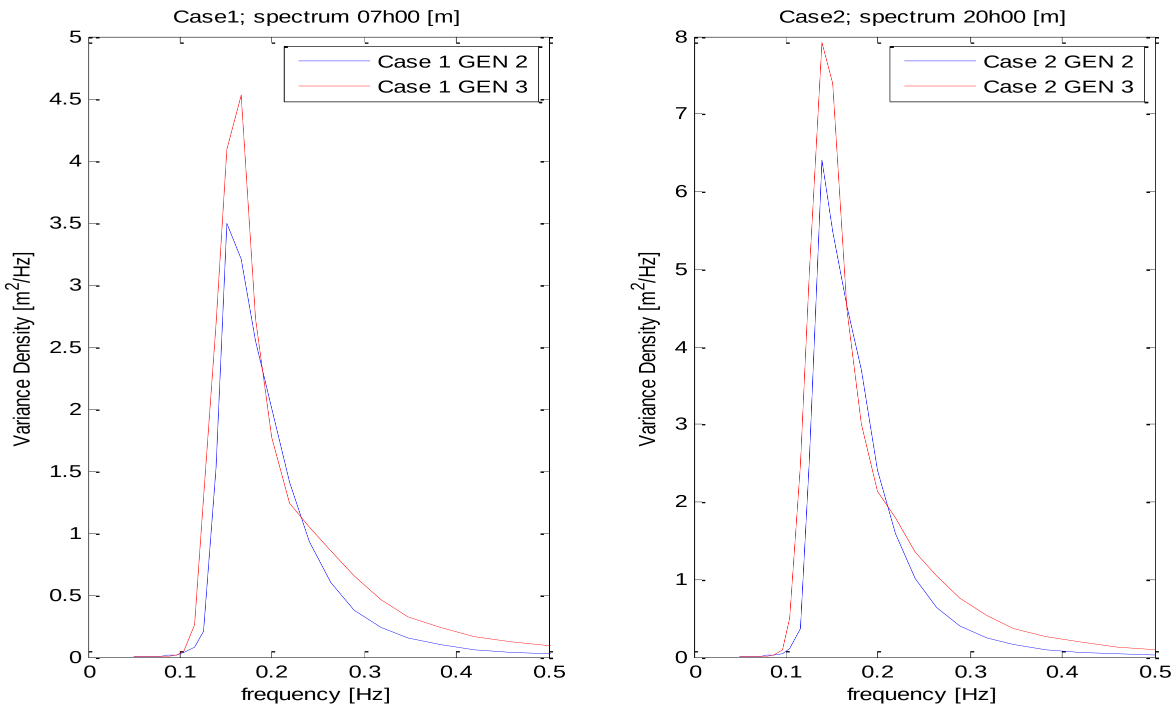

Figure 11: Variance density spectra for case 1 and 2.

The difference between the two formulae comes mainly from the value for C_{drag}. SWAN in generation 2 takes this value as a constant; generation 3 let it depend on the wind velocity. In the case of storms the measured wind velocity lies well above 7.5 m/s (in case 2 up to 23 m/s). The calculated U_* in generation 3 will therefore have a larger value than in generation 2, resulting in a larger value for A.

The exponential wind growth term, *BE*, is calculated in generation 2 by the modified formula of Snyder *et al.* (1981):

$$B = \max[0, \beta_2 \frac{5}{2\pi} \frac{\rho_a}{\rho_w} \left(\frac{U_{10}}{\sigma/k} \cos(\theta - \theta_w) - \beta_3 \right)] \sigma \qquad (5.5)$$

in which:

$\beta_2 = 0.59$

$\beta_3 = 0.12$

In generation 3 the exponential wind growth term is calculated by the formula of Komen *et al.* (1984):

$$B = \max[0, 0.25 \frac{\rho_a}{\rho_w} \left(28 \frac{U_*}{c} \cos(\theta - \theta_w) - 1 \right)] \sigma \qquad (5.6)$$

In which c is the phase velocity.

U_* is calculated by (5.4) giving B, the exponential wave growth term, again a larger value in generation 3 than when ran in generation 2.

SWAN in generation 3 uses, especially for the higher wind velocities, larger values for the linear and exponential wind growth terms. From the theory it was already said that the transfer of wind energy to the waves occurs mostly at near the peak of the spectrum and at the mid-range frequencies, which explains the higher frequency peak in generation 3.

5.2.2 SWAN model validation

The use of larger wind growth terms in generation 3 is also seen in results for calculated values of the significant wave height. The two graphs on top in figure 11 show the results for generation 2 (left) and generation 3 (right). Especially the computed values by SWAN generation 3 for the location D-Day match very well with the hindcasted values.

Towards the first peak the values for Antifer and buoy LHA are overestimated, but the second peak for buoy LHA seems to fit well. Looking at the results for generation 2 it can be concluded that the second peak of the storm is underestimated (for all three positions).

The two graphs in the middle show results for the measured and computed mean wave period for generation 2 (left) and generation 3 (right). It can be seen that both generations largely underestimate the mean wave period. Having a closer look at the results for the mean wave period, two other phenomena are also striking: The measured mean wave period for buoy LHA gives the highest value of the three points, while it is expected that Antifer would give the highest value (which is also confirmed by the results of SWAN and measurements of the significant wave height and the peak wave period). Also the results for the estimated mean wave period in generation 2 are better than for generation 3, while it is expected that generation 3 would be more accurate.

The peak wave period is well computed by SWAN, both in generation 2 and 3. This is also the case for the other four cases (see appendix C).

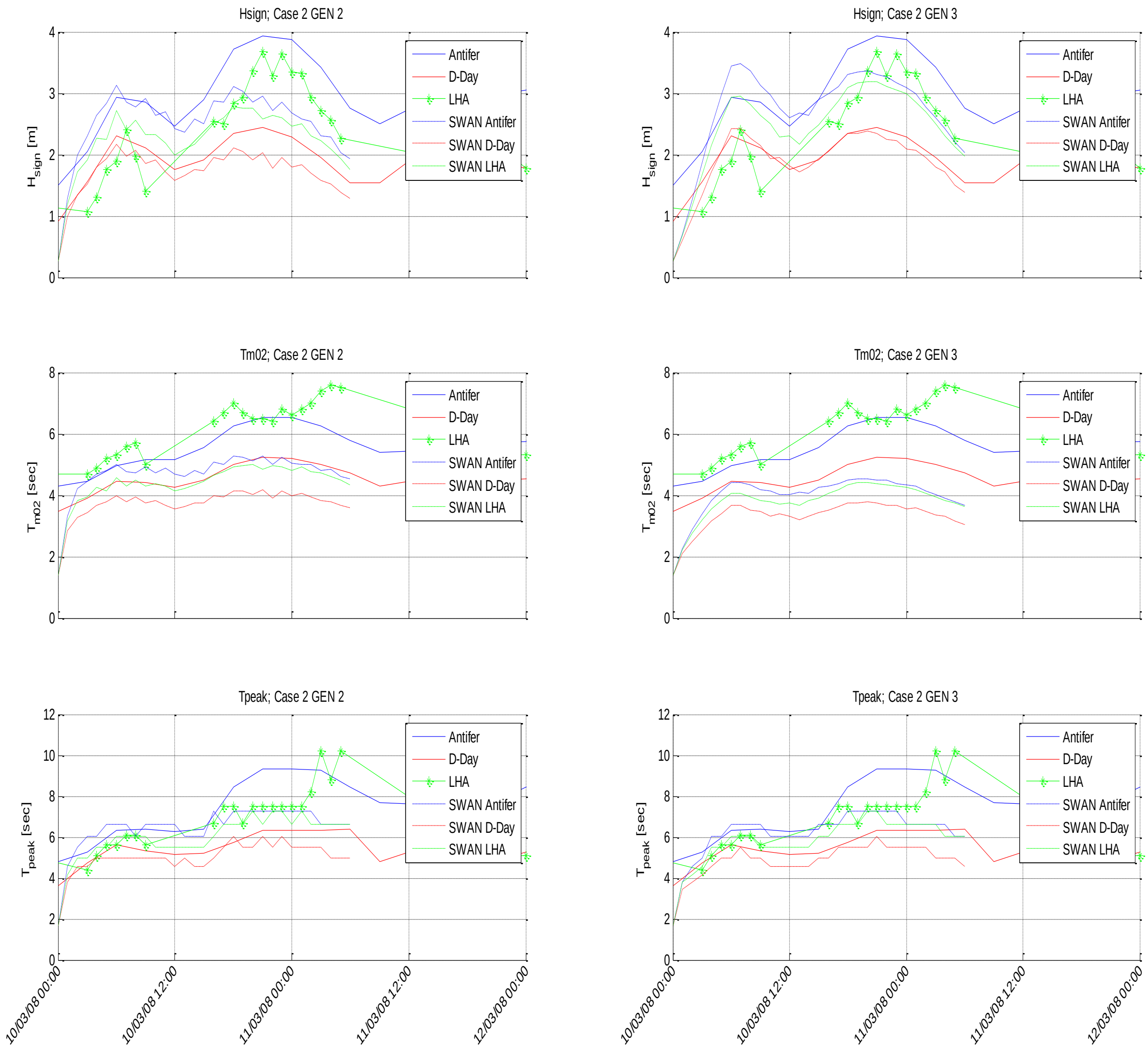

Figure 12: SWAN results for Hsign, Tm02 and Tpeak for generation 2 (left) and generation 3 (right).

Comparing the results of all the storm cases, it can be concluded that SWAN in generation 3 gives more accurate results for the estimated significant wave height than generation 2. Figure 12 shows the results of the measured and computed (generation 3) significant wave heights for cases 1, 3, 4 and 5.

Case 1 gives good results for the point Antifer. D-day and LHA are both overestimated. Case 3 gives good results for the point D-Day (like case 2), the results for buoy LHA are also not too bad, just slightly overestimated. The results by SWAN for point Antifer are underestimated. Case 4 gives very accurate results for point D-Day, the predictions for Antifer are also very accurate during the first thirteen hours, afterwards they are underestimated. Buoy LHA is overestimated during the first fifteen hours; the last nine are very accurate. Finally case 5 gives again very accurate results for point D-Day. Buoy LHA remains slightly overestimated, Antifer is somewhat underestimated.

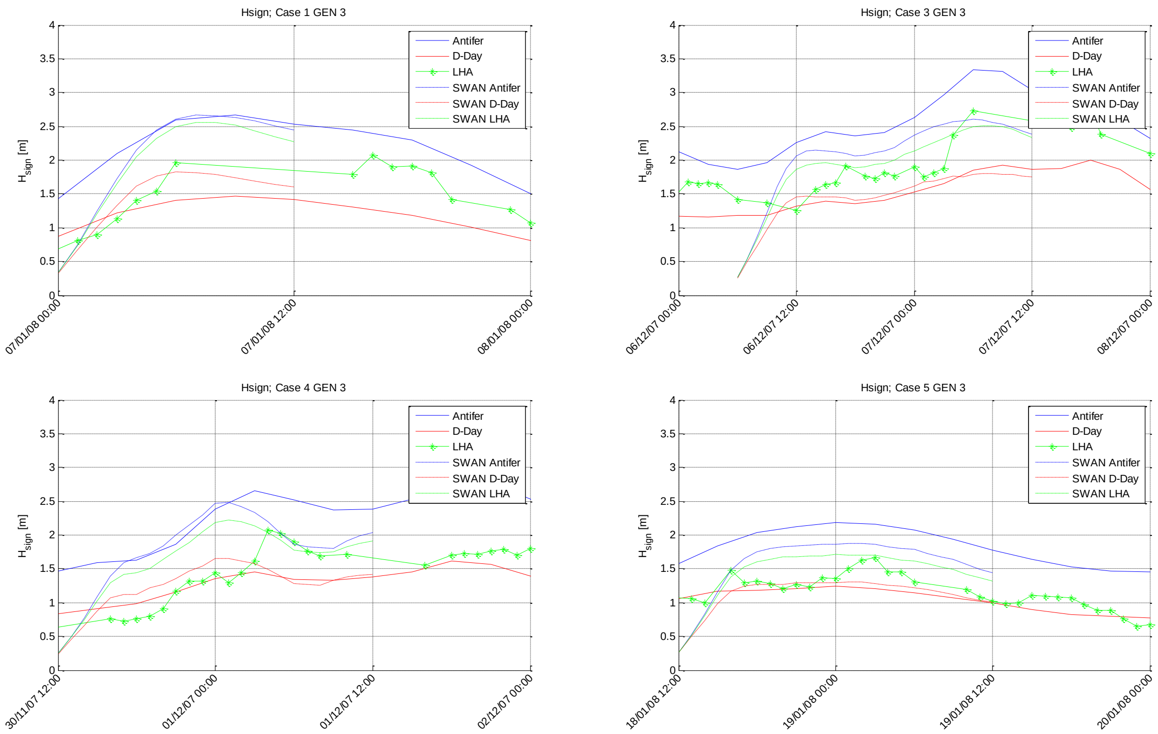

Figure 13: Hsign for cases 1, 3, 4 and 5 in SWAN generation 3.

Together with case 2, the following can be concluded for the calculation of the significant wave height by SWAN for the storm cases: The point D-Day is very accurate calculated by SWAN, only in case 1 there is a slight overestimation; however this can be explained by the twenty percent of added wind for this case. The results for buoy LHA are also good; they follow the main trend of the measured values, however sometimes they are slightly overestimated. Point Antifer is always (except from case 1, twenty percent wind added) underestimated.

A possible explanation for the underestimation of the significant wave height at point Antifer can be found in the forcing of the system. In SWAN the only imposed force on the system is the wind. However, looking at the position of point Antifer in the Bay of the River Seine, exposure to background swell coming from the English Channel is to be expected, which should result in higher waves. On the contrary this is not the case for point D-Day, which lies more protected behind the Cotentin Peninsula.

5.2.3 Mean Wave Period

Coming back to the results for the mean wave period, the results in case 2 are also confirmed in the other cases (see appendix C). The values are all underestimated and the two phenomena, the measured values at buoy LHA being larger than at Antifer and that generation 2 gives more accurate results, occur as well.

The underestimation of the mean wave period by SWAN is also found and explained in other literature. A main cause for the underestimation can be found in the (incomplete) computation of the wave-wave interactions.

Bottema and Beyer (2001) excluded depth induced breaking (by working with moderate winds) and bottom friction (by working with short fetches) in their tests. What remained where the 'deep water source terms'. Still they found a large underestimation of wave periods.

Gorman and Neilson (1999) found significant differences between SWAN's quadruplet DIA-method and exact solutions for the quadruplet wave-wave interactions, not only in shallow waters, but also in deep water conditions. This suggests that the quadruplet interactions (and the DIA-method) may indeed be the key to the problem of wave period underestimation.

The reason for the higher measured values of the mean wave period at buoy LHA, compared to Antifer, may be lying in the hindcasting method used to produce the data at Antifer (and D-Day). These hindcasting methods produce, in coastal regions, results with errors up to over twenty percent (Magne *et al.* 2010 (in submitting)). And, since the method of hindcasting makes use of numerical integration schemes (just like SWAN), it can be expected that this error comes in a form of an underestimation of the mean wave period. With the data being underestimated at Antifer, it is possible for the data of LHA, which are real time measured, to lie above those for Antifer.

An explanation for the more accurate (larger) results for the mean wave period in generation 2 compared to generation 3, can be found in the moments of the wave spectra. The mean wave period is calculated as:

$$T_{m02} = \sqrt{\frac{m_0}{m_2}} \qquad (5.7)$$

With m_0 and m_2 respectively the zeroth and second order moment of the variance density spectrum. Looking again at figure 9, it can be seen that the second order moment of the variance density spectrum in generation 3 is larger than the second order moment in generation 2 (the spectra for generation 3 are wider). Higher values for the second order moments will result in smaller values for the mean wave periods.

5.2.4 Study case; Case 2

Storm case 2 has been found to be the most interesting case of the five. Figure 13 gives both input and results for this case. In the left-top of the figure, the measured wave height (left axis) and wind velocity (right axis) are given. The storm actually consists of two peak events, a first peak is visible after six hours, a second after twenty hours. It is interesting to see that, while the largest wind velocity is measured at the first peak, the highest measured waves are found at the second peak. The graph left-down gives the computed results by SWAN, the behaviour is confirmed for buoy LHA: while the wind velocity goes down, the wave height increases at the second peak.

An explanation can be found in the two graphs on the right hand side: On the top the input for wind velocity (left axis) and wind direction (right axis) is given. The wind during the first peak blows pure south (180 degrees), it than turns towards the west (260-270 degrees) during the second peak. Waves at the second peak, which are coming from the west, are well able to meet some left over wave action from the south, which was created during the first storm. This meeting of waves from different directions will result in the creation of higher waves. This can be confirmed by the two dimensional spectrum at LHA just before the peak of the second storm, which is given in the bottom-right in the figure. The direction of the peak points towards the east, however influence towards the north is also visible.

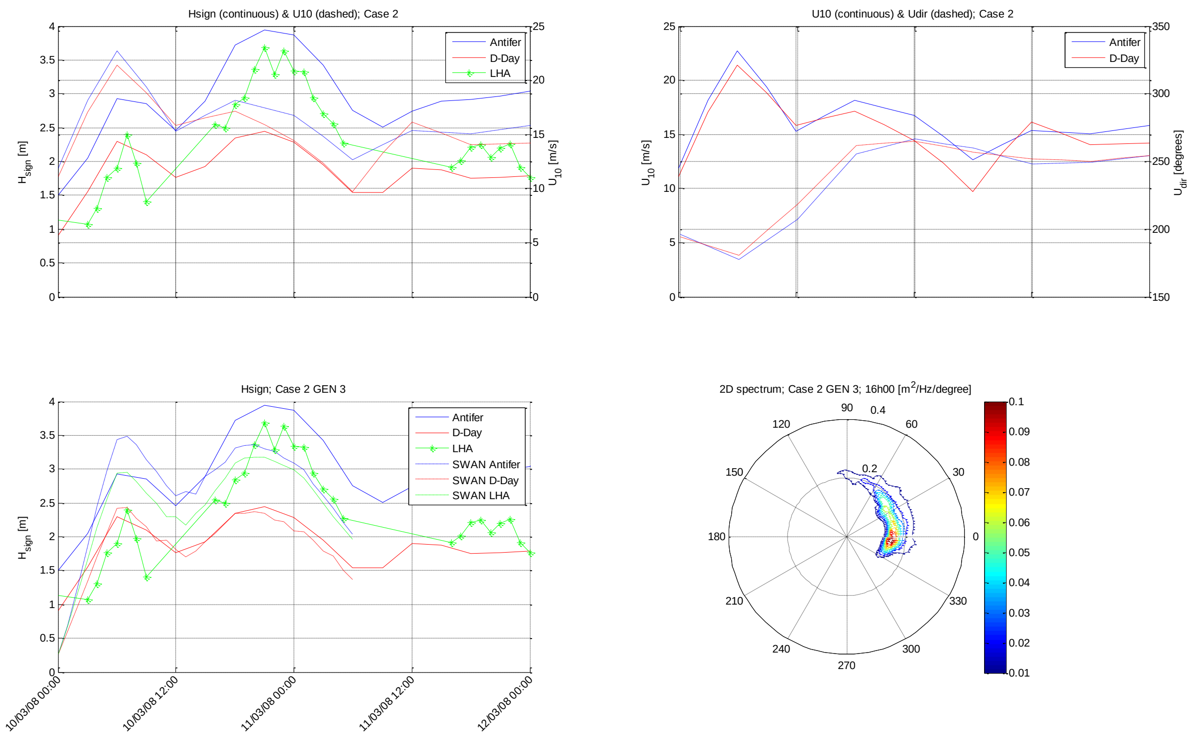

Figure 14: Input and results case 2, SWAN generation 3.

5.3 2-D modelling (new bathymetry)

Results following from SWAN for the three near-shore placed buoys do not coincide with the results that were measured by the buoys. In 5.3.1 observations on the measurements by the buoys will be discussed, only concerning the significant wave height. In paragraph 5.3.2 accompanying explanations of the observations will be discussed. In 5.3.3 results of the modelling in SWAN will be shown for each case individually. In paragraph 5.3.4 it is tried to discuss general patterns in results following from 5.3.3. 5.3.5 Handles in short the (underestimated) results for the mean wave period calculated by SWAN. In 5.3.6 explanations are tried to be found for the general patterns discussed in 5.3.4. Finally in 5.3.7 case 3 is used as a study case and its results are investigated somewhat more thoroughly.

5.3.1 Observations buoy measurements

Figures 15 till 19 give, for all cases, the measured (continuous) and computed (dashed) results for the significant wave height for the three near-shore placed buoys; Musoir Nord, Musoir Sud and LH17. In total four general and one particular observation can be seen in the results following from the buoy measurements.

Musoir Nord, Musoir Sud and LH17 are all influenced by the tide; the tidal wave (which is plotted with the black dashed-dotted line, y-axis on the left) is clearly visible in all plots for the significant wave height.

Looking at Musoir Sud and Musoir Nord, the difference between significant wave heights for high and low tide is of the same size (the amplitude is of the same order of size). However the significant wave height measured at Musoir Sud is (apart from a small period in case 3) always larger than the significant wave height at Musoir Nord.

During low tide, the significant wave height measured at LH17 is of the same size as at Musoir Sud. During high tide the significant wave height at LH17 is clearly smaller than both at Musoir Sud and Musoir Nord; the difference between values of significant wave height during high and low tide at LH17 is smaller.

Horizontal asymmetry can be observed in the measurements for the significant wave height. Case 3 forms a good example: Going from low to high water the plot is steeper than the plot for going from high to low water.

A fifth observation is only done in case 4: The highest measured significant wave height, for all the three buoys, happens after high tide (01/12/2007; 06h00), while following the general pattern of the other cases, it should take place just before high tide.

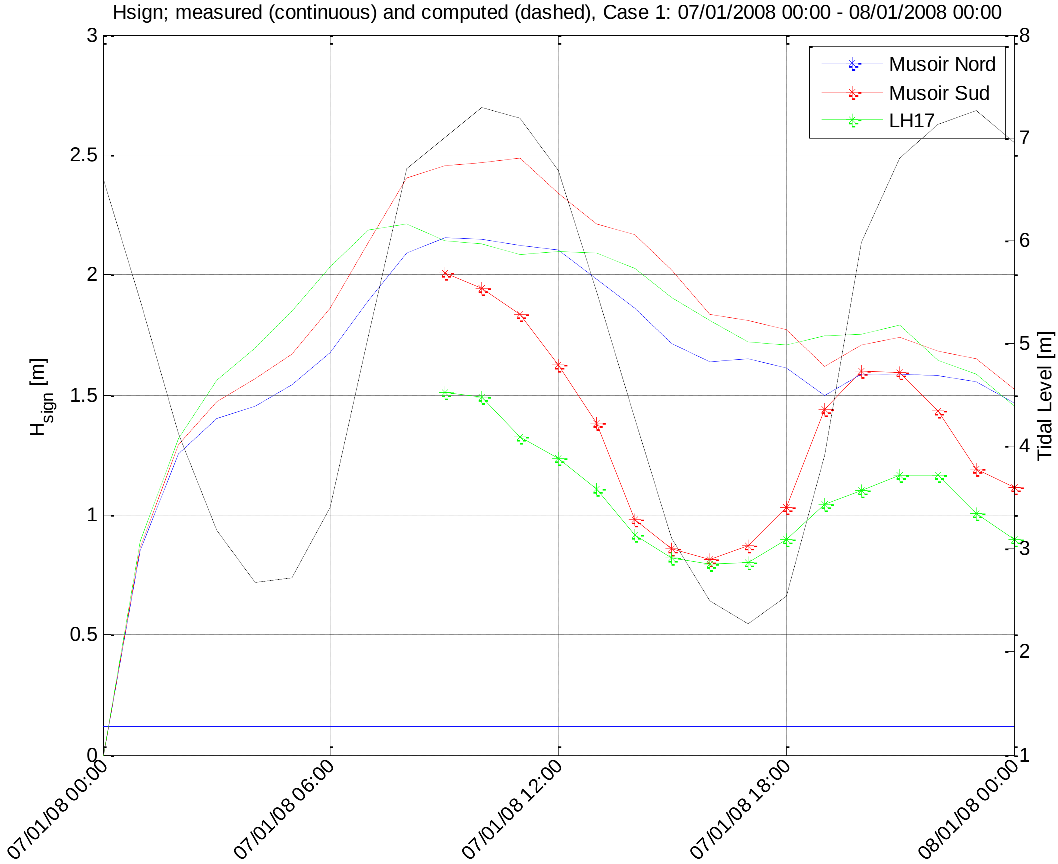

Figure 15: Significant wave height, measured and computed, case 1.

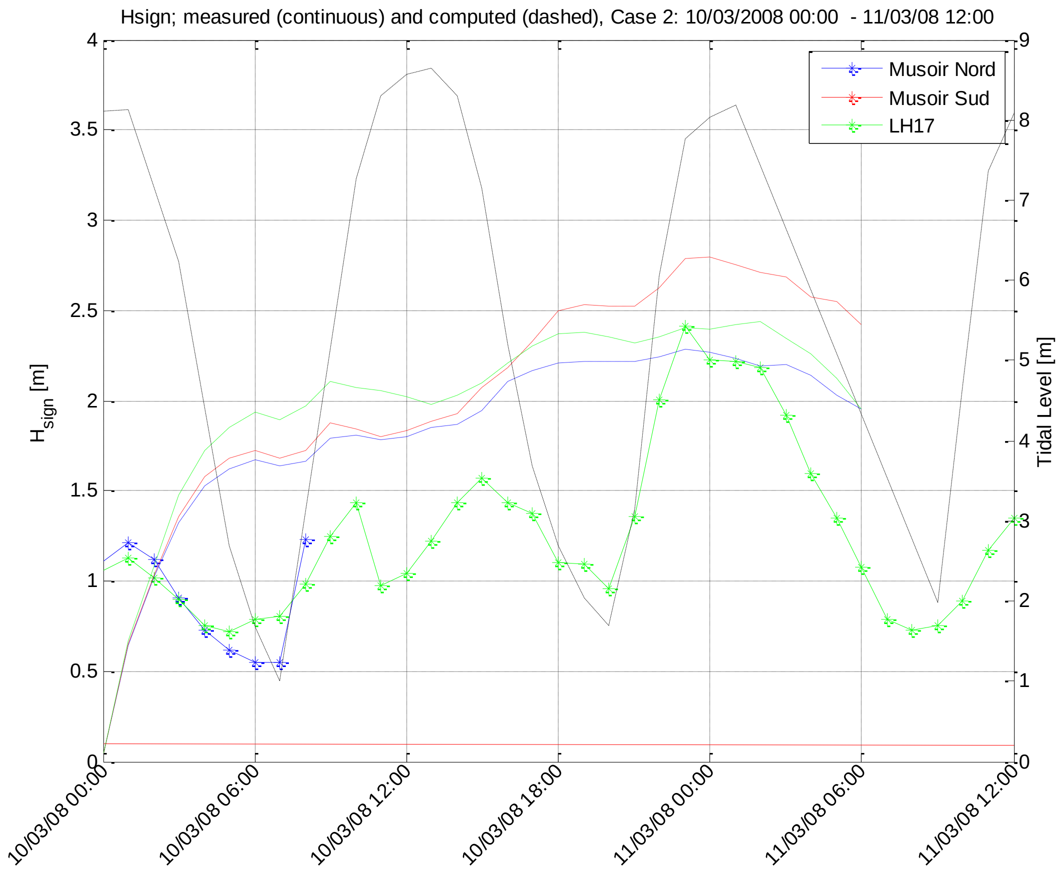

Figure 16: Significant wave height, measured and computed, case 2.

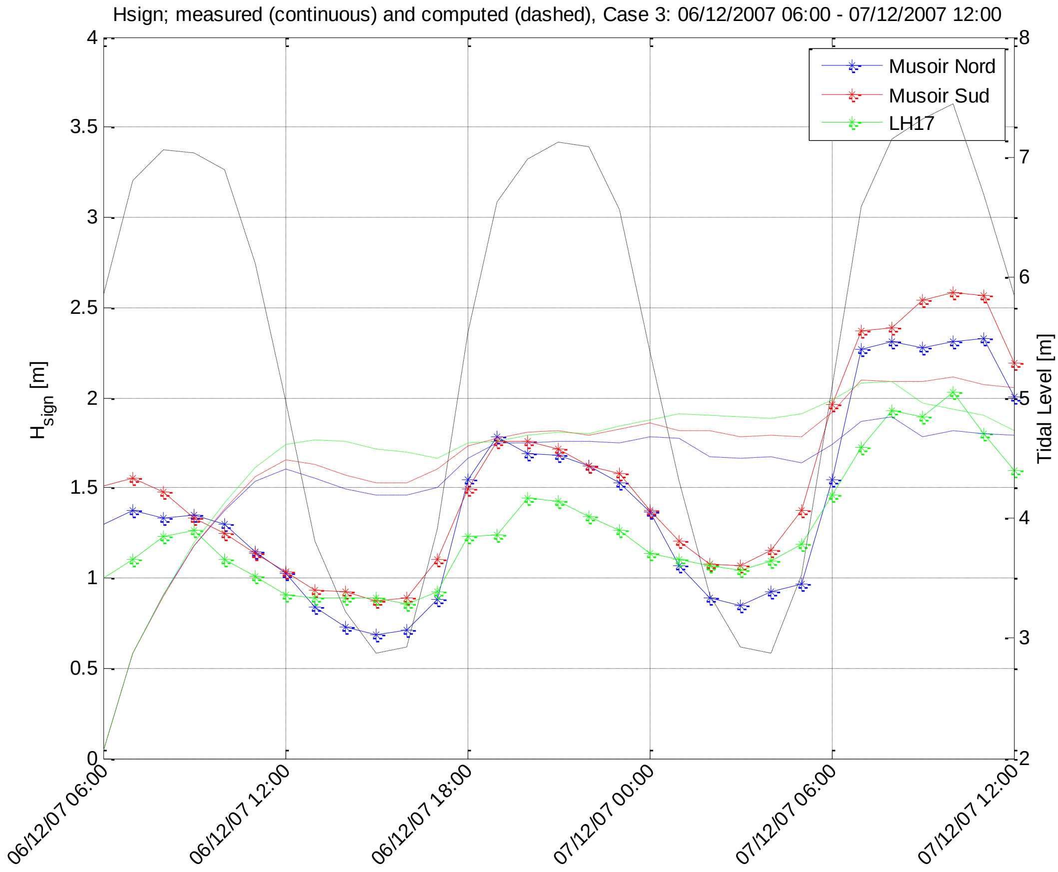

Figure 17: Significant wave height, measured and computed, case 3.

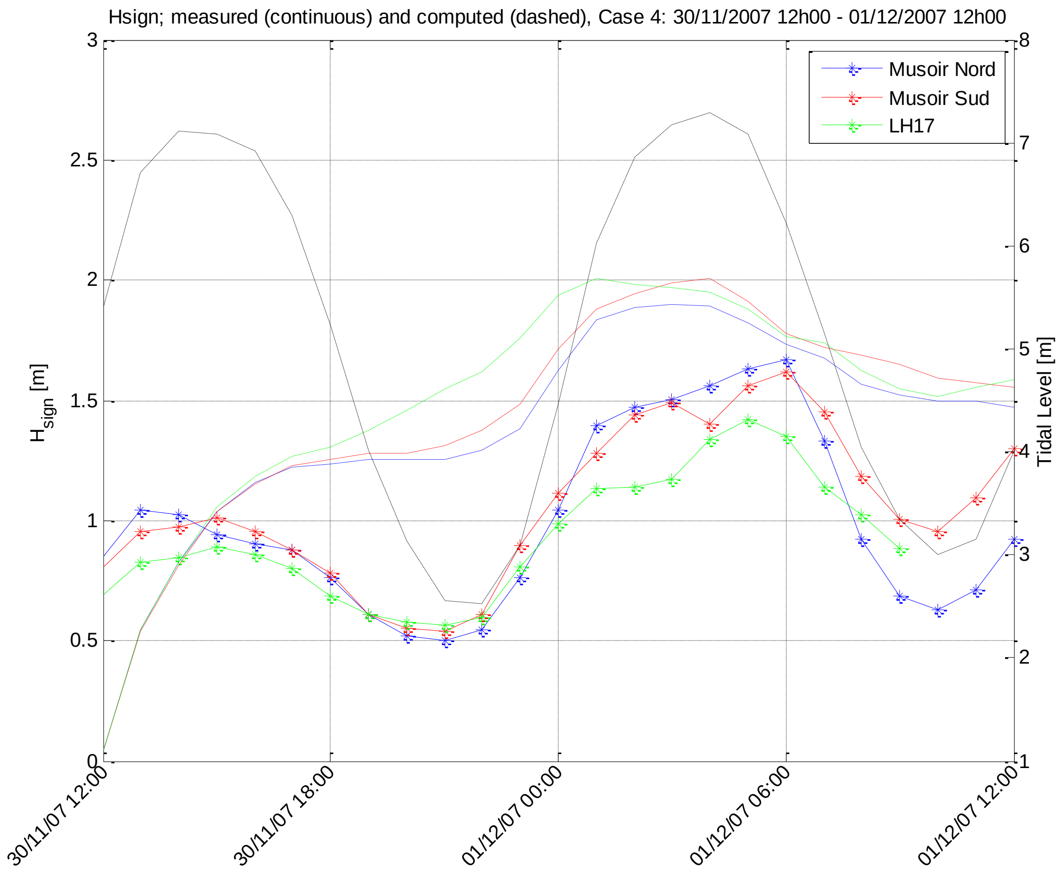

Figure 18: Significant wave height, measured and computed, case 4.

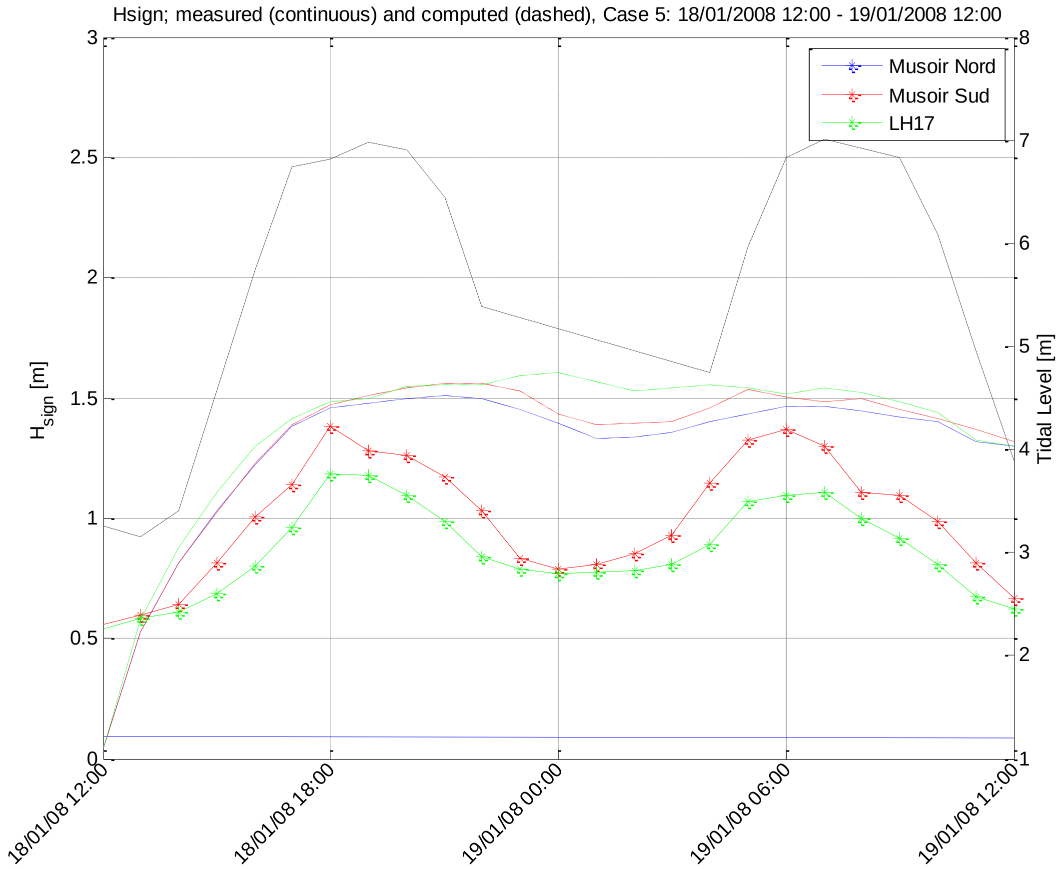

Figure 19: Significant wave height, measured and computed, case 5.

5.3.2 Explanations observations buoy measurements

The well visible influence of the tide on the results of the significant wave height in the Bay of the River Seine lies in the bathymetry. The bathymetry at the northern bank in the head of the River Seine is, apart from the newly dredged navigation channel, shallow. With the large tide imposed this gives well observable differences in measured significant wave height during high and low tide.

In order to clarify the differences in wave height between Musoir Nord and Musoir Sud it is necessary to have a close look at the bathymetry and the involved processes in the head of the River Seine. Figure 20 gives the positions of the three buoys within the new bathymetry. Musoir Sud lies at the western boundary of the newly dredged navigation channel. Waves propagating from the Bay of the River Seine towards the east will break depth induced at the shallow parts in front of buoy Musoir Sud. This will give a decrease in significant wave height, both at Musoir Sud and Musoir Nord.

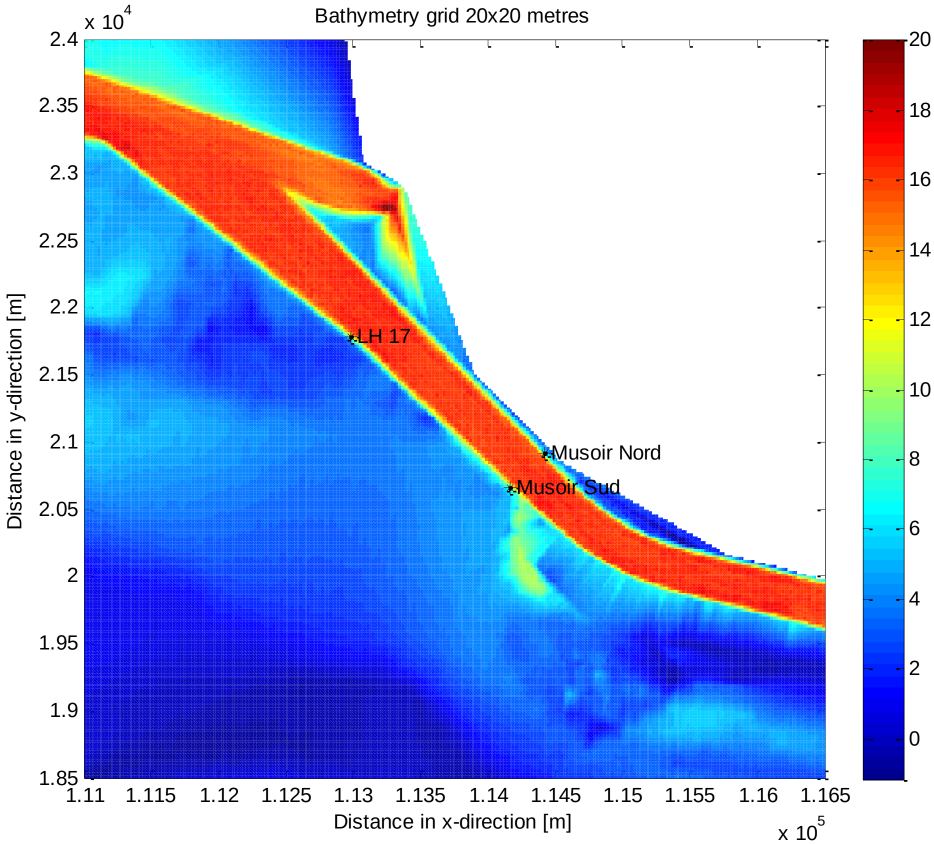

Figure 20: Position of the three near-shore buoys in the head of the River Seine.

After Musoir Sud the waves will meet the navigation channel and refraction occurs. Dependable on the critical angle of incidence, waves will cross the access channel or will be reflected away. Snell's law says:

$$\frac{\sin \vartheta}{c} = \text{constant} \qquad (5.8)$$

$$\frac{\sin \vartheta_1}{c_1} = \frac{\sin \vartheta_2}{c_2} \qquad (5.9)$$

$$\sin \vartheta_2 = \sin \vartheta_1 * \frac{c_2(h_2)}{c_1(h_1)} \qquad (5.10)$$

With h_2 being the depth of the access channel, which is larger than h_1, the water depth west of the access channel, θ is the angle with the normal of the access channel under which the waves come in and leave.

$$h_2 > h_1 \Rightarrow c_2 > c_1 \Rightarrow \frac{c_2}{c_1} > 1$$

Substituting this in (5.10) gives a minimum angle of wave incidence for refraction, since the sine term on the left hand side in (5.10) can never be larger than one. For example with an angle of incidence of 70 degrees and a value of c_2 divided by c_1 of 1.2, the following happens:

$$\sin \vartheta_2 \; = \; \sin \vartheta_1 * \frac{c_2(h_2)}{c_1(h_1)}$$

$$\sin \vartheta_2 \; = \; 0.94 \; * \; 1.2 \; \approx \; 1.13$$

This is impossible to satisfy. The critical angle of incidence is the value of θ_1 for which θ_2 equals 90 degrees:

$$\vartheta_{crit} = \arcsin \frac{(c_1)}{(c_2)} \quad (5.11)$$

If the waves come in under an angle larger than the critical angle of incidence, total reflection will occur.

Some rough calculations give that for low water (+1.0 m. CD) in the head of the River Seine the critical angle of incidence is about 45 degrees, during high water (+8.0 m. CD) the angle is 66 degrees.

Under all five storm cases, the waves come in from the west to northwest. With the position of the access channel in the head of the River Seine, this means that the angle of incoming waves is always larger than the critical angle of incidence. In all storm cases the waves will not be refracted into the channel and therefore the wave height at the eastern boundary of the channel (at Musoir Nord) will be smaller than at the western boundary. If waves however would refract into the channel, the wave height would also decrease, due to an increase in wave speed, which is depth induced.

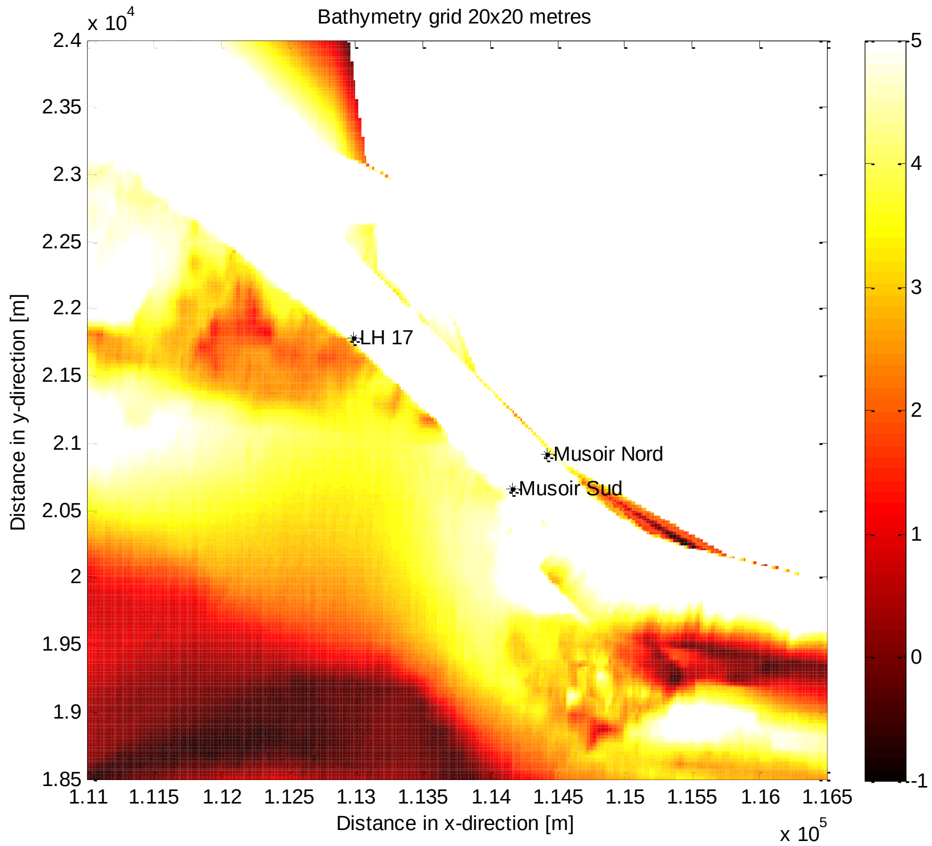

Figure 21: The bathymetry in the head of the River Seine.

The difference for results between buoys LH17 and Musoir Sud lies also in the bathymetry. Looking west of the two buoys (figure 21), which is the direction for the incoming waves, the bathymetry in front of LH17 is shallower than in front of Musoir Sud. During low water the water depth west of both buoys is of such limited depth that it no longer gives real differences in significant wave height (all waves will break). During high tide the difference in depths west of LH17 and Musoir Sud is more observed by the waves, due to the increased overall depth. This results in more waves to break on the shallow flats in front of LH17 than in front of Musoir Sud.

The existence of horizontal asymmetry has to be found on a larger scale than solely the Bay of the River Seine: A tidal wave near-shore consists of a set of tidal components. The base is a M2 tide, a sinusoidal tidal wave. Differences in bathymetry give rise to higher order tidal components, like M4 and M6 components.

For the Bay of the River Seine, the tide propagates from the Atlantic Ocean through the English Channel into the Bay. At the Atlantic the bathymetry shows over 4000 metres of depth, coming towards the shore it meets the continental shelf which gives a quick rise to a depth of roughly 100 metres. This sudden change in bathymetry gives rise to the higher order tidal components and transforms the sinusoidal M2 wave into a horizontal asymmetric tidal wave.

In order to clarify the peak for the significant wave height after high water, instead of before in case 4; 01/12/2007 03h00 - 06h00, it is necessary to look for a second event happening, besides the wind sea generated waves.

Looking at the input/validation data for case 4 in Appendix C, the graph for the peak period shows a peak at 01/12/2007 between 05h00 and 10h00. Such a peak indicates a swell event, which, combined with the wind sea generated waves, gives rise to a larger significant wave height.

5.3.3 SWAN results; individual cases

See again figures 15 till 19 for the measured (constant) and computed (dashed) results of significant wave height. Since a lot of difference exists between the measured and computed values and constant patterns are hard to observe at first eyesight, hereunder are, per individual case, all observations written down. If a quick explanation can be given to clarify an observation it is done.

<u>Case 1:</u>

The results by SWAN for Musoir Nord, Musoir Sud and LH17 follow the pattern of the modelled results of the three off-shore buoys; Antifer, D-Day and LHA (see Appendix E). The peak of the storm is for all six buoys modelled at 07/01/2008; 09h00, which is just before high tide. Afterwards the modelled significant wave height, for all six buoys again, decreases smoothly. At 07/01/2008; 23h00 the next high tide is recorded, the significant wave height for the three off-shore buoys (both modelled and recorded) is not visibly influenced.

The results following from the buoys Musoir Sud and LH17 (Musoir Nord was out of service) show a clear influence of tide on the significant wave height (Musoir Sud 70 centimetres difference, LH17 40 centimetres), however the modelled results only give a difference of five to ten centimetres. Just before high tide the measured and modelled wave heights for Musoir Sud are close to each other (07/01/2008; 08h00 and 20h00); however during low tide the measured results give much smaller values than SWAN calculates (differences of up to one metre). The results from SWAN for buoy LH17 are always largely overestimated.

Case 2:

The three off-shore buoys recorded two peaks during this storm; SWAN also models these two peaks. Musoir Sud and Musoir Nord were out of service, LH17 only recorded a peak in the results during the storm for the second peak (10/03/2008; 23h00). The results by SWAN for the three near-shore buoys show more or less the same pattern: The significant wave height grows steadily towards the second peak, which has the same height as measured.

The explanation for the non-recording, both measured and modelled, of the first peak by the near-shore buoys can be found in the tide. During the first peak for the off-shore results (10/03/2008; 07h00), it is low tide, the influence of the tide on the measured results for the buoys near-shore is (as in the other cases) clearly present. The computed results by SWAN for the significant wave height at 07h00 lie over one metre higher than the measured results, however low tide prevent results from giving a peak. The peak at 10/03/2008; 23h00 is visible in both the measurements at LH17 as in the results by SWAN: It is an event that happens around high tide.

The values of significant wave height for buoy LH17 that follow from the measurements and from the SWAN calculations, are, for the peak just before high tide, the same.

Case 3:

Case 3 is the most interesting case, since it gives a full coverage of measurements by the three near-shore buoys. The computations by SWAN cover a period of 30 hours, including two times high and two times low tide.

As in the other cases, the near-shore buoys follow for the SWAN computations the behaviour of the three off-shore buoys; they steadily grow towards the peak of the storm between 07h00 and 10h00; 07/12/2007. Again low tide is not seen back in the SWAN results, while in the measurements it is well observed.

Just before high tide (06/12/2007; 19h00 and 07/12/2007; 07h00) results for the measured and computed significant wave heights at Musoir Sud and Musoir Nord are the same. For LH17 only the results at the second peak coincide with each other, however during a somewhat longer period (from 08h00 till 11h00), also during and just after high tide.

Case 4:

The SWAN computations for the three near-shore buoys follow again the tendency of the three off-shore buoys. Low tide is at 30/11/2007; 22h00, which causes for Musoir Nord and Musoir Sud a ‘pause’ in the SWAN results for the growth of significant wave height. From 30/11/2007; 22h00 on, high tide starts and the growth of significant wave height continues. This ‘pause’ is not visible in results for buoy LH17.

A bit awkward is that the coincidence of the measured and computed significant wave height for Musoir Sud and Musoir Nord now not only happens before, but also after high tide (01/12/2007; 06h00, high tide recorded at 04h00). The explanation lies into a swell event, as already explained in 5.3.2.

Case 5:

Buoy Musoir Nord recorded no measurements. The tendency of the results by SWAN for the near-shore buoys is again to follow the results of the off-shore buoys.

The calculated and measured values for buoy Musoir Sud coincide both times before high tide (18/01/2008; 18h00 and 19/01/2008; 06h00). The calculations for the significant wave height by SWAN for buoy LH17 are overestimated.

The influence of the tide is larger on the measured values than on the computed values. Low tide is only little visible in the results for buoys Musoir Nord and Musoir Sud (a level drop of 25 centimetres, while the measurements give 60 centimetres). The SWAN results for buoy LH17 show no influence of low tide and thereby follow the tendency of results for the three off-shore placed buoys (both computed as measured).

5.3.4 SWAN results; general patterns

The significant wave height modelled in SWAN differs a lot from the measured significant wave height by the buoys. In the SWAN results the tidal influence is only little visible, however measurements by the buoys give a difference of 0.5 to 1.0 metres between high and low tide. Especially SWAN results for buoy LH17 show little to no influence of low tide on its results.

For the peak storm events that take place during high tide the SWAN results for Musoir Sud give the highest significant wave height in case 1 and case 2; peak 2. For the peak storm events of case 3 and case 4, SWAN calculates more or less the same significant wave height for Musoir Sud and LH17. In all cases (also for the two storms taking place during low tide) Musoir Nord has the smallest computed significant wave height, which is due to the already discussed refraction effect of waves over the access channel. Heading towards the four peak events discussed, the results for Musoir Nord follow Musoir Sud, but finally Musoir Sud gives the highest values during the peak events. This behaviour is confirmed by the measurements.

While heading for the peak events, SWAN always computes the largest significant wave height for LH17. It is only just before the peak event that results of Musoir Sud reach or even overtake the results of LH17. During the peak events of case 1, case 2; peak 2, case 3 and case 4, the significant wave height computed for LH17 is always larger than for Musoir Nord.

The two other peak events (case 2; peak 1 and case 5) occur during low tide and SWAN gives the largest value of significant wave height for LH17, followed by Musoir Sud and Musoir Nord, which show a little influence by the low tide.

In cases 1, 2, 3 and 5 the coincidence of measured and computed results happens always just before high tide. Results by SWAN for Musoir Sud and Musoir Nord do always (if measured) coincide with the measurements. Calculations for LH17 only coincide during the actually peak of the storm events for case 2; peak 2 and case 3, in all other cases the significant wave height is overestimated by SWAN.

5.3.5 Mean Wave Period

The computed results for the mean wave period by SWAN on the 20 by 20 metres grid show, as for the off-shore buoys, a large underestimation of mean wave period compared to the measured values. Figure 22 gives measured and computed results of all six positions in the Bay for case 3 and case 4.

For the explanation of the underestimated mean wave period by SWAN is referred to chapter 5.2.3.

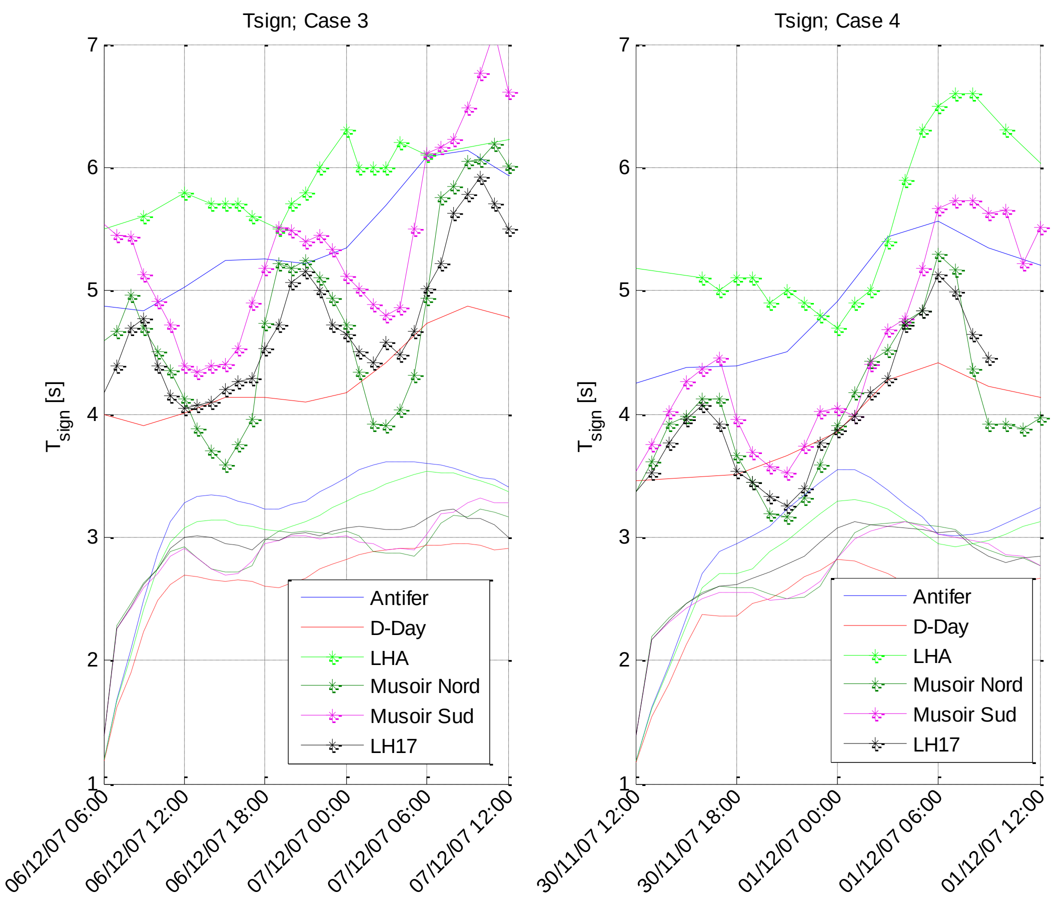

Figure 22: Mean Wave Period, computed (dashed) and measured (continuous).

5.3.6 Explanations SWAN observations

As follows from the previous paragraphs it is hard to interpret results, since measured and computed values do not coincide with each other. A first thought to clarify observations, was to look at the possible influence of a tidal current on the measured results, since this tidal current is not incorporated in the SWAN model.

Three-dimensional calculations (Telemac) provide for different tidal ranges accompanying tidal currents in the head of the River Seine. Figures 27 and 29 give the plots of the measured (continuous) and computed (dashed) significant wave height. The black dashed-dotted line is the recorded tide at buoy Le Havre, dashed-dotted in magenta is the tide following from Telemac calculations, the continuous line in magenta is the tidal current that follows from Telemac (left axis, [m/s]). Figure 27 shows the results for case 2, figure 28 for case 3. Appendix F provides the graphs for all cases.

Looking back at figures 15 till 19 it can be seen that the tidal range for cases 1, 3, 4 and 5 is about five metres, the used Telemac calculations for these cases are all the same. Case 2 has a tidal range of over seven metres; Telemac calculations for a larger tidal range and a stronger tidal current have been used.

In figure 29 it can be seen that just before high tide the tidal current is at its maximum, with a value of about 0.7 metres per second (positive values mean a current flowing from the Bay into the river). This is also the moment (just before high tide) that SWAN results for Musoir Nord and Musoir Sud coincide with the measurements by the buoys. Case 2 formed an exception on the other cases, since it showed a coincidence of measurements and calculations for buoy LH17, while in the other cases the calculated significant wave height for LH17 was always overestimated.

The answer for this single observation might be lying in the larger tidal current being present during case 2 (up to 1.55 metres per second, see figure 27). The measured values of significant wave height by the buoys are affected by the tidal current by the fact that this current can be opposite to the direction of the waves.

A thought was that the wave-current interaction might be the answer to differences between calculated and measured wave heights. Hereafter, in 5.3.7, it is shown that for most cases in this research the influence of tidal currents on waves is of second order. Concluding: Also the non-presence of a tidal current in the SWAN model is not the total, or general, answer to the differences in measured and computed results for wave height.

It looks like the combination of the very complicated bathymetry in the head of the River Seine, together with the large imposed tidal range makes it too difficult for SWAN to properly calculate results. A possible key may be lying in the breaking wave parameter γ (wave height to depth ratio): The case concerns a double barred beach and is not well comparable with the Bay of the River Seine, but Ruessink *et al.* (2001) found a systematic overestimation of up to 60 percent in the inner bar trough of the double-barred beach at Egmond aan Zee (Netherlands), but far better model-data agreement (without systematic overestimations) in the outer bar trough. In a next research Ruessink *et al.* (2003) concluded that that would mean that the used breaking wave parameter γ (wave height to depth ratio) should not be cross-shore constant, but should depend on the local wave number k and water depth d. The calculations for the Bay of the River Seine show the same tendency: Calculations for the three off-shore placed buoys give good results, coming near-shore the calculations are overestimated, especially during low tide.

5.3.7 Wave-current interaction

Figures 28 and 30 (case 2 and 3) give the direction of the waves calculated by SWAN and the direction of the tidal current calculated by Telemac. Hereunder both cases are treated separately. First theory by Jonsson (1990) will be described, he performed a lot of research on wave-current interaction. Hereafter case 2 and 3 will be elaborated with the help of Jonsson´s research. In this research on the bay of the River Seine we are interested in the refraction of waves by a horizontally sheared tidal current (Soulsby *et al.*, 1993).

Jonsson (1990) describes how a simple relation comes to an existence if pure current refraction is considered. He starts from a steady wave transformation by a current over a horizontal bed and ignores further dissipation. With a simple sign convention he makes it that the angle of incidence β, which is the angle between the normal N and the wave orthogonal (see Figures 23, 24), always lies between 0° and 90°.

Figure 24 gives a sketch of the Jonssons situation. The current goes from left to right, under an angle δ with the x-axis. The angle α is from the x-axis to the wave orthogonal. This makes δ - α the angle between the wave orthogonal and the current direction. Jonsson than gives for the determination of the wavelength L :

$$\sqrt{\frac{h}{L}\tanh kh} = \sqrt{\frac{h}{L_0}}\left(1 - \frac{U\cos(\delta-\alpha)T_a}{h}\frac{h}{L}\right) \quad (5.12)$$

For shallow water there is an explicit solution to Equation 5.12:

$$L = \left(U\cos(\delta-\alpha) + \sqrt{gh}\right)T_a \quad (5.13)$$

In which U is the current velocity, g the gravity acceleration, h the water depth and T_a the absolute wave period.

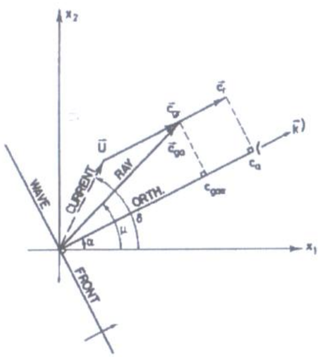

Figure 23: Horizontal plan view with wave ray, absolute group velocity, it scomponent in orthogonal direction, absolute wave speed an wave number (from Jonsson, 1990).

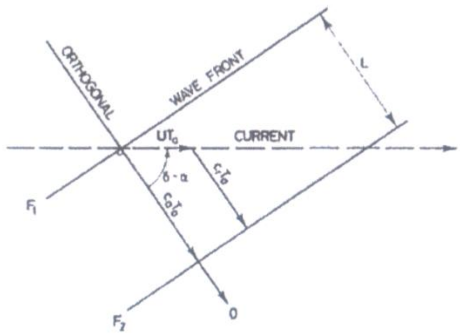

Figure 24: Waves in a homogeneous current field (from Jonsson, 1990).

Jonsson continues and looks at a wave field travelling from a region 1 influenced by a certain current, to a region 2 influenced by another current (Figure 25 and 26). He assumes the values of T_a, h, U_1, U_2, the angle of incidence β_1 and wave height H_1 known. With those he determines wavelength L_1 from a special wave table. Since $\frac{\delta k_x}{\delta y} = 0$ and therefore also $\frac{\delta k_y}{\delta x} = 0$; $\frac{L}{\sin \beta} = constant$. Therefore $U_2 \sin \beta_2 := U \cos(\delta - \alpha)$, which makes for the determination of L_2:

$$\sqrt{\frac{h}{L_2} \tanh k_2 h} = \sqrt{\frac{h}{L_0}} \left[1 - \frac{U_2 \sin \beta_1 T_a}{L_1}\right] \quad (5.14)$$

For the determination of H_2 Jonssson (1990) finds:

$$\frac{H_2}{H_1} = \sqrt{\frac{1 + G_1}{1 + G_2}} \sqrt{\frac{\sin 2\beta_1}{\sin 2\beta_2}} \quad (5.15)$$

In which $G = \frac{2kh}{\sinh 2kh}$. Both in deep as shallow water this equation (5.13) reduces to Longuet-Higgins and Stewart´s (1961) expression:

$$\frac{H_2}{H_1} = \sqrt{\frac{\sin 2\beta_1}{\sin 2\beta_2}} \quad (5.16)$$

Minimum wave height occurs in region 2 when the angle between current and wave height is 45°.

All theory above is somewhat short, for a full description we make reference to Jonssons article (1990).

For our research we start from Equation 5.13. It is clear that if the angle between the wave orthogonal and the current is 90°, there is no first order influence on the wavelength. From equation 5.16 it follows that the wave height in that case is also not influenced. If the current acts in the same direction as the waves, it is called a following current and it will lengthen the waves. If it acts opposing it will shorten the waves. Shorter waves will become steeper until they break.

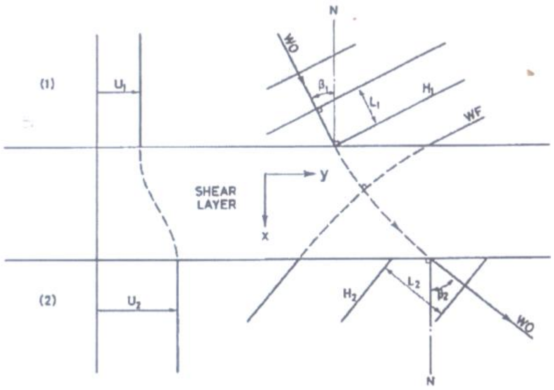

Figure 25: Waves refracting across a shear current from region 1 to 2 (from Jonsson and Skovgaard, 1979).

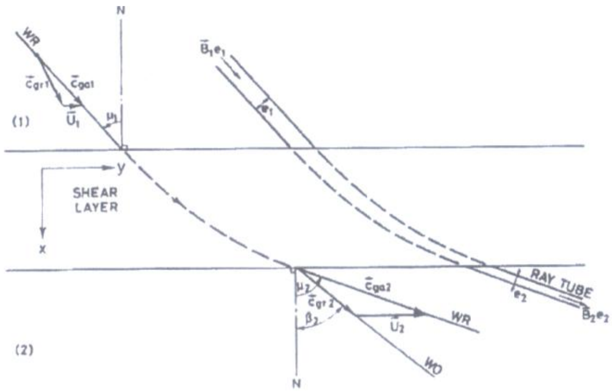

Figure 26: Wave ray WR and ray tube passing the shear layer of figure 25 (form Jonsson, 1990).

In Tables 6 and 7 Cases 2 and 3 are split up in four periods. For each, the angle between current and waves is given and also whether the current is following or opposing.

Case 2	Direction:	*δ (current):*	*α (waves):*	*δ – α:*	Effect:
01:00 – 07:00	Following	300°	25°	85°	None
07:00 – 10:00	Following	120°	40°	80°	None
15:00 – 20:00	Opposing	300°	70°	(-)50°	Shortens
20:00 – 23:00	Following	120°	90°	30°	Lengthens

Table 6: Case 2, angles between current and waves during different periods.

Case 3	Direction:	*δ (current):*	*α (waves):*	*δ – α:*	Effect:
10:00 – 15:00	Opposing	300°	70°	(-)50°	Shortens
16:00 – 20:00	Following	120°	75°	45°	Lengthens
21:00 – 03:00	Opposing	300°	80°	(-)40°	Shortens
04:00 – 07:00	Following	120°	90°	30°	Lengthens

Table 7: Case 3, angles between current and waves during different periods.

For Case 2 the first period 01:00 – 10:00, with 85° and 80°, there is no first order influence of the current on the wave height. The third period, the current is opposing and close to the 45° minimum wave height criterion (Equation 5.16). The fourth period the current is following under an angle of 30°. The wave will lengthen by Equation 5.13, which will bring the wave height down.

In Case 3 all periods have angles between current and waves of about 45°, which is the minimum wave height criterion. The following currents will decrease wave height, the opposing will work increasing.

The comparison of SWAN results with the measurements for Case 2 give that for 01:00 till 10:00, the tidal current has not influenced the wave height. If the tidal current would have been included in the SWAN calculations, results would remain over predicted. The third period would shorten and thereby grow the wave height. SWAN results are already over predicted, differences would only increase with a tidal current included. The fourth period would bring the wave height somewhat down; that would give better results. However towards the end of this period measured and calculated wave heights are already coinciding (10/03/2008 23:00).

For Case 3 calculated and measured values are already better coinciding. During periods 1 and 3 including a tidal current in SWAN, would not give satisfying results. The current is opposing and the wave height should grow. However the SWAN calculations are already above the measured values. The following currents (periods 2 and 4) will bring the wave height down. Therefore new calculations for those periods with a tidal current included, would give good results.

In general we can conclude that for this research, besides Case 3; periods 2 and 4, the tidal current in the Bay of the River Seine does not change the wave height in first order.

5.3.8 Study case; Case 3

Case 3 is found an interesting study case since it has a full coverage of measurements by all three buoys. The SWAN run covers a period of 30 hours of calculations, which gives the possibility to compare results during twice high and twice low water.

In figure 24 it is well observable that both times just before high water (06/12/2007; 18h00 – 20h00 and 07/12/2007; 06h00 – 08h00) the measured and calculated wave heights correspond with each other. Low tide (06/12/2007; 15h00 – 16h00 and 07/12/2007; 03h00 – 04h00) shows a little influence (a drop of ten centimetres) on the buoys Musoir Nord and Musoir Sud. Low tide shows no visible influence on buoy LH17.

Figure 27 shows the 2D variance density spectra for the buoys LHA, LH17, Musoir Nord and Musoir Sud at 06/12/2007; 21h00. The spectrum for buoy LHA has one clear peak at 355 degrees with an accompanying frequency of 0.18 Hertz (see figure 28, 1D variance density spectra). 21h00 is at high tide, measured and computed wave heights for Musoir Nord and Musoir Sud do still fairly coincide.

Going more near-shore, the next buoy that is met, is LH17. The 2D spectrum here shows two peak directions (at 15 and 330 degrees with respect to the east); the peak frequency is 0.18 Hertz. These two peaks are caused by the total reflection of incoming waves on the access channel (see chapter 5.3.2; critical angle of incidence). The angle of incoming waves at 15 degrees, with respect to the normal to the access channel, is larger than the critical angle of incidence for refraction occurring. The incoming waves are reflected back under an angle of 330 degrees, which causes the second peak in the 2D spectrum.

Results for Musoir Sud are even more scattered over different directions, also the 1D spectrum has a wider shape; waves are less uniform concerning their period. However still two peaks are visible, waves come in under an angle of 15 degrees and are reflected back under an angle of 350 degrees. The last buoy is Musoir Nord; one clear peak is visible for a wave direction of 5 degrees.

The same pattern for the four buoys can be observed during the next high tide, 07/12/2007; 10h00 (see Appendix H, 1D and 2D variance density spectra at different times for case 3). Waves at buoy LHA are still fairly uniform, the peak direction lies between 5 and 330 degrees, the accompanying peak frequency is 0.17 Hertz. Buoy LH17 has a clear peak for incoming waves under an angle of 15 degrees, the waves leave under an angle of 320 degrees. Two small peaks (5 and 20 degrees) are visible; the 1D spectrum gives an accompanying frequency of 0.13 Hertz. These peaks are probably caused by the complicated bathymetry west of LH17; waves come in under 20 degrees and leave under an angle 5 degrees. Results at Musoir Sud are completely scattered between 10 and 300 degrees, the 1D spectrum also tells that the value for the peak frequency has a wide range. These phenomena are all caused by the complicated bathymetry west of buoy Musoir Sud. The results for buoy Musoir Nord are less scattered, both for the 1D and 2D spectrum, however this time two peak directions are visible at 330 and 350 degrees.

It is not possible to see a constant line in results for the variance density spectra. If for example the two spectra for the two high tides are compared, it is not possible to see regularities or clear differences with the spectra during low tide.

One observation that can be done is that the 2D spectra for Musoir Sud become more and more scattered in both direction and frequency as the storm grows. Musoir Nord is more regular, only towards the peak of the storm (07/12/2007; 12h00) results become more scattered. Buoy LH17 seems to show the most regular results of the near-shore buoys. Two peaks are constant present, one for the incoming waves, under an angle of roughly 10 degrees, another for the outgoing waves at an angle of 330 degrees.

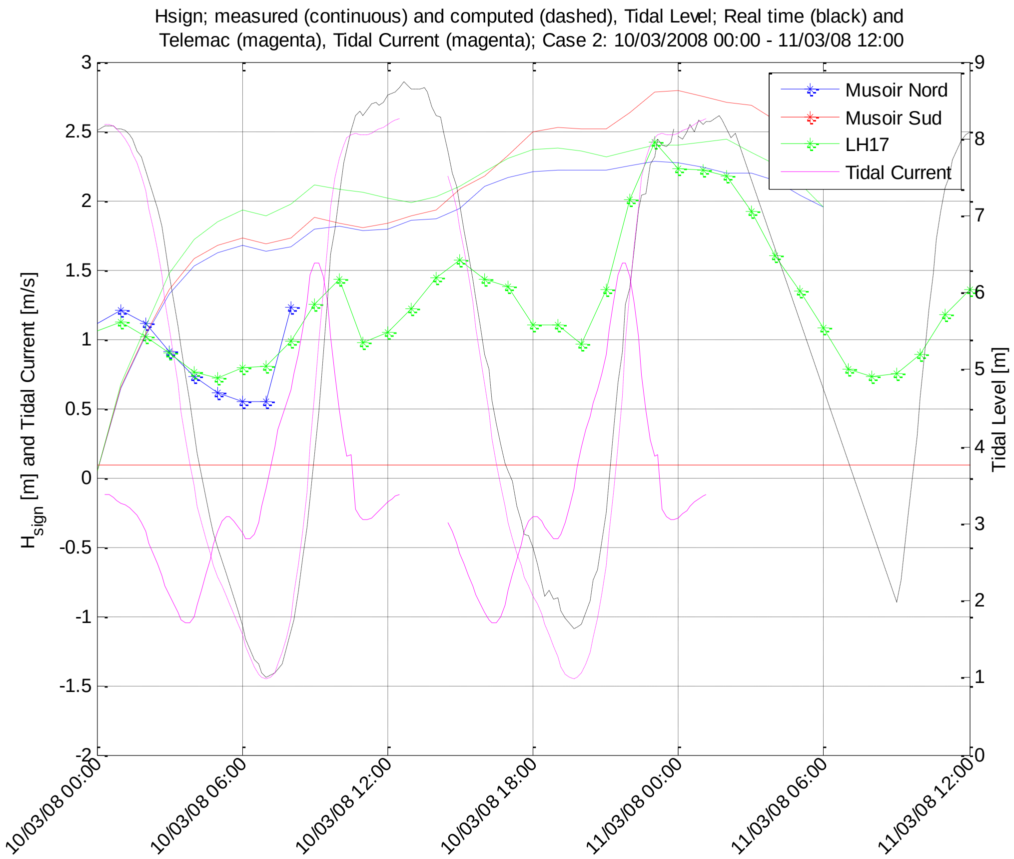

Figure 27: Measured, SWAN and Telemac results; case 2.

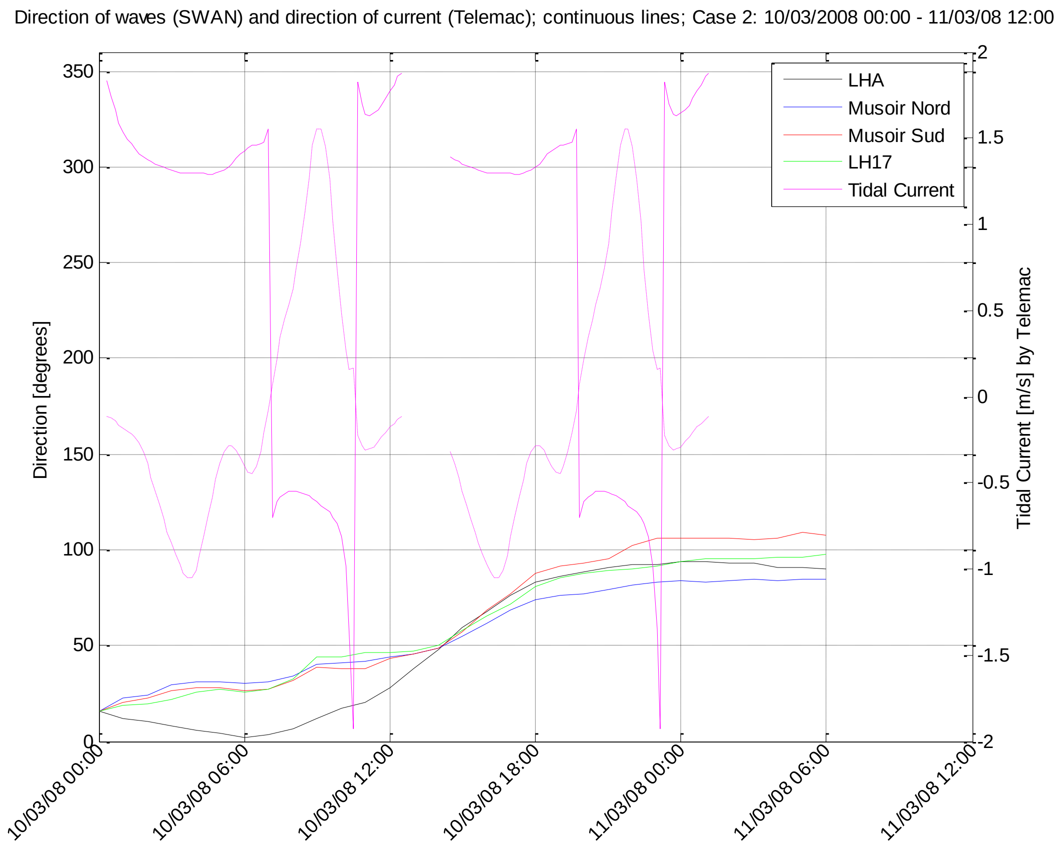

Figure 28: Direction of waves (SWAN) and current (Telemac); case 2.

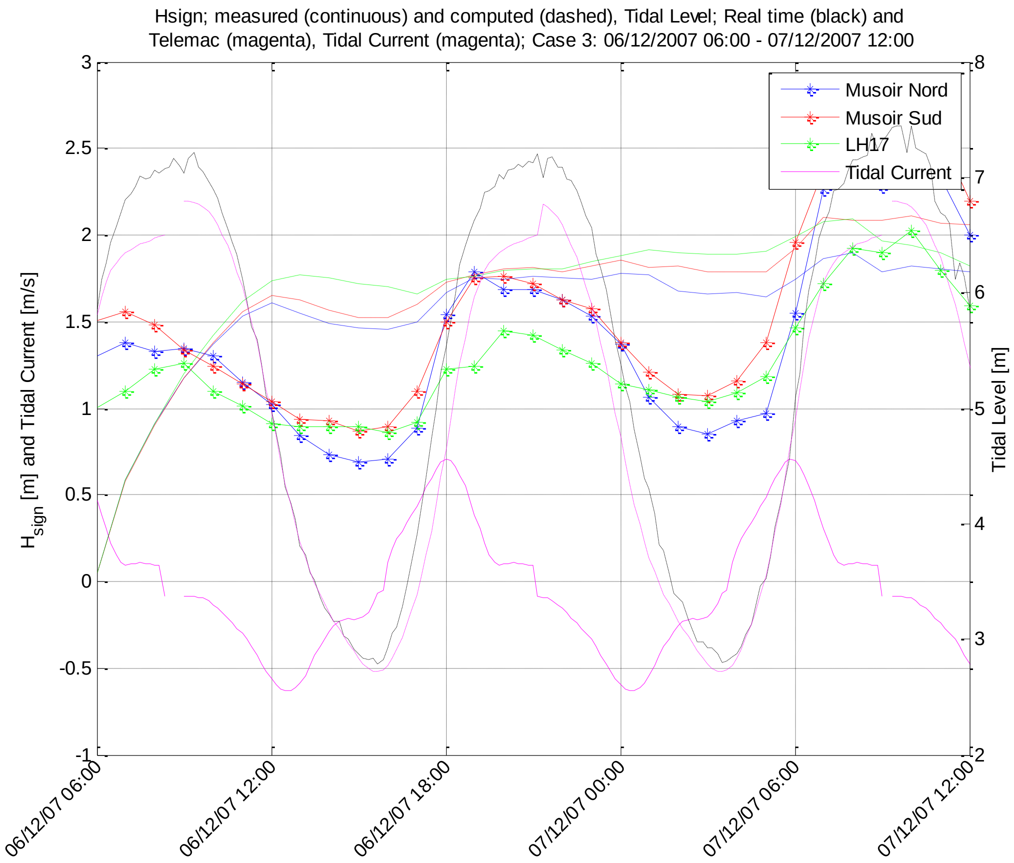

Figure 29: Measured, SWAN and Telemac results; case 3.

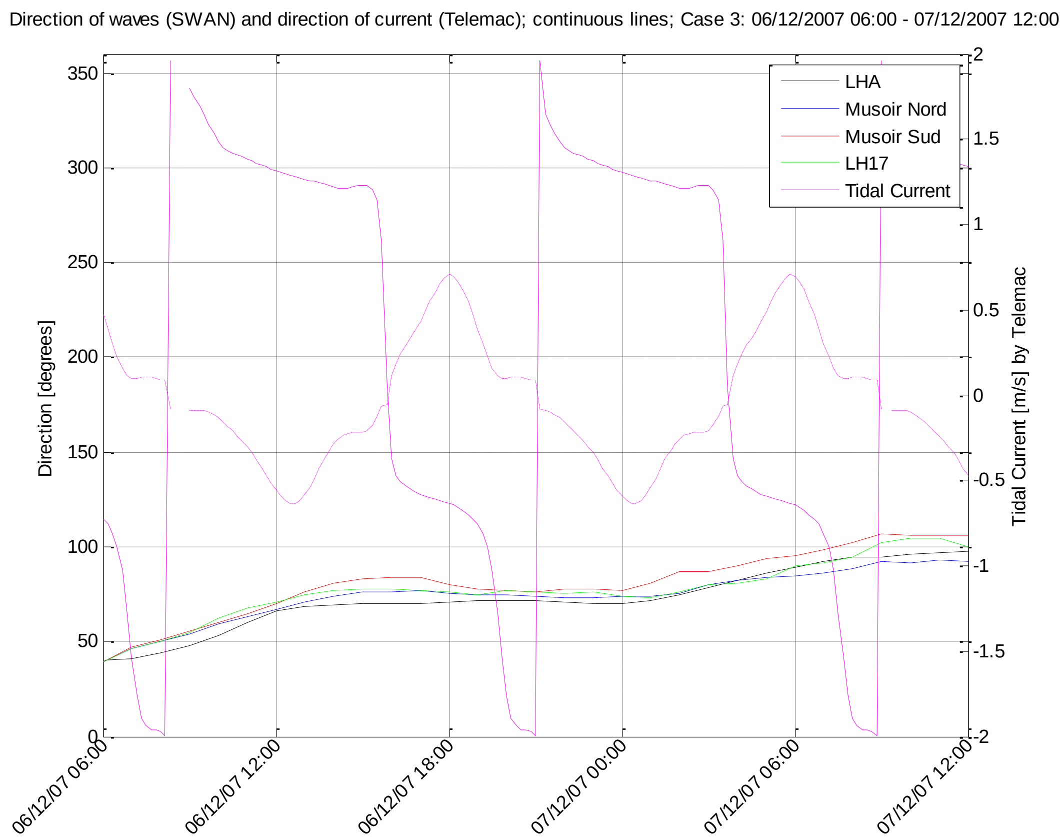

Figure 30: Direction of waves (SWAN) and current (Telemac); case 3.

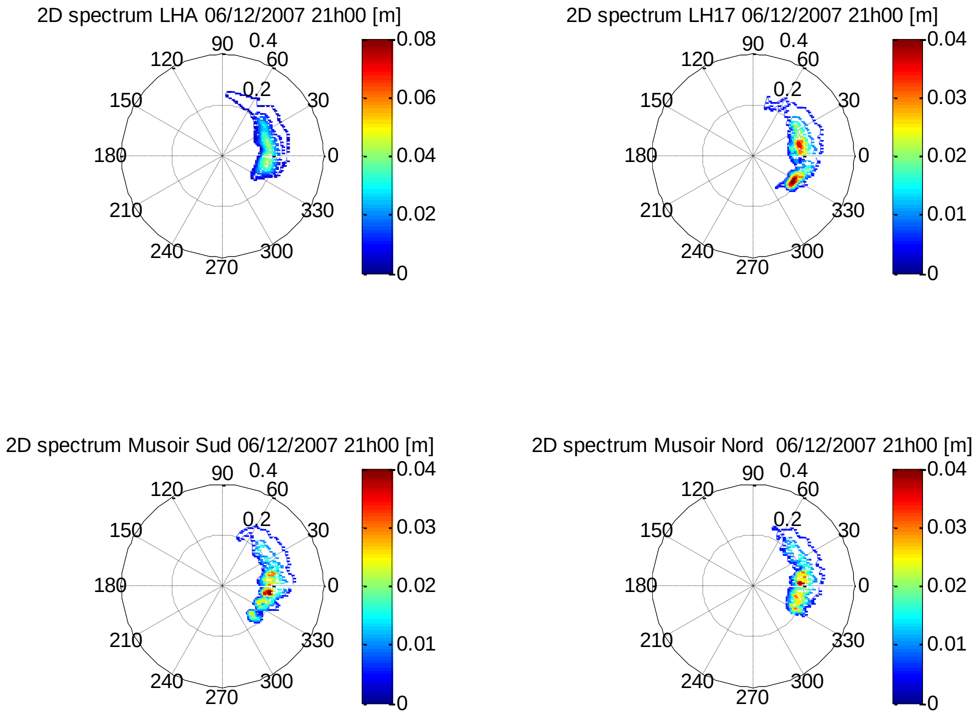

Figure 31: 2D variance density spectra for LHA, LH17, Musoir Sud and Musoir Nord; 06/12/2007; 21h00.

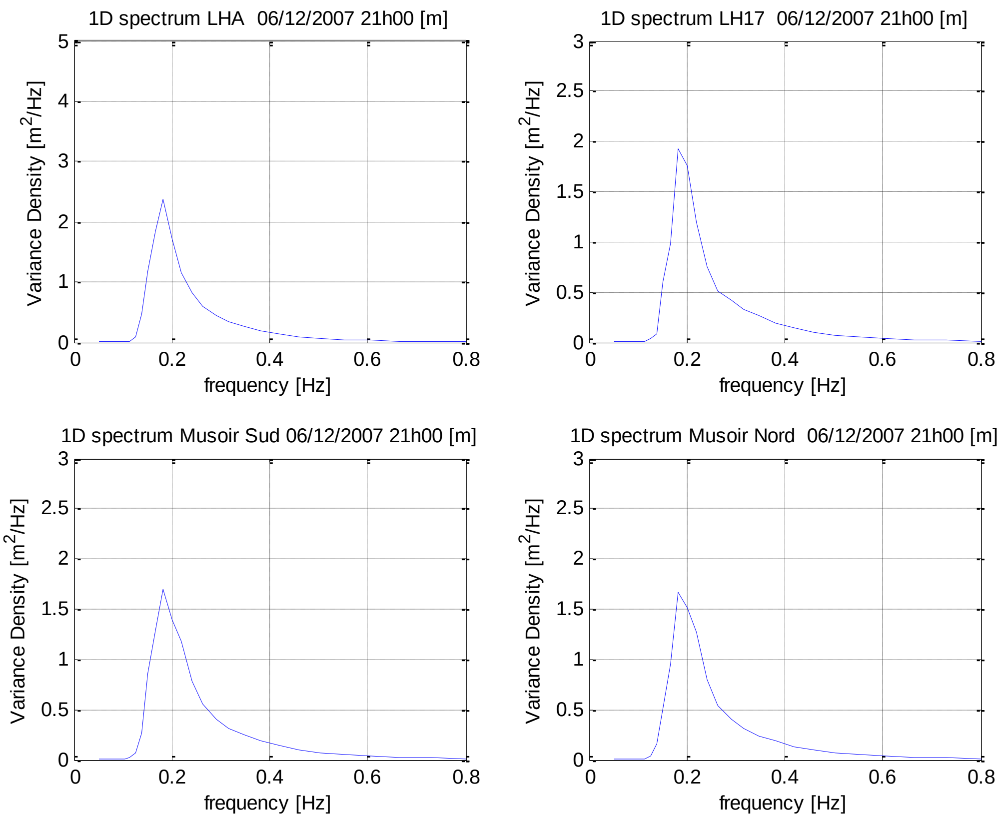

Figure 32: 1D variance density spectra for LHA, LH17, Musoir Sud and Musoir Nord; 06/12/2007; 21h00.

6 Conclusions

The calculation of significant wave height by SWAN in generation 3 gives more accurate results than in generation 2. For the three off-shore placed buoys, SWAN generation 3 gives well comparable results to the measured results. Generation 2 underestimates the significant wave height somewhat.

The calculation of the mean wave period is always largely underestimated by SWAN, for both generations. This is a known problem and also widely described in literature.

While SWAN generation 3 gives good results for the off-shore placed buoys, coming towards the near-shore, results do not match with the measurements by the buoys. Tidal influence is little to not visible in SWAN and the near shore modelled results tent to follow the off-shore results.

It looks like the bathymetry in the head of the River Seine is too complicated for SWAN to proper model results. Besides the problem of the bathymetry, also too much processes play a role in the head of the River Seine, which are not all incorporated into the model. One of the ideas where the problem might be lying is in the constant wave breaking parameter γ.

From the study case on case 3 it can however be concluded that the modelling of refraction or total reflection over an access channel is properly done by SWAN.

7 References

Brevik, I., Aas, B., 1979, Flume experiments on waves and currents I. Rippled bed, Coastal Engineering 3, 149-177

Brevik, I., 1980, Flume experiments on waves and currents II. Smooth bed, Coastal Engineering 4, 89-110

Bottema, M., Beyer, D., 2001, Evaluation of the SWAN model for the Dutch IJsselmeer area, Ocean wave measurement and analysis, 580-589

Gorman, R.M., Neilson, C.G., 1999, Modelling shallow water wave wave generation and transformation in an intertidal estuary, Coastal Engineering 36, 197-217

Holthuijsen, L.H., 2007, Waves in Oceanic and Coastal Waters, Cambridge University Press

Jonsson, I.G., 1990, Wave-current interactions. In: B. Le Mehauté and D.M. Hanes (eds), The Sea, vol.9A, Wiley-Interscience, New York, 65-120

Magne, R., Ardhuin, F., Roland, A., (2010 in submitting), Prévisions et rejeux des états de mer du globe à la plage, European Journal of Environmental and Civil Engineering (in french)

Ruessink, B.G., Miles, J.R., Feddersen, F., Guza, R.T., Elgar, S., 2001, Modelling the alongshore current on barred beaches, Journal of Geophysical Research 106, 22451-22463

Ruessink, B.G., Walstra, D.J.R., Southgate, H.N., 2003, Calibration and verification of a parametric wave model on barred beaches, Coastal Engineering 48, 139-149

Soulsby, R.L., Hamm, L., Klopman, G., Myrhaug, D., Simons, R.R., Thomas, G.P., 1993, Wave-current interaction within and outside the bottom boundary layer, Coastal Engineering, 21, 41-69

SWAN team, 2009, SWAN user manual, Delft University of Technology, 125 pp.

SWAN team, 2009, SWAN scientific and technical documentation SWAN cycle III version 40.72 ABCDE, Delft University of Technology, website

Used websites:

- www.wikipedia.org
    - Le Havre
    - Seine

- http://www.havre-port.net/pahweb.html

- http://hist-geo.ac-rouen.fr/site/IMG/jpg/EcluseFluvialePort2000_petiteimage.jpg

Appendix A: SWAN settings storm runs off-shore

case:	1.1	1.2	2.1	2.2	3.1	3.2	4.1	4.2	5.1	5.2
storm:	Jan I	Jan I	8	8	3.2	3.2	3.1	3.1	Jan III	Jan III
date:	6-9 jan. '08	6-9 jan. '08	9-13 mar. '08	9-13 mar. '08	5-8 dec. '07	5-8 dec. '07	30 n.-5 dec. '07	30 n.-5 dec. '07	17-21 jan. '08	17-21 jan. '08
SWAN generation:	GEN 2	GEN 3 (K)	GEN 2	GEN 3 (K)	GEN 2	GEN 3 (K)	GEN 2	GEN 3 (K)	GEN 2	GEN 3 (K)
nonstationary:	yes	yes	yes	yes	yes	yes	yes	yes	yes	yes
max. no. iterations:	5	5	5	5	5	5	5	5	5	5
delta t:	1 hour	1 hour	1 hour	1 hour	1 hour	1 hour	1 hour	1 hour	1 hour	1 hour
nx:	136	136	136	136	136	136	136	136	136	136
delta x:	1000 m.	1000 m.	1000 m.	1000 m.	1000 m.	1000 m.	1000 m.	1000 m.	1000 m.	1000 m.
ny:	67	67	67	67	67	67	67	67	67	67
delta y:	1000 m.	1000 m.	1000 m.	1000 m.	1000 m.	1000 m.	1000 m.	1000 m.	1000 m.	1000 m.
n theta:	144	144	144	144	144	144	144	144	144	144
delta theta:	2.5 degrees	2.5 degrees	2.5 degrees	2.5 degrees	2.5 degrees	2.5 degrees	2.5 degrees	2.5 degrees	2.5 degrees	2.5 degrees
n sigma:	30	30	30	30	30	30	30	30	30	30
sigma low:	0.05 Hz	0.05 Hz	0.05 Hz	0.05 Hz	0.05 Hz	0.05 Hz	0.05 Hz	0.05 Hz	0.05 Hz	0.05 Hz
sigma high:	0.8 Hz	0.8 Hz	0.8 Hz	0.8 Hz	0.8 Hz	0.8 Hz	0.8 Hz	0.8 Hz	0.8 Hz	0.8 Hz
wind forcing:	2 buoys +20%	2 buoys +20%	2 buoys	2 buoys	2 buoys	2 buoys	2 buoys	2 buoys	2 buoys	2 buoys
boundary forcing:	No	No	No	No	No	No	No	No	No	No
initial condition:	Rest	Rest	Rest	Rest	Rest	Rest	Rest	Rest	Rest	Rest
bottom friction:	off	off	off	off	off	off	off	off	off	off
triads:	off	on	off	on	off	on	off	on	off	on
quadruplets:	off	on	off	on	off	on	off	on	off	on
whitecapping:	on	on	on	on	on	on	on	on	on	on

variations:		
max. no. iterations:	1	3
grid size:	500x500	2000x2000
computational scheme:	BSBT scheme	
bottom friction:	on	

Appendix B: SWAN settings storm runs new bathymetry

For the settings of the runs on the 1000 by 1000 metres grid is referred to appendix A, runs in generation 3. Hereunder follow the settings for the nested runs on the 100 by 100 and 20 by 20 metres runs.

case:	1, nested 100	1, nested 20	2, nested 100	2, nested 20	3, nested 100	3, nested 20	4, nested 100	4, nested 20	5, nested 100	5, nested 20
storm:	Jan I	Jan I	8	8	3.2	3.2	3.1	3.1	Jan III	Jan III
date:	6-9 jan. '08	6-9 jan. '08	9-13 mar. '08	9-13 mar. '08	5-8 dec. '07	5-8 dec. '07	30 n.-5 dec. '07	30 n.-5 dec. '07	17-21 jan. '08	17-21 jan. '08
SWAN generation:	GEN 3 (K)	GEN 3 (K)	GEN 3 (K)	GEN 3 (K)	GEN 3 (K)	GEN 3 (K)	GEN 3 (K)	GEN 3 (K)	GEN 3 (K)	GEN 3 (K)
nonstationary:	yes	yes	yes	yes	yes	yes	yes	yes	yes	yes
max. no. iterations:	5	5	5	5	5	5	5	5	5	5
delta t:	1 hour	1 hour	1 hour	1 hour	1 hour	1 hour	1 hour	1 hour	1 hour	1 hour
nx:	160	130	160	130	160	130	160	130	160	130
delta x:	100 m.	20 m.	100 m.	20 m.	100 m.	20 m.	100 m.	20 m.	100 m.	20 m.
ny:	160	130	160	130	160	130	160	130	160	130
delta y:	100 m.	20 m.	100 m.	20 m.	100 m.	20 m.	100 m.	20 m.	100 m.	20 m.
n theta:	144	144	144	144	144	144	144	144	144	144
delta theta:	2.5 degrees	2.5 degrees	2.5 degrees	2.5 degrees	2.5 degrees	2.5 degrees	2.5 degrees	2.5 degrees	2.5 degrees	2.5 degrees
n sigma:	30	30	30	30	30	30	30	30	30	30
sigma low:	0.05 Hz	0.05 Hz	0.05 Hz	0.05 Hz	0.05 Hz	0.05 Hz	0.05 Hz	0.05 Hz	0.05 Hz	0.05 Hz
sigma high:	0.8 Hz	0.8 Hz	0.8 Hz	0.8 Hz	0.8 Hz	0.8 Hz	0.8 Hz	0.8 Hz	0.8 Hz	0.8 Hz
wind forcing:	2 buoys +20%	2 buoys +20%	2 buoys	2 buoys	2 buoys	2 buoys	2 buoys	2 buoys	2 buoys	2 buoys
boundary forcing:	RUN 1000	RUN 100	RUN 1000	RUN 100	RUN 1000	RUN 100	RUN 1000	RUN 100	RUN 1000	RUN 100
initial condition:	Rest	Rest	Rest	Rest	Rest	Rest	Rest	Rest	Rest	Rest
bottom friction:	off	off	off	off	off	off	off	off	off	off
triads:	off	on	off	on	off	on	off	on	off	on
quadruplets:	off	on	off	on	off	on	off	on	off	on
whitecapping:	on	on	on	on	on	on	on	on	on	on

Appendix C: Wave parameters storm cases

Case 1

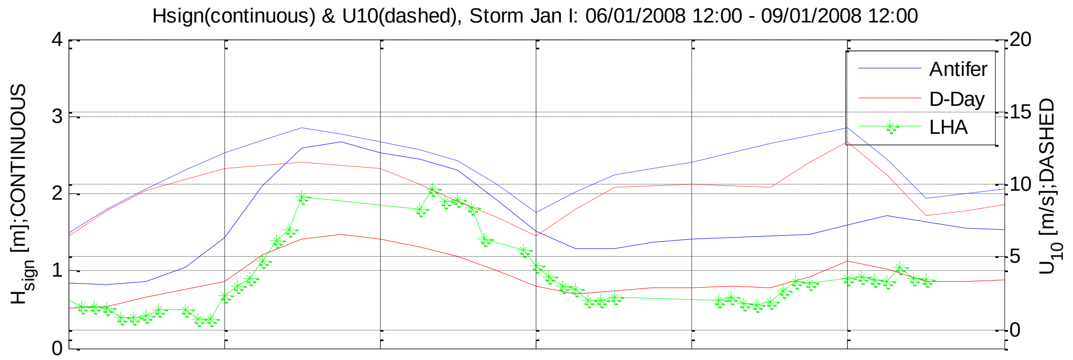

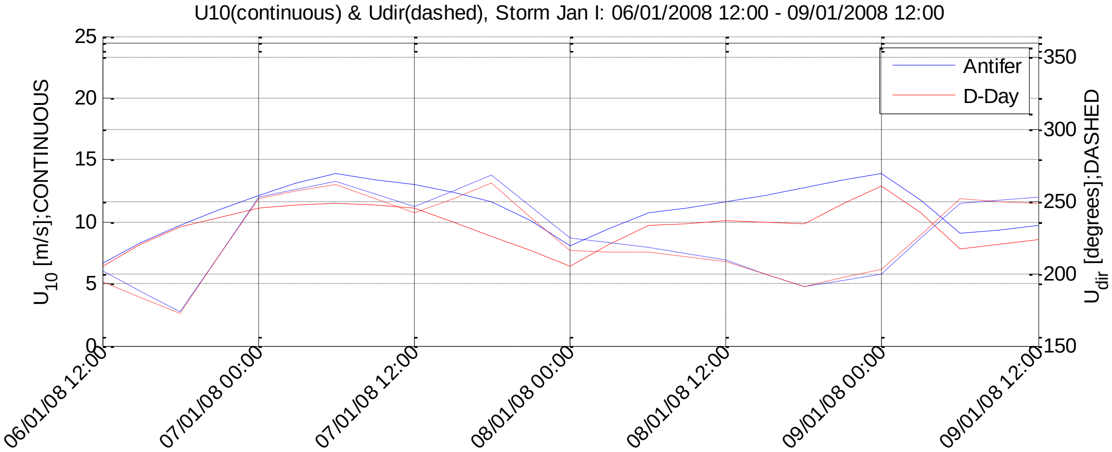

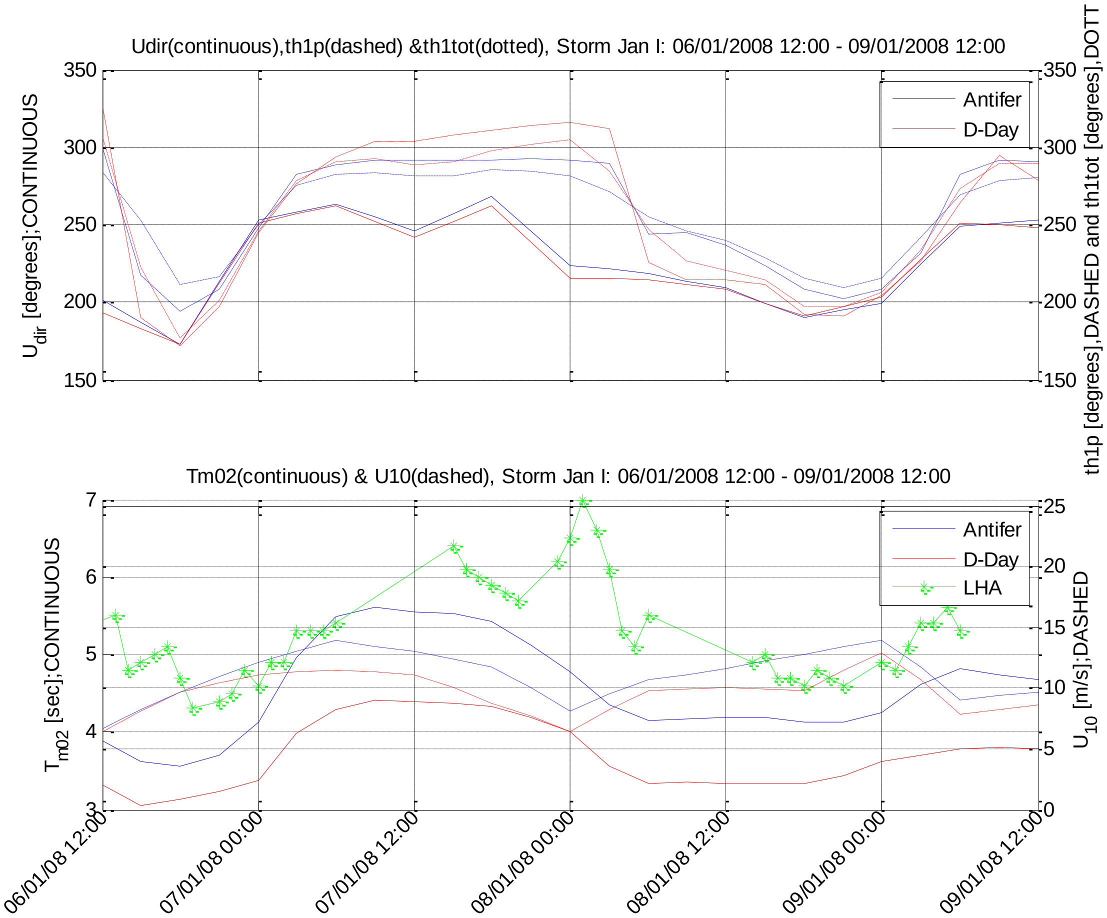
Udir(continuous),th1p(dashed) &th1tot(dotted), Storm Jan I: 06/01/2008 12:00 - 09/01/2008 12:00
U_dir [degrees];CONTINUOUS
th1p [degrees],DASHED and th1tot [degrees],DOTT
Antifer
D-Day
Tm02(continuous) & U10(dashed), Storm Jan I: 06/01/2008 12:00 - 09/01/2008 12:00
T_m02 [sec];CONTINUOUS
U_10 [m/s];DASHED
Antifer
D-Day
LHA
06/01/08 12:00
07/01/08 00:00
07/01/08 12:00
08/01/08 00:00
08/01/08 12:00
09/01/08 00:00
09/01/08 12:00

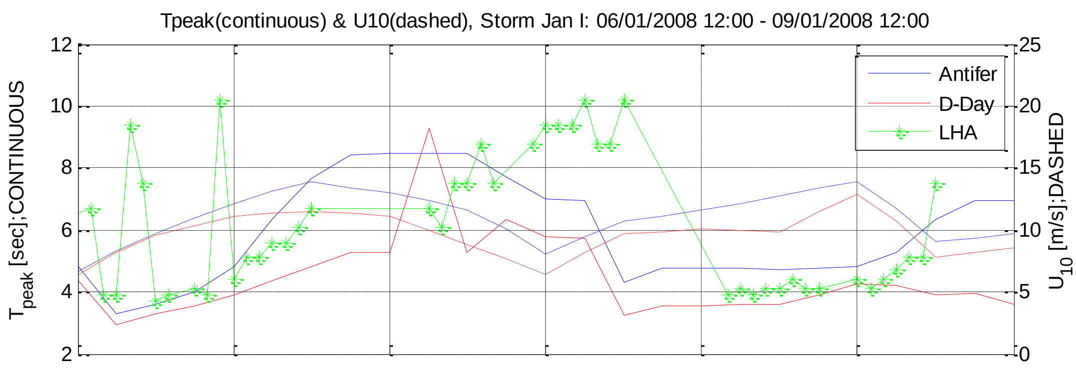

Tpeak(continuous) & U10(dashed), Storm Jan I: 06/01/2008 12:00 - 09/01/2008 12:00
T_peak [sec];CONTINUOUS
U_10 [m/s];DASHED
Antifer
D-Day
LHA
12
10
8
6
4
2
25
20
15
10
5
0

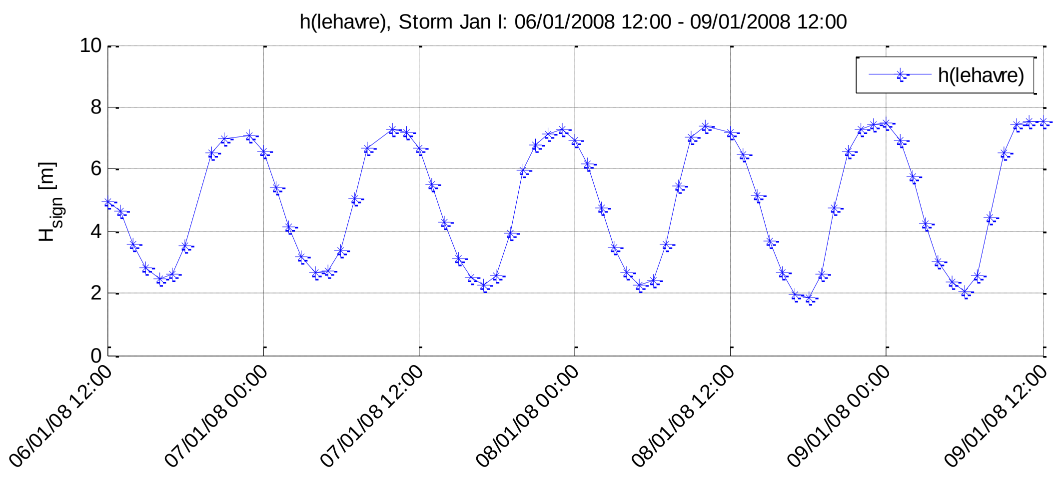

h(lehavre), Storm Jan I: 06/01/2008 12:00 - 09/01/2008 12:00
H_sign [m]
h(lehavre)
10
8
6
4
2
0
06/01/08 12:00
07/01/08 00:00
07/01/08 12:00
08/01/08 00:00
08/01/08 12:00
09/01/08 00:00
09/01/08 12:00

Case 2.

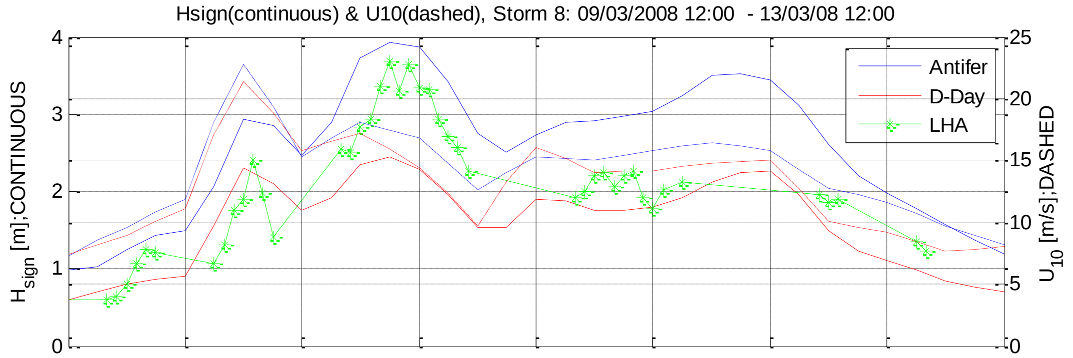
Hsign(continuous) & U10(dashed), Storm 8: 09/03/2008 12:00 - 13/03/08 12:00
H_sign [m];CONTINUOUS
U_10 [m/s];DASHED
Antifer
D-Day
LHA

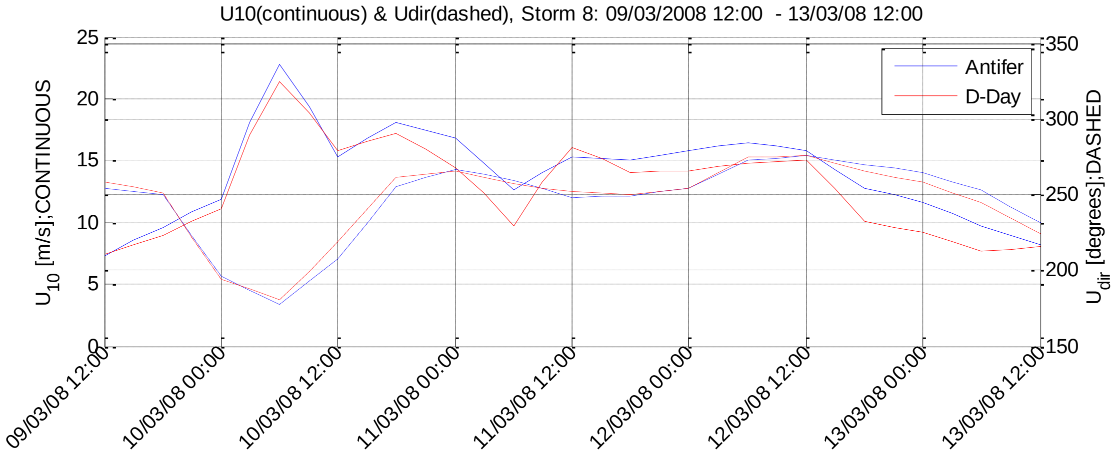
U10(continuous) & Udir(dashed), Storm 8: 09/03/2008 12:00 - 13/03/08 12:00
U_10 [m/s];CONTINUOUS
U_dir [degrees];DASHED
Antifer
D-Day
09/03/08 12:00
10/03/08 00:00
10/03/08 12:00
11/03/08 00:00
11/03/08 12:00
12/03/08 00:00
12/03/08 12:00
13/03/08 00:00
13/03/08 12:00

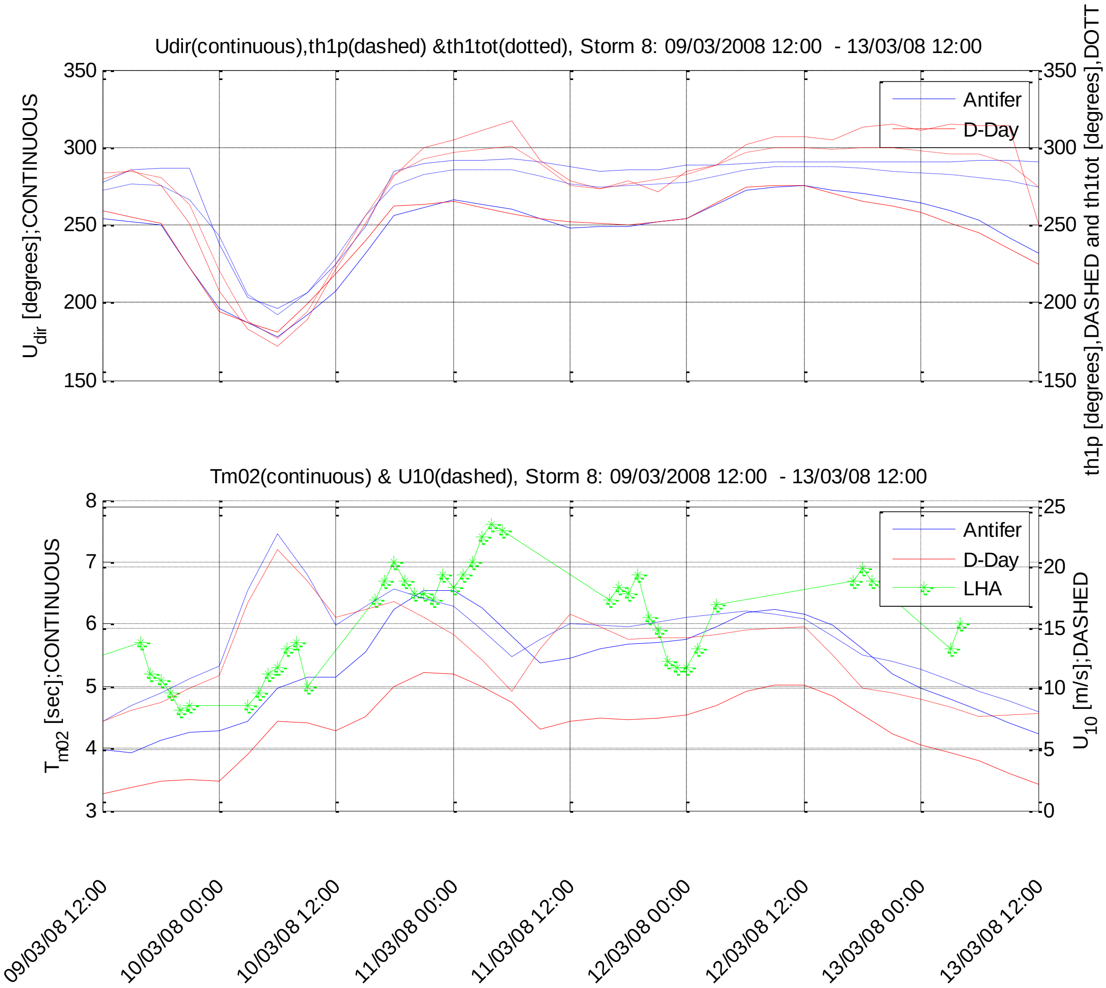
Udir(continuous),th1p(dashed) &th1tot(dotted), Storm 8: 09/03/2008 12:00 - 13/03/08 12:00
U_dir [degrees];CONTINUOUS
th1p [degrees],DASHED and th1tot [degrees],DOTT
Antifer
D-Day
Tm02(continuous) & U10(dashed), Storm 8: 09/03/2008 12:00 - 13/03/08 12:00
T_m02 [sec];CONTINUOUS
U_10 [m/s];DASHED
LHA
09/03/08 12:00
10/03/08 00:00
10/03/08 12:00
11/03/08 00:00
11/03/08 12:00
12/03/08 00:00
12/03/08 12:00
13/03/08 00:00
13/03/08 12:00

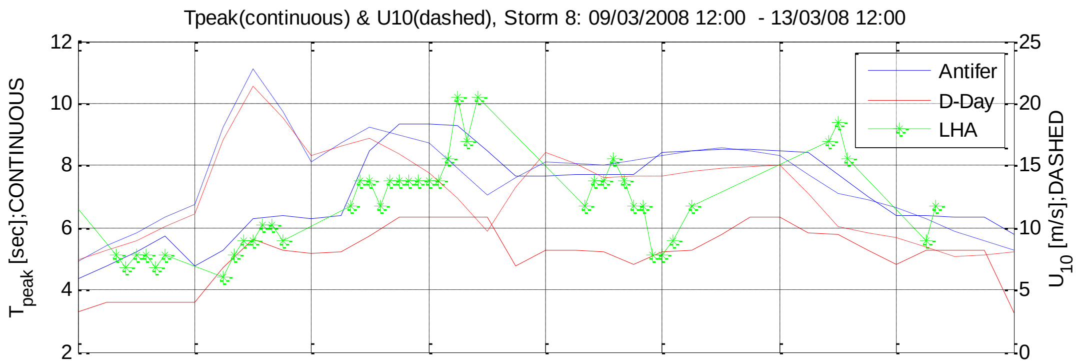
Tpeak(continuous) & U10(dashed), Storm 8: 09/03/2008 12:00 - 13/03/08 12:00
T_peak [sec];CONTINUOUS
U_10 [m/s];DASHED
Antifer
D-Day
LHA
12
10
8
6
4
2
25
20
15
10
5
0

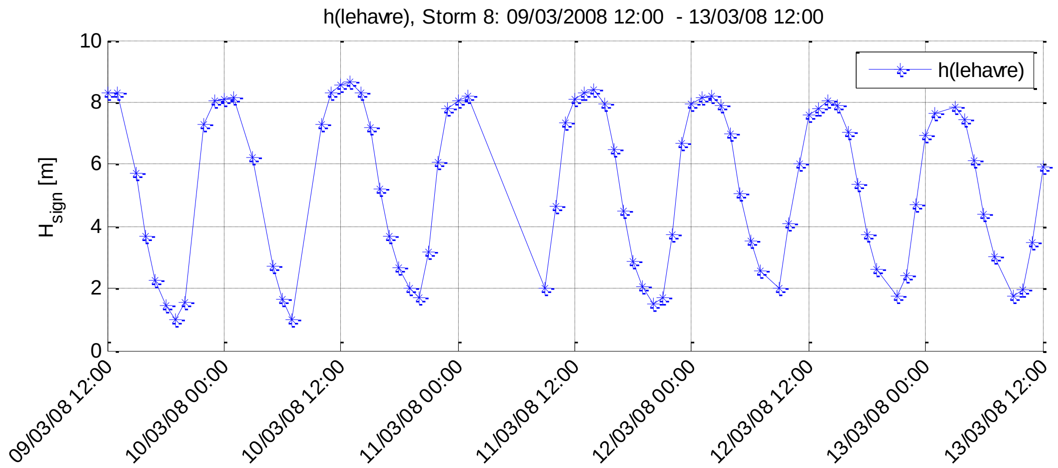
h(lehavre), Storm 8: 09/03/2008 12:00 - 13/03/08 12:00
H_sign [m]
h(lehavre)
10
8
6
4
2
0
09/03/08 12:00
10/03/08 00:00
10/03/08 12:00
11/03/08 00:00
11/03/08 12:00
12/03/08 00:00
12/03/08 12:00
13/03/08 00:00
13/03/08 12:00

Case 3.

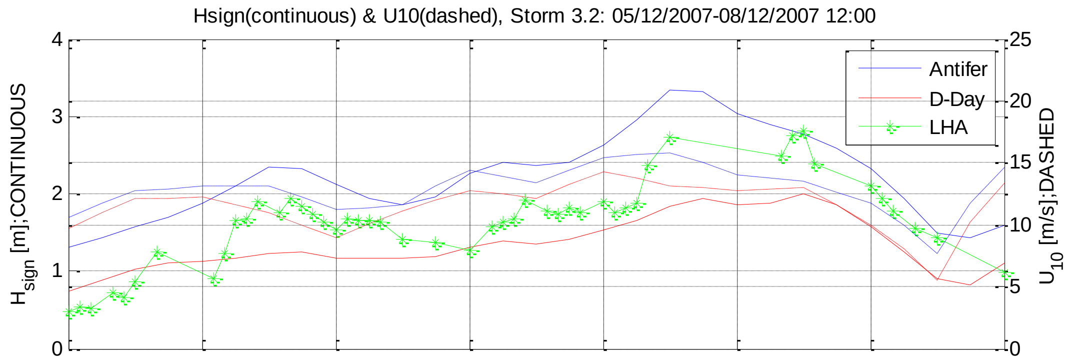

Hsign(continuous) & U10(dashed), Storm 3.2: 05/12/2007-08/12/2007 12:00
Antifer
D-Day
LHA
Hsign [m];CONTINUOUS
U10 [m/s];DASHED

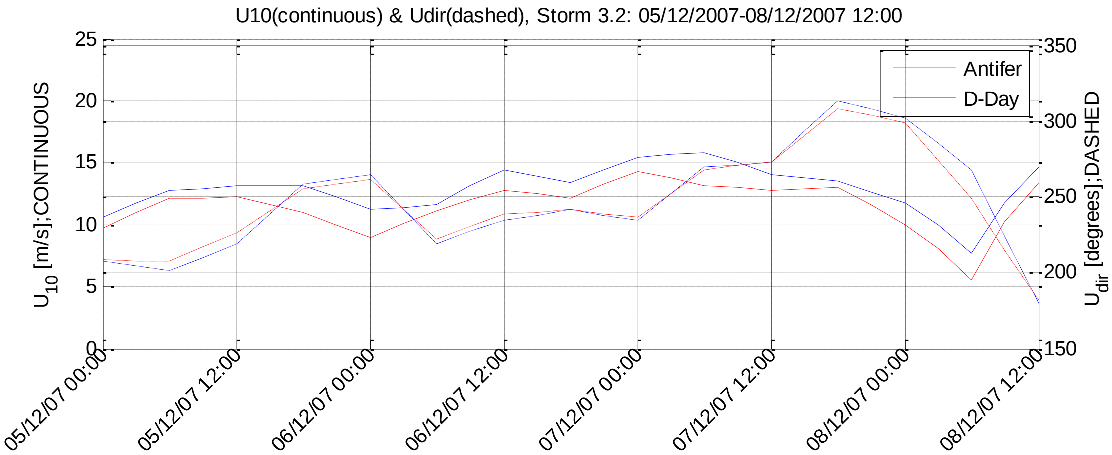

U10(continuous) & Udir(dashed), Storm 3.2: 05/12/2007-08/12/2007 12:00
Antifer
D-Day
U10 [m/s];CONTINUOUS
Udir [degrees];DASHED
05/12/07 00:00
05/12/07 12:00
06/12/07 00:00
06/12/07 12:00
07/12/07 00:00
07/12/07 12:00
08/12/07 00:00
08/12/07 12:00

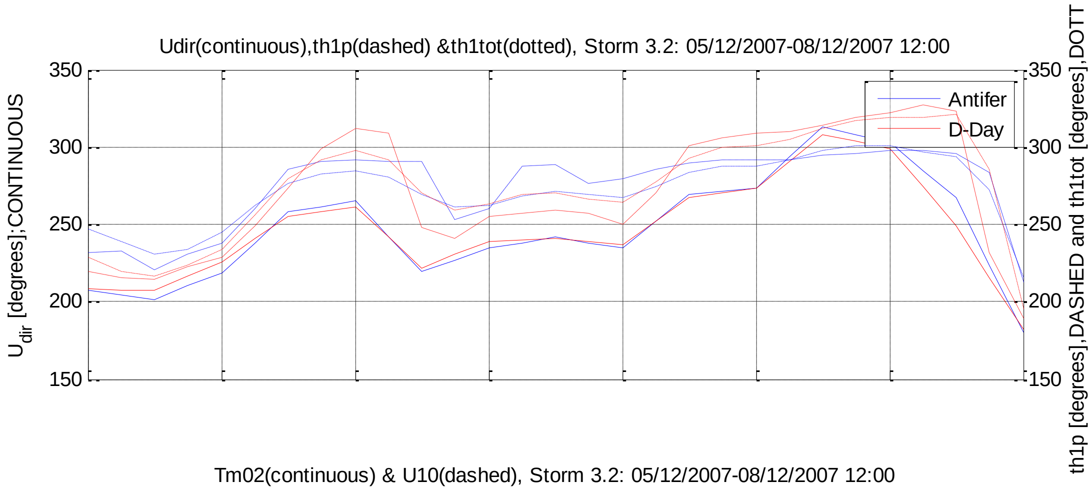

Udir(continuous),th1p(dashed) &th1tot(dotted), Storm 3.2: 05/12/2007-08/12/2007 12:00
U_dir [degrees];CONTINUOUS
th1p [degrees],DASHED and th1tot [degrees],DOTT
Antifer
D-Day

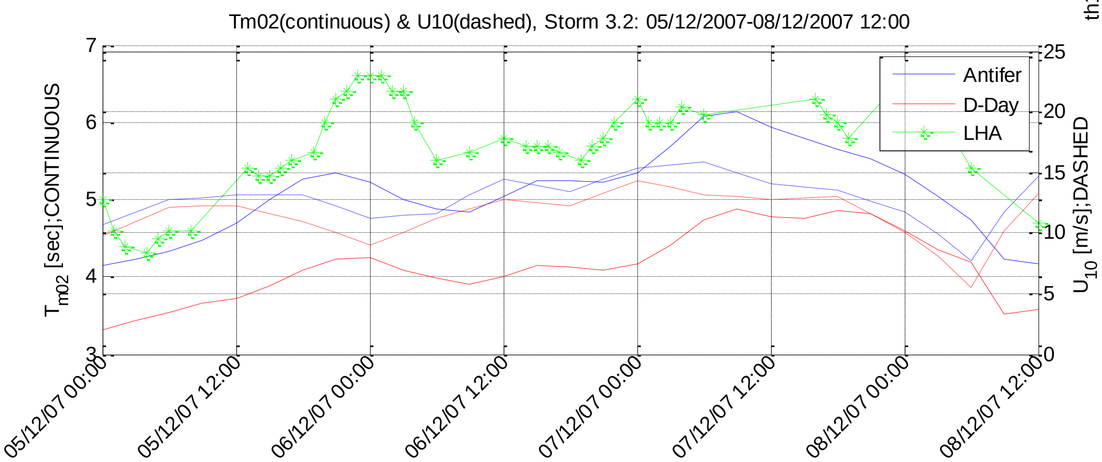

Tm02(continuous) & U10(dashed), Storm 3.2: 05/12/2007-08/12/2007 12:00
T_m02 [sec];CONTINUOUS
U_10 [m/s];DASHED
Antifer
D-Day
LHA
05/12/07 00:00
05/12/07 12:00
06/12/07 00:00
06/12/07 12:00
07/12/07 00:00
07/12/07 12:00
08/12/07 00:00
08/12/07 12:00

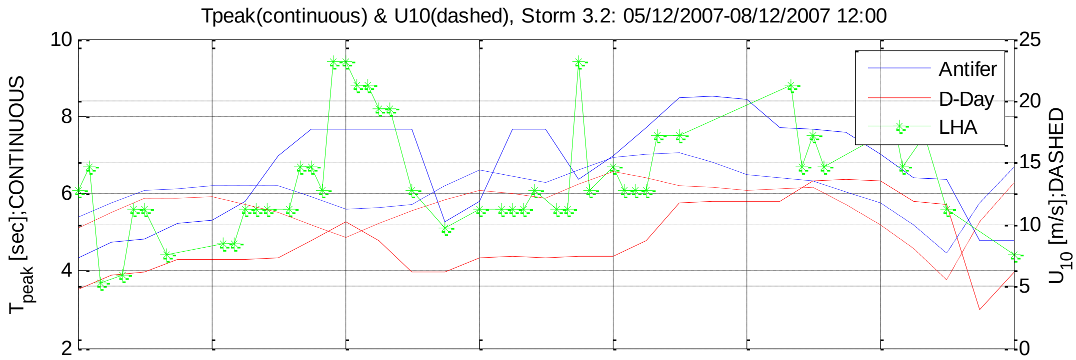
Tpeak(continuous) & U10(dashed), Storm 3.2: 05/12/2007-08/12/2007 12:00
Antifer
D-Day
LHA
Tpeak [sec];CONTINUOUS
U10 [m/s];DASHED

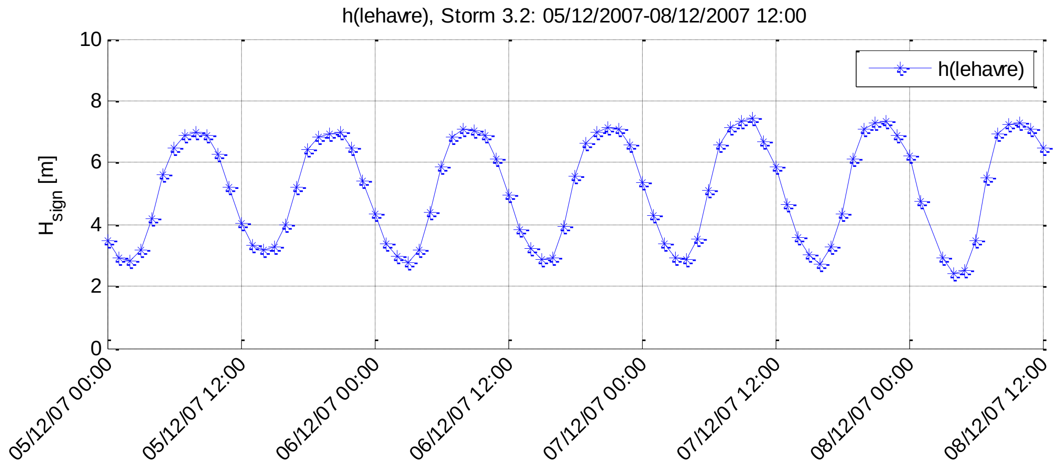
h(lehavre), Storm 3.2: 05/12/2007-08/12/2007 12:00
h(lehavre)
Hsign [m]
05/12/07 00:00
05/12/07 12:00
06/12/07 00:00
06/12/07 12:00
07/12/07 00:00
07/12/07 12:00
08/12/07 00:00
08/12/07 12:00

Case 4.

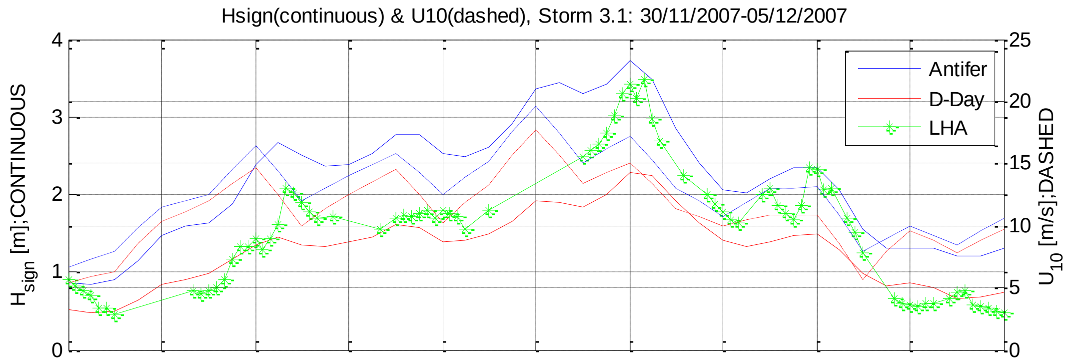
Hsign(continuous) & U10(dashed), Storm 3.1: 30/11/2007-05/12/2007
H_sign [m];CONTINUOUS
U_10 [m/s];DASHED
Antifer
D-Day
LHA
0
1
2
3
4
0
5
10
15
20
25

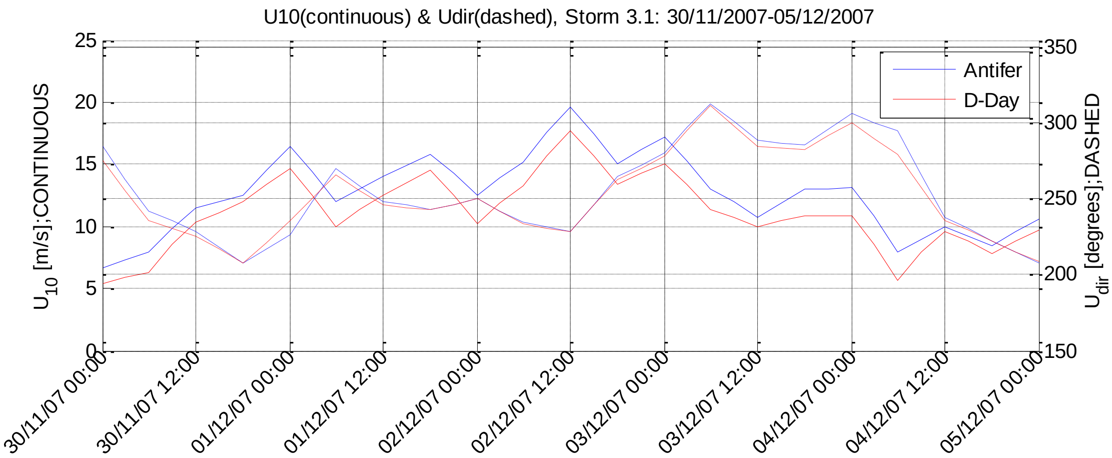
U10(continuous) & Udir(dashed), Storm 3.1: 30/11/2007-05/12/2007
U_10 [m/s];CONTINUOUS
U_dir [degrees];DASHED
Antifer
D-Day
0
5
10
15
20
25
150
200
250
300
350
30/11/07 00:00
30/11/07 12:00
01/12/07 00:00
01/12/07 12:00
02/12/07 00:00
02/12/07 12:00
03/12/07 00:00
03/12/07 12:00
04/12/07 00:00
04/12/07 12:00
05/12/07 00:00

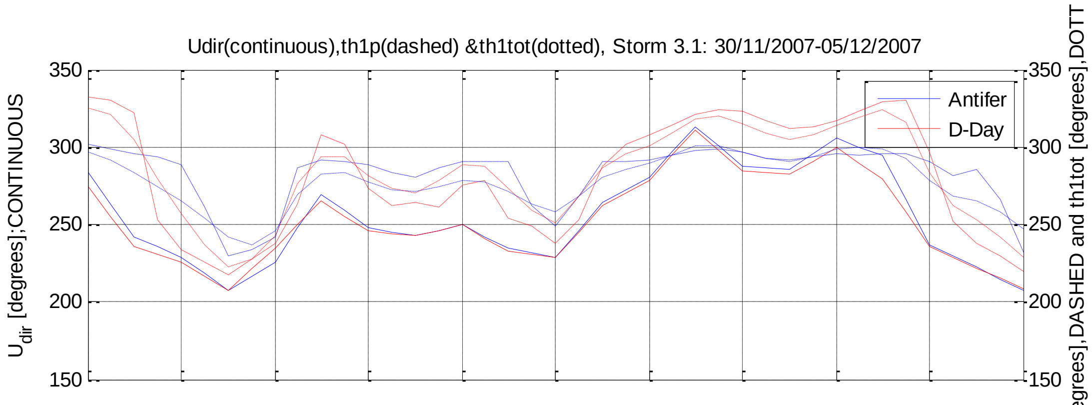
Udir(continuous),th1p(dashed) &th1tot(dotted), Storm 3.1: 30/11/2007-05/12/2007
U_dir [degrees];CONTINUOUS
th1p [degrees],DASHED and th1tot [degrees],DOTT
Antifer
D-Day
350
300
250
200
150

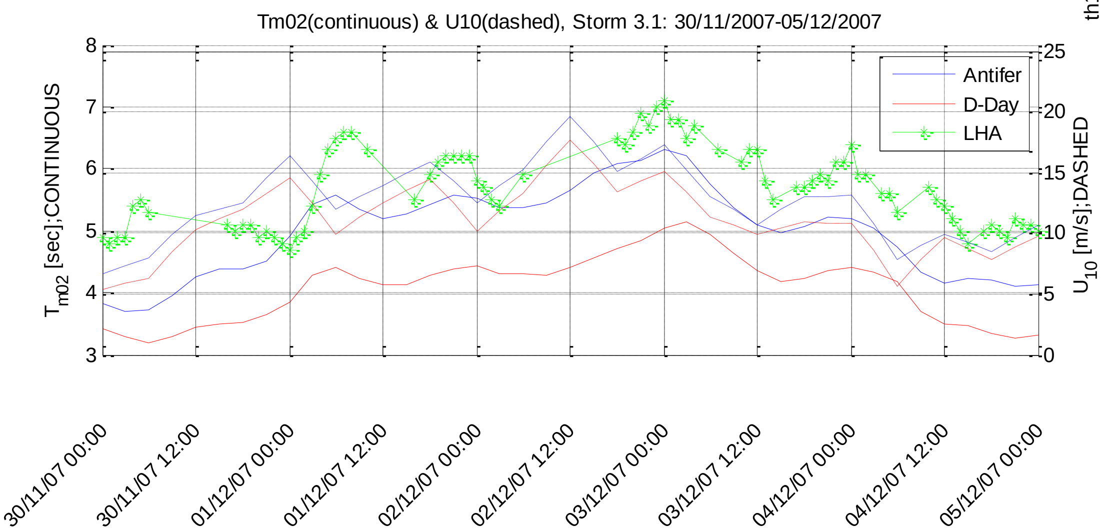
Tm02(continuous) & U10(dashed), Storm 3.1: 30/11/2007-05/12/2007
T_m02 [sec];CONTINUOUS
U_10 [m/s];DASHED
Antifer
D-Day
LHA
30/11/07 00:00
30/11/07 12:00
01/12/07 00:00
01/12/07 12:00
02/12/07 00:00
02/12/07 12:00
03/12/07 00:00
03/12/07 12:00
04/12/07 00:00
04/12/07 12:00
05/12/07 00:00

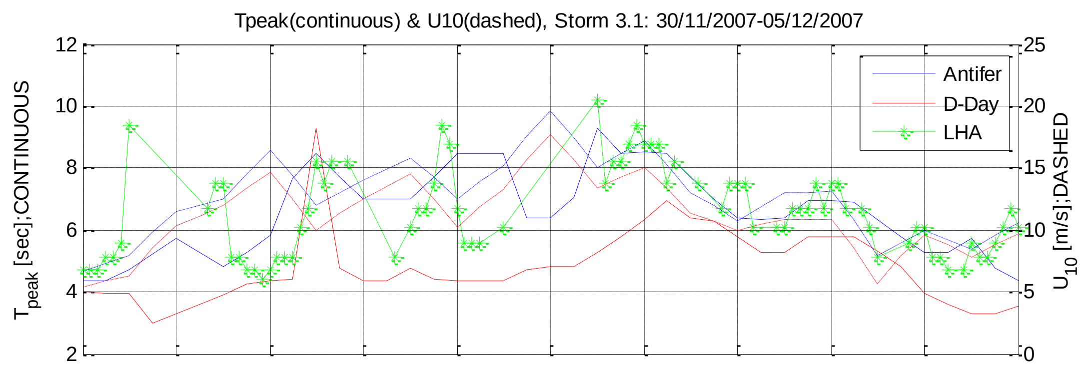

Tpeak(continuous) & U10(dashed), Storm 3.1: 30/11/2007-05/12/2007
Antifer
D-Day
LHA
T_peak [sec];CONTINUOUS
U_10 [m/s];DASHED

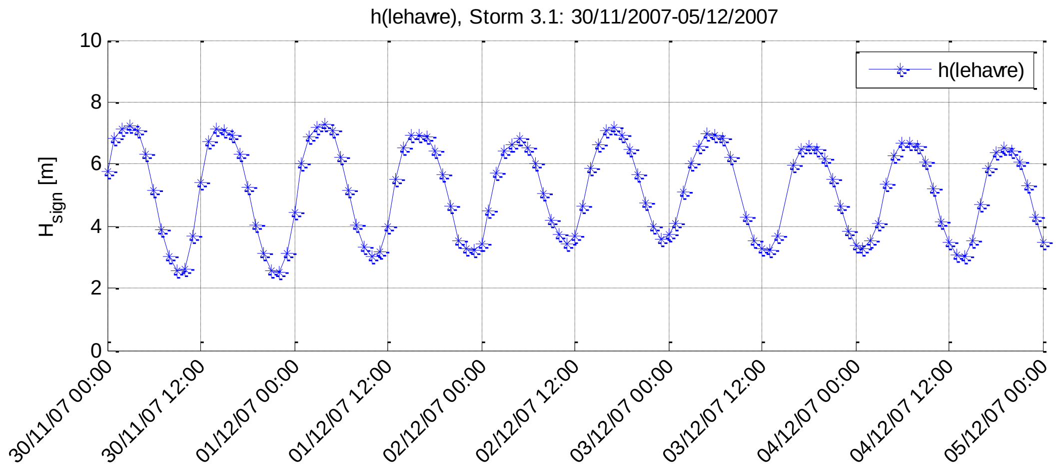

h(lehavre), Storm 3.1: 30/11/2007-05/12/2007
h(lehavre)
H_sign [m]
30/11/07 00:00
30/11/07 12:00
01/12/07 00:00
01/12/07 12:00
02/12/07 00:00
02/12/07 12:00
03/12/07 00:00
03/12/07 12:00
04/12/07 00:00
04/12/07 12:00
05/12/07 00:00

Case 5.

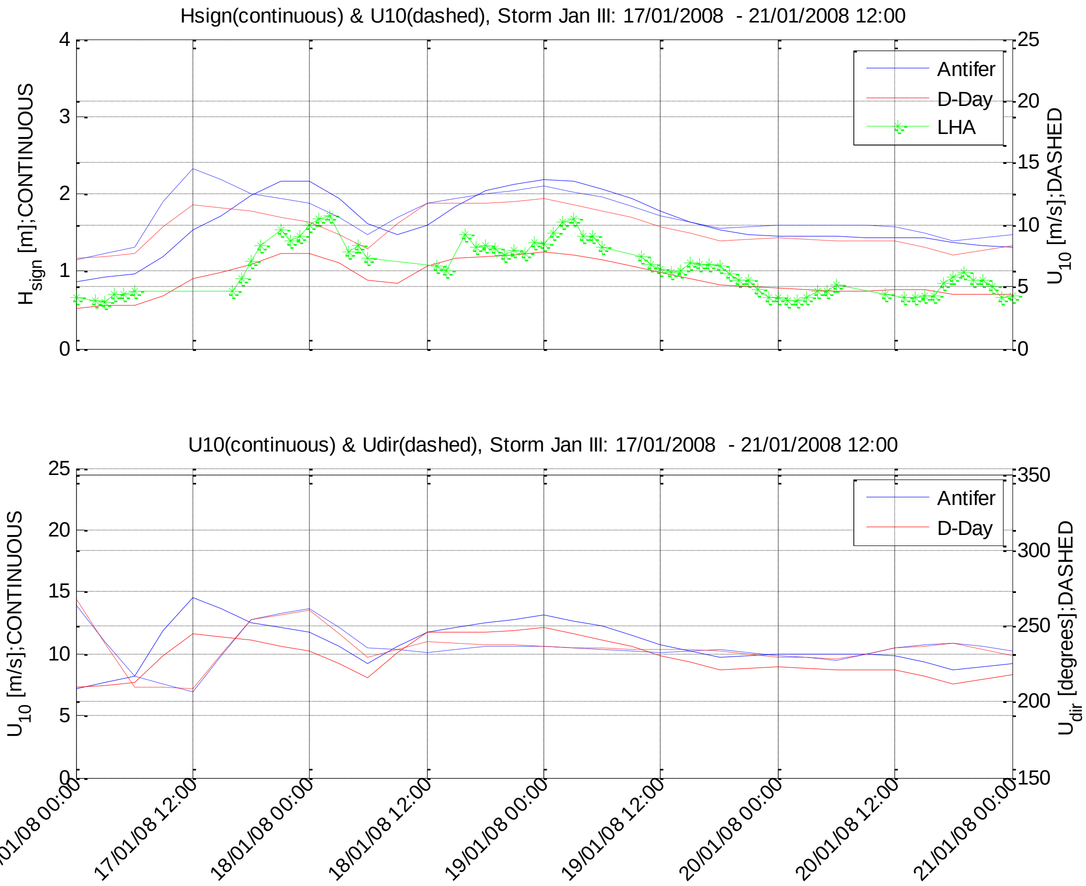

Hsign(continuous) & U10(dashed), Storm Jan III: 17/01/2008 - 21/01/2008 12:00
Antifer
D-Day
LHA
H_sign [m];CONTINUOUS
U_10 [m/s];DASHED
U10(continuous) & Udir(dashed), Storm Jan III: 17/01/2008 - 21/01/2008 12:00
Antifer
D-Day
U_10 [m/s];CONTINUOUS
U_dir [degrees];DASHED
17/01/08 00:00
17/01/08 12:00
18/01/08 00:00
18/01/08 12:00
19/01/08 00:00
19/01/08 12:00
20/01/08 00:00
20/01/08 12:00
21/01/08 00:00

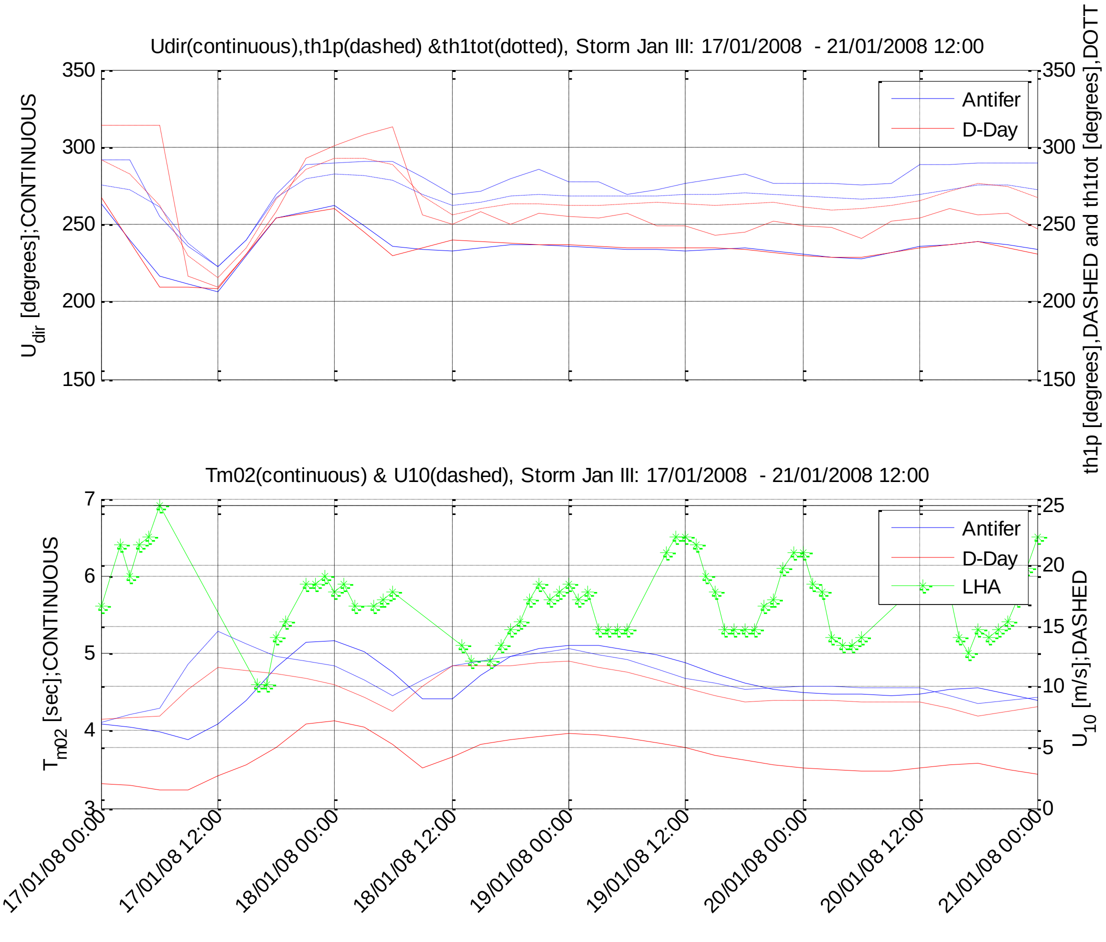
Udir(continuous),th1p(dashed) &th1tot(dotted), Storm Jan III: 17/01/2008 - 21/01/2008 12:00
U_{dir} [degrees];CONTINUOUS
th1p [degrees],DASHED and th1tot [degrees],DOTT
Antifer
D-Day
Tm02(continuous) & U10(dashed), Storm Jan III: 17/01/2008 - 21/01/2008 12:00
T_{m02} [sec];CONTINUOUS
U_{10} [m/s];DASHED
Antifer
D-Day
LHA
17/01/08 00:00
17/01/08 12:00
18/01/08 00:00
18/01/08 12:00
19/01/08 00:00
19/01/08 12:00
20/01/08 00:00
20/01/08 12:00
21/01/08 00:00

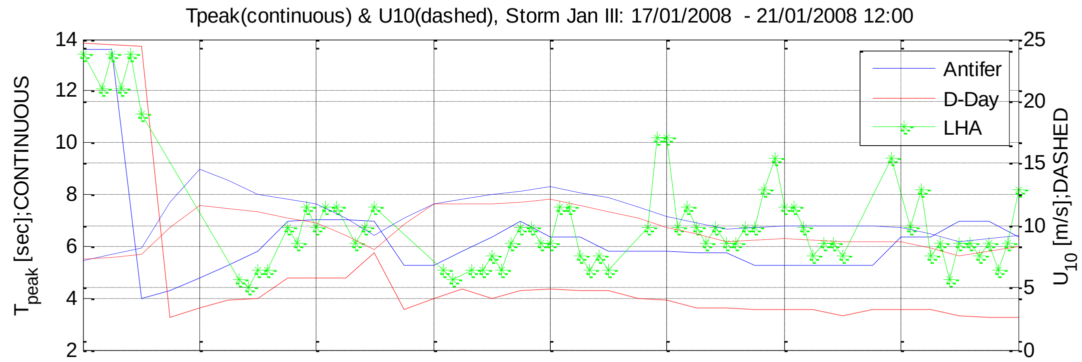
Tpeak(continuous) & U10(dashed), Storm Jan III: 17/01/2008 - 21/01/2008 12:00
T_peak [sec];CONTINUOUS
U_10 [m/s];DASHED
Antifer
D-Day
LHA

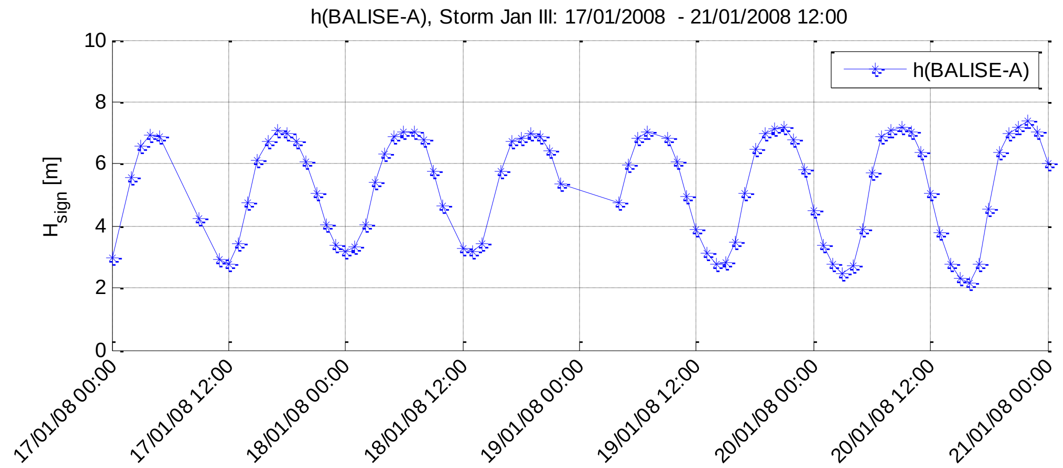
h(BALISE-A), Storm Jan III: 17/01/2008 - 21/01/2008 12:00
H_sign [m]
h(BALISE-A)
17/01/08 00:00
17/01/08 12:00
18/01/08 00:00
18/01/08 12:00
19/01/08 00:00
19/01/08 12:00
20/01/08 00:00
20/01/08 12:00
21/01/08 00:00

Appendix D: SWAN results storm cases off-shore

Case 1.1

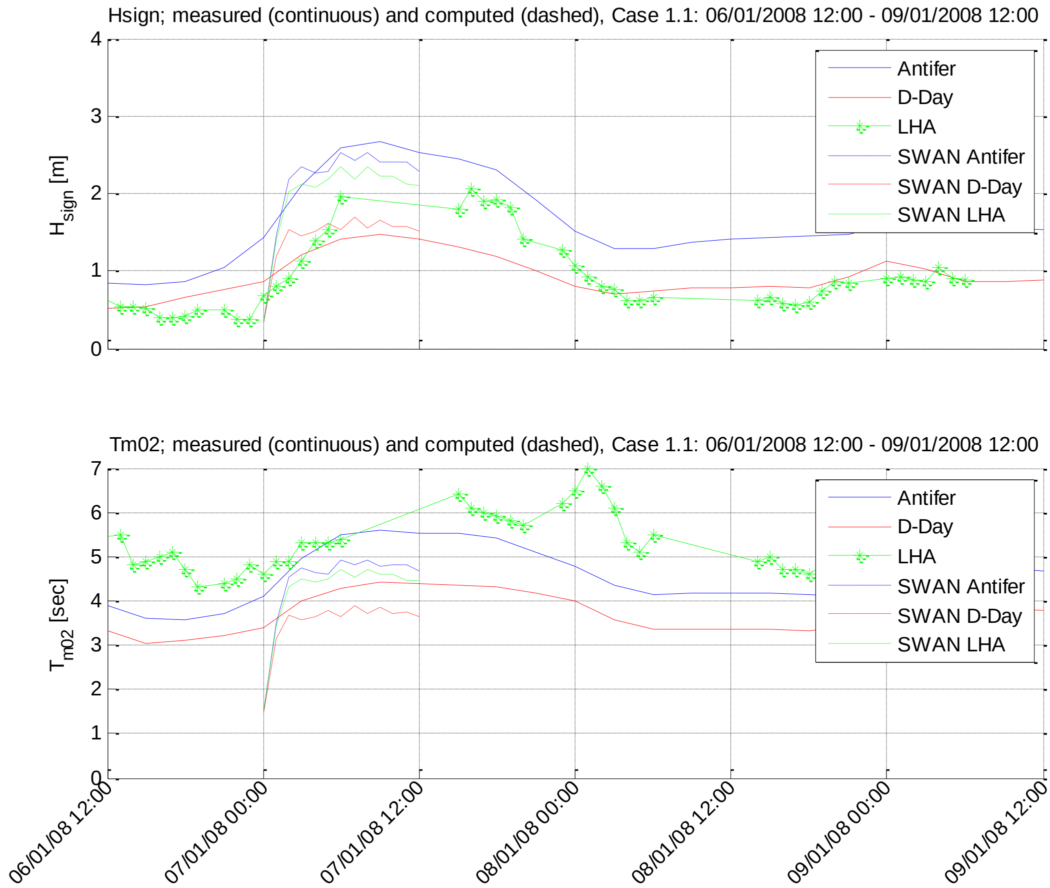


Tpeak; measured (continuous) and computed (dashed), Case 1.1: 06/01/2008 12:00 - 09/01/2008 12:00
12
10
8
6
4
2
0
T_{peak} [sec]
Antifer
D-Day
LHA
SWAN Antifer
SWAN D-Day
SWAN LHA

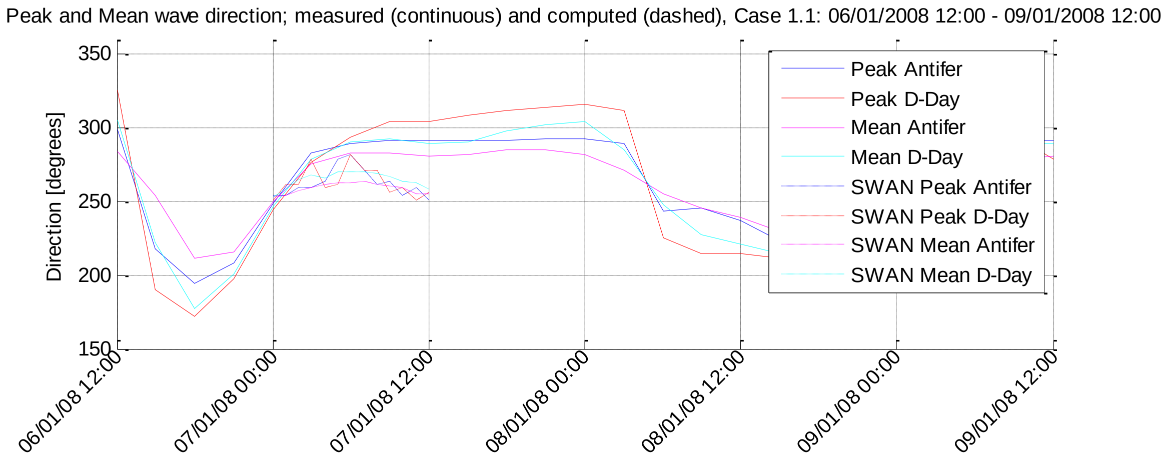
Peak and Mean wave direction; measured (continuous) and computed (dashed), Case 1.1: 06/01/2008 12:00 - 09/01/2008 12:00
350
300
250
200
150
Direction [degrees]
Peak Antifer
Peak D-Day
Mean Antifer
Mean D-Day
SWAN Peak Antifer
SWAN Peak D-Day
SWAN Mean Antifer
SWAN Mean D-Day
06/01/08 12:00
07/01/08 00:00
07/01/08 12:00
08/01/08 00:00
08/01/08 12:00
09/01/08 00:00
09/01/08 12:00

Case 1.2

Hsign; measured (continuous) and computed (dashed), Case 1.2: 06/01/2008 12:00 - 09/01/2008 12:00
H_sign [m]
Antifer
D-Day
LHA
SWAN Antifer
SWAN D-Day
SWAN LHA

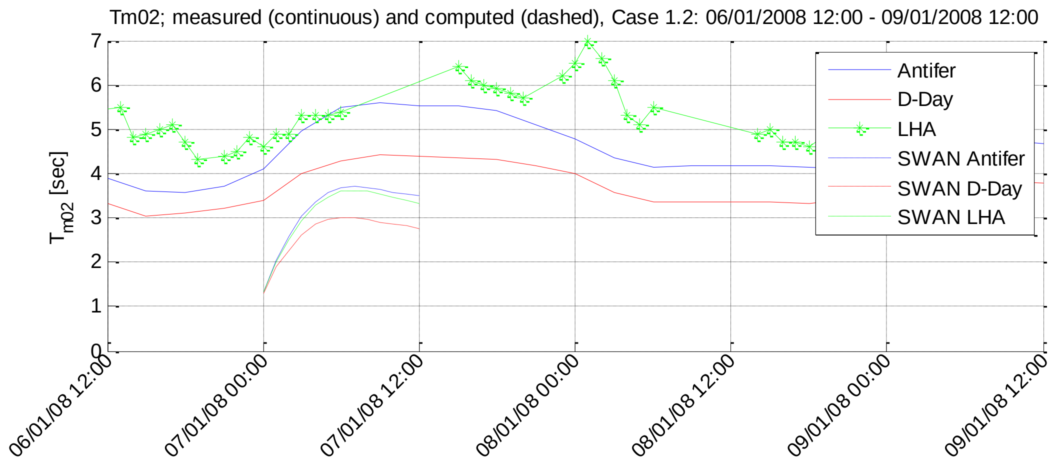

Tm02; measured (continuous) and computed (dashed), Case 1.2: 06/01/2008 12:00 - 09/01/2008 12:00
T_m02 [sec]
Antifer
D-Day
LHA
SWAN Antifer
SWAN D-Day
SWAN LHA
06/01/08 12:00
07/01/08 00:00
07/01/08 12:00
08/01/08 00:00
08/01/08 12:00
09/01/08 00:00
09/01/08 12:00

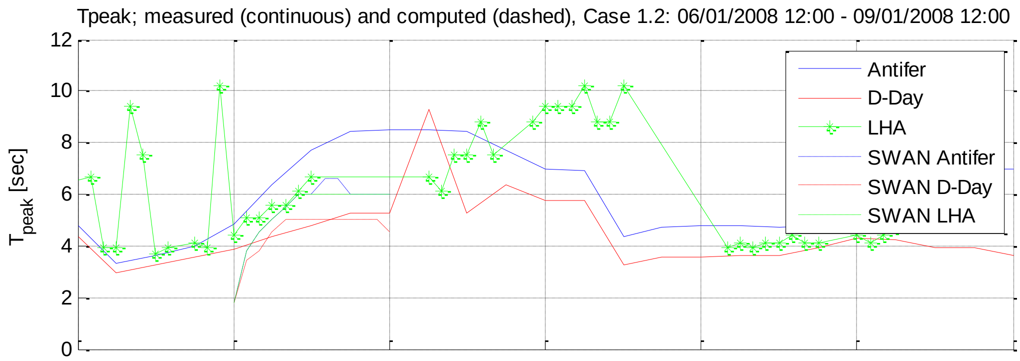
Tpeak; measured (continuous) and computed (dashed), Case 1.2: 06/01/2008 12:00 - 09/01/2008 12:00
T_{peak} [sec]
0
2
4
6
8
10
12
Antifer
D-Day
LHA
SWAN Antifer
SWAN D-Day
SWAN LHA

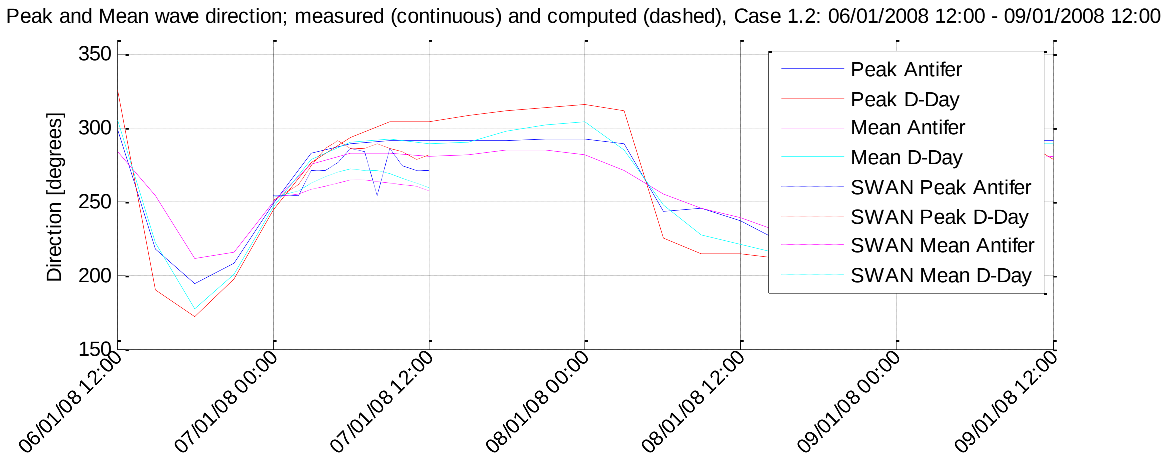
Peak and Mean wave direction; measured (continuous) and computed (dashed), Case 1.2: 06/01/2008 12:00 - 09/01/2008 12:00
Direction [degrees]
150
200
250
300
350
Peak Antifer
Peak D-Day
Mean Antifer
Mean D-Day
SWAN Peak Antifer
SWAN Peak D-Day
SWAN Mean Antifer
SWAN Mean D-Day
06/01/08 12:00
07/01/08 00:00
07/01/08 12:00
08/01/08 00:00
08/01/08 12:00
09/01/08 00:00
09/01/08 12:00

Case 2.1

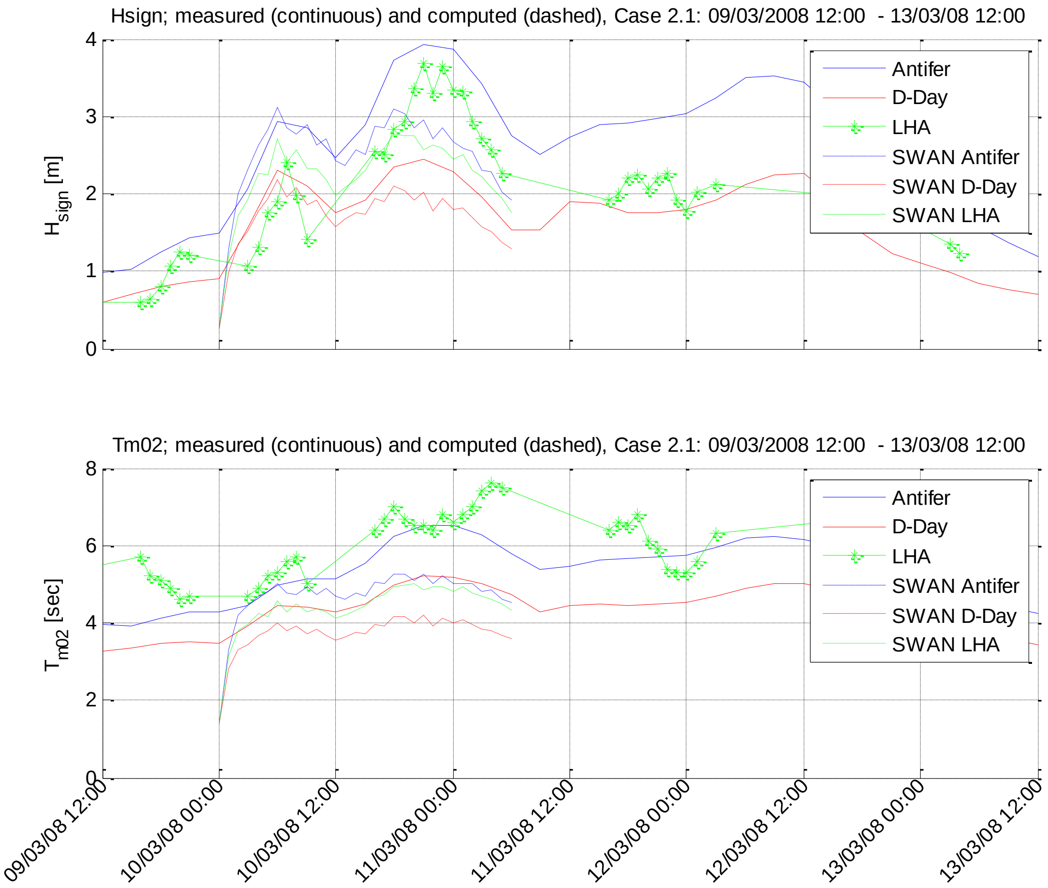

Hsign; measured (continuous) and computed (dashed), Case 2.1: 09/03/2008 12:00 - 13/03/08 12:00
Hsign [m]
Antifer
D-Day
LHA
SWAN Antifer
SWAN D-Day
SWAN LHA
Tm02; measured (continuous) and computed (dashed), Case 2.1: 09/03/2008 12:00 - 13/03/08 12:00
Tm02 [sec]
09/03/08 12:00
10/03/08 00:00
10/03/08 12:00
11/03/08 00:00
11/03/08 12:00
12/03/08 00:00
12/03/08 12:00
13/03/08 00:00
13/03/08 12:00

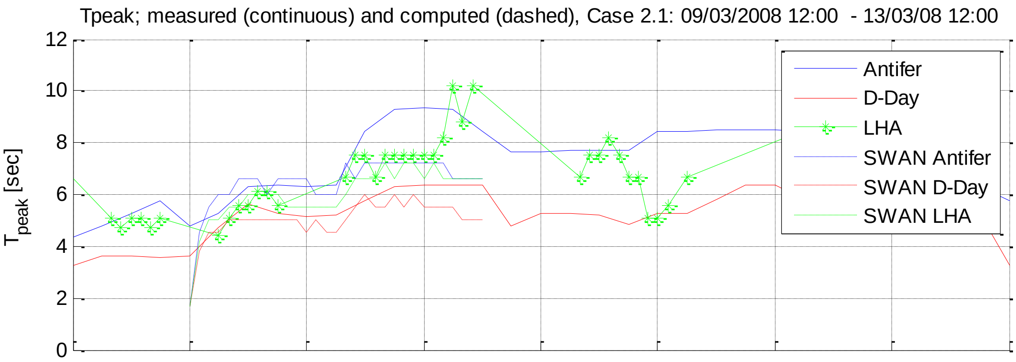

Tpeak; measured (continuous) and computed (dashed), Case 2.1: 09/03/2008 12:00 - 13/03/08 12:00
T peak [sec]
12
10
8
6
4
2
0
Antifer
D-Day
LHA
SWAN Antifer
SWAN D-Day
SWAN LHA

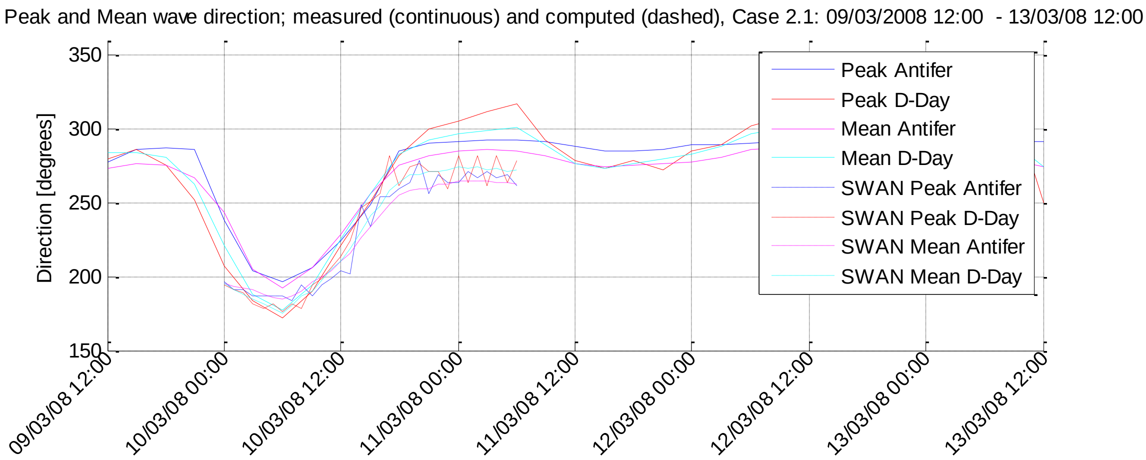

Peak and Mean wave direction; measured (continuous) and computed (dashed), Case 2.1: 09/03/2008 12:00 - 13/03/08 12:00
Direction [degrees]
350
300
250
200
150
Peak Antifer
Peak D-Day
Mean Antifer
Mean D-Day
SWAN Peak Antifer
SWAN Peak D-Day
SWAN Mean Antifer
SWAN Mean D-Day
09/03/08 12:00
10/03/08 00:00
10/03/08 12:00
11/03/08 00:00
11/03/08 12:00
12/03/08 00:00
12/03/08 12:00
13/03/08 00:00
13/03/08 12:00

Case 2.2

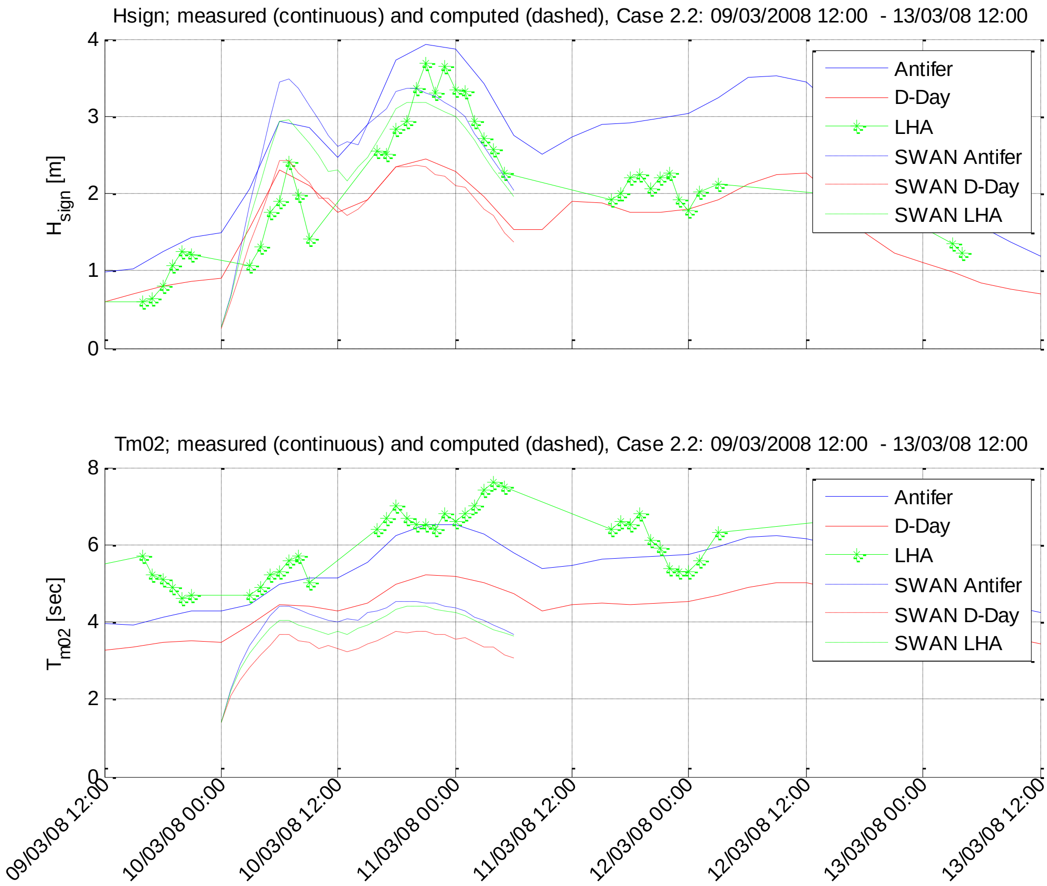

Hsign; measured (continuous) and computed (dashed), Case 2.2: 09/03/2008 12:00 - 13/03/08 12:00
H_{sign} [m]
Antifer
D-Day
LHA
SWAN Antifer
SWAN D-Day
SWAN LHA
Tm02; measured (continuous) and computed (dashed), Case 2.2: 09/03/2008 12:00 - 13/03/08 12:00
T_{m02} [sec]
09/03/08 12:00
10/03/08 00:00
10/03/08 12:00
11/03/08 00:00
11/03/08 12:00
12/03/08 00:00
12/03/08 12:00
13/03/08 00:00
13/03/08 12:00

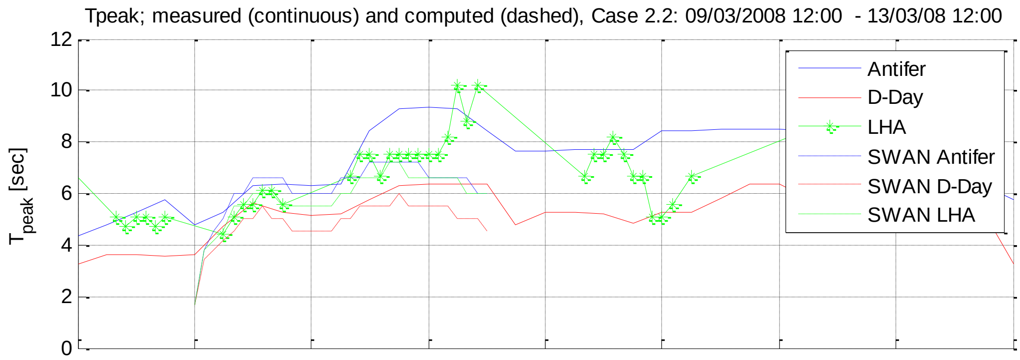
Tpeak; measured (continuous) and computed (dashed), Case 2.2: 09/03/2008 12:00 - 13/03/08 12:00
12
10
8
6
4
2
0
T peak [sec]
Antifer
D-Day
LHA
SWAN Antifer
SWAN D-Day
SWAN LHA

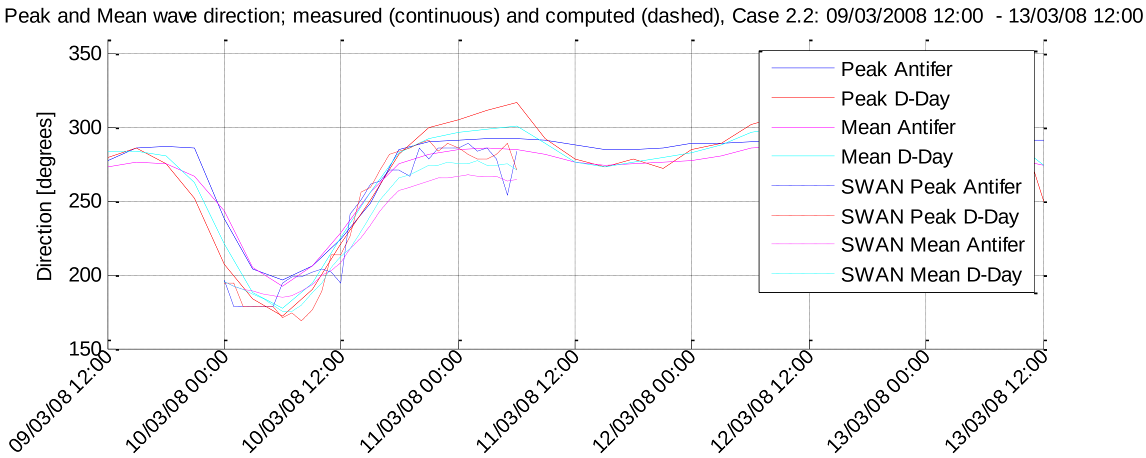
Peak and Mean wave direction; measured (continuous) and computed (dashed), Case 2.2: 09/03/2008 12:00 - 13/03/08 12:00
350
300
250
200
150
Direction [degrees]
Peak Antifer
Peak D-Day
Mean Antifer
Mean D-Day
SWAN Peak Antifer
SWAN Peak D-Day
SWAN Mean Antifer
SWAN Mean D-Day
09/03/08 12:00
10/03/08 00:00
10/03/08 12:00
11/03/08 00:00
11/03/08 12:00
12/03/08 00:00
12/03/08 12:00
13/03/08 00:00
13/03/08 12:00

Case 3.1

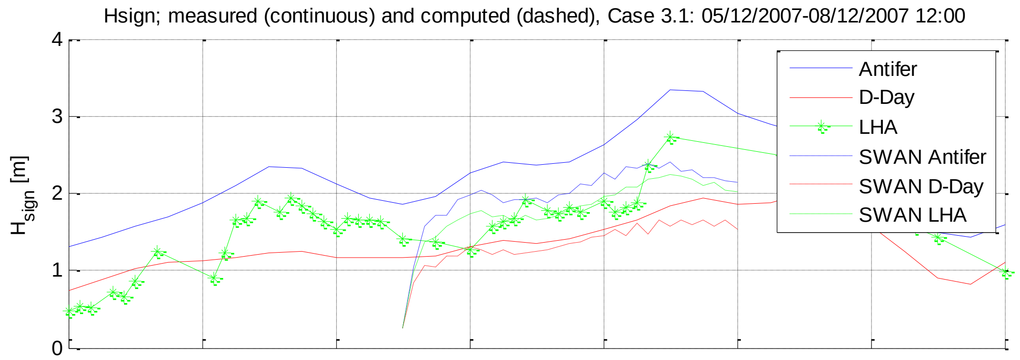
Hsign; measured (continuous) and computed (dashed), Case 3.1: 05/12/2007-08/12/2007 12:00
H_sign [m]
0
1
2
3
4
Antifer
D-Day
LHA
SWAN Antifer
SWAN D-Day
SWAN LHA

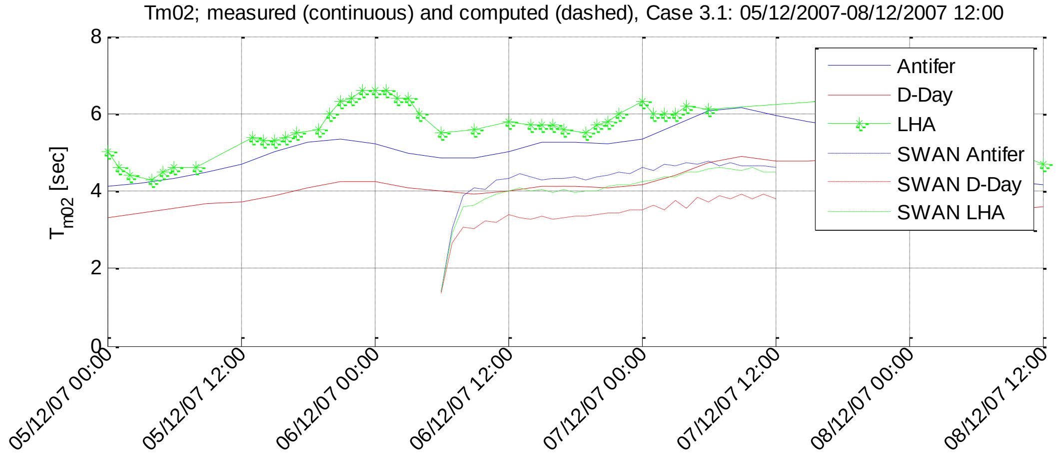
Tm02; measured (continuous) and computed (dashed), Case 3.1: 05/12/2007-08/12/2007 12:00
T_m02 [sec]
0
2
4
6
8
Antifer
D-Day
LHA
SWAN Antifer
SWAN D-Day
SWAN LHA
05/12/07 00:00
05/12/07 12:00
06/12/07 00:00
06/12/07 12:00
07/12/07 00:00
07/12/07 12:00
08/12/07 00:00
08/12/07 12:00

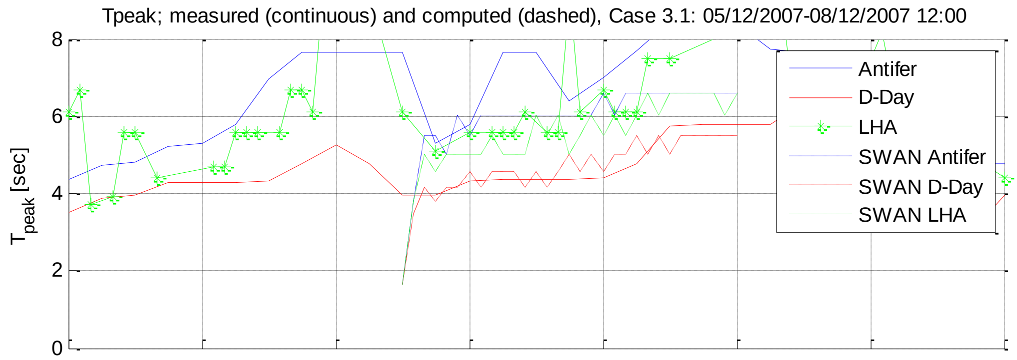
Tpeak; measured (continuous) and computed (dashed), Case 3.1: 05/12/2007-08/12/2007 12:00
T_{peak} [sec]
8
6
4
2
0
Antifer
D-Day
LHA
SWAN Antifer
SWAN D-Day
SWAN LHA

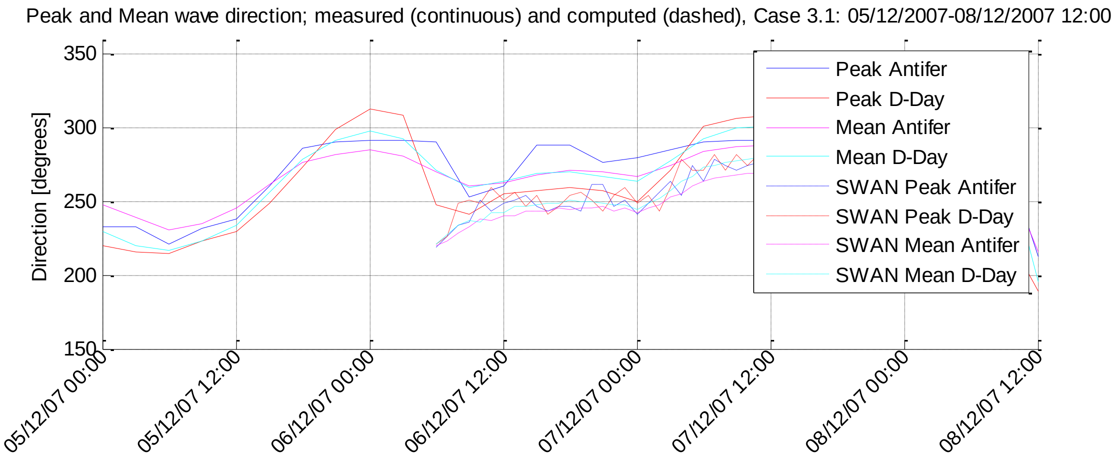
Peak and Mean wave direction; measured (continuous) and computed (dashed), Case 3.1: 05/12/2007-08/12/2007 12:00
Direction [degrees]
350
300
250
200
150
Peak Antifer
Peak D-Day
Mean Antifer
Mean D-Day
SWAN Peak Antifer
SWAN Peak D-Day
SWAN Mean Antifer
SWAN Mean D-Day
05/12/07 00:00
05/12/07 12:00
06/12/07 00:00
06/12/07 12:00
07/12/07 00:00
07/12/07 12:00
08/12/07 00:00
08/12/07 12:00

Case 3.2


Hsign; measured (continuous) and computed (dashed), Case 3.2: 05/12/2007-08/12/2007 12:00
H_sign [m]
Antifer
D-Day
LHA
SWAN Antifer
SWAN D-Day
SWAN LHA
Tm02; measured (continuous) and computed (dashed), Case 3.2: 05/12/2007-08/12/2007 12:00
T_m02 [sec]
Antifer
D-Day
LHA
SWAN Antifer
SWAN D-Day
SWAN LHA
05/12/07 00:00
05/12/07 12:00
06/12/07 00:00
06/12/07 12:00
07/12/07 00:00
07/12/07 12:00
08/12/07 00:00
08/12/07 12:00

Tpeak; measured (continuous) and computed (dashed), Case 3.2: 05/12/2007-08/12/2007 12:00

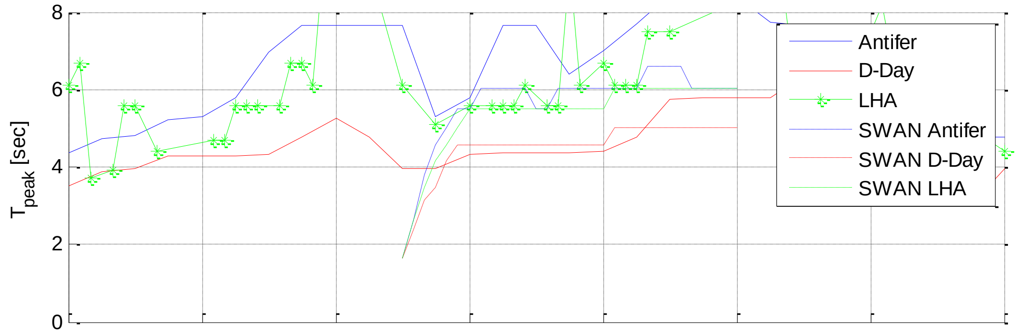

Peak and Mean wave direction; measured (continuous) and computed (dashed), Case 3.2: 05/12/2007-08/12/2007 12:00

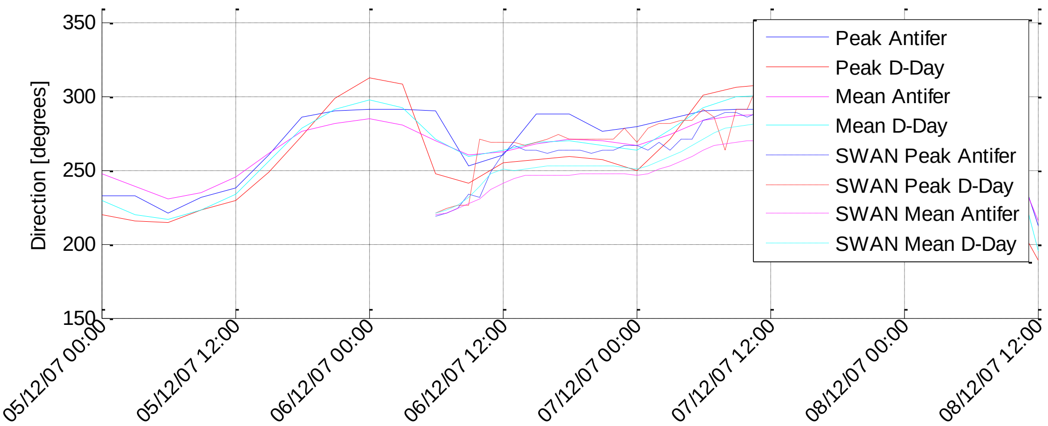

Case 4.1

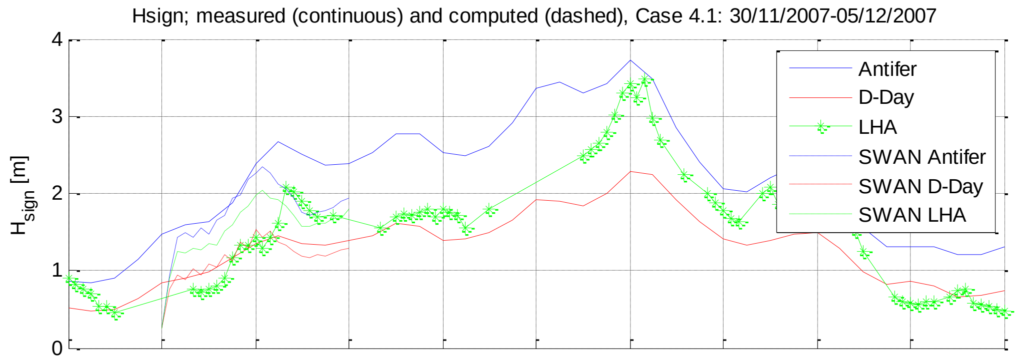
Hsign; measured (continuous) and computed (dashed), Case 4.1: 30/11/2007-05/12/2007
H_{sign} [m]
0
1
2
3
4
Antifer
D-Day
LHA
SWAN Antifer
SWAN D-Day
SWAN LHA

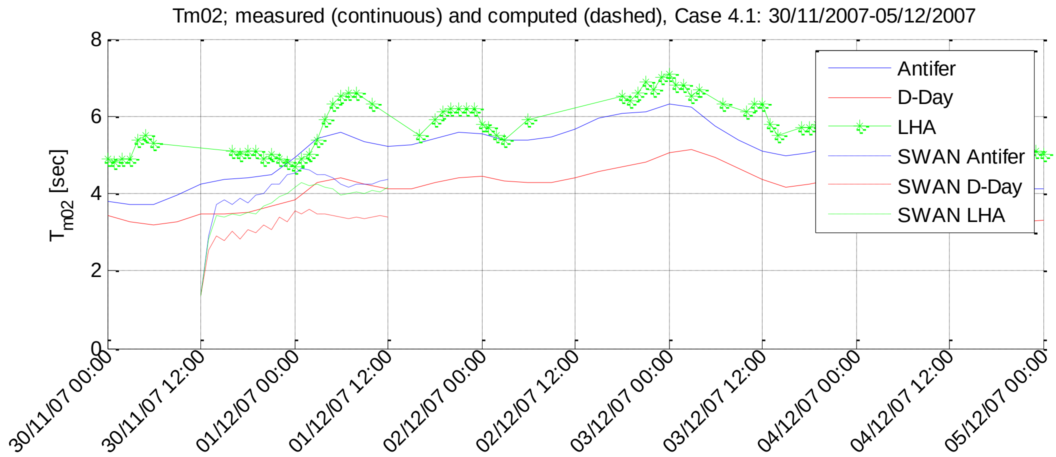
Tm02; measured (continuous) and computed (dashed), Case 4.1: 30/11/2007-05/12/2007
T_{m02} [sec]
0
2
4
6
8
Antifer
D-Day
LHA
SWAN Antifer
SWAN D-Day
SWAN LHA
30/11/07 00:00
30/11/07 12:00
01/12/07 00:00
01/12/07 12:00
02/12/07 00:00
02/12/07 12:00
03/12/07 00:00
03/12/07 12:00
04/12/07 00:00
04/12/07 12:00
05/12/07 00:00

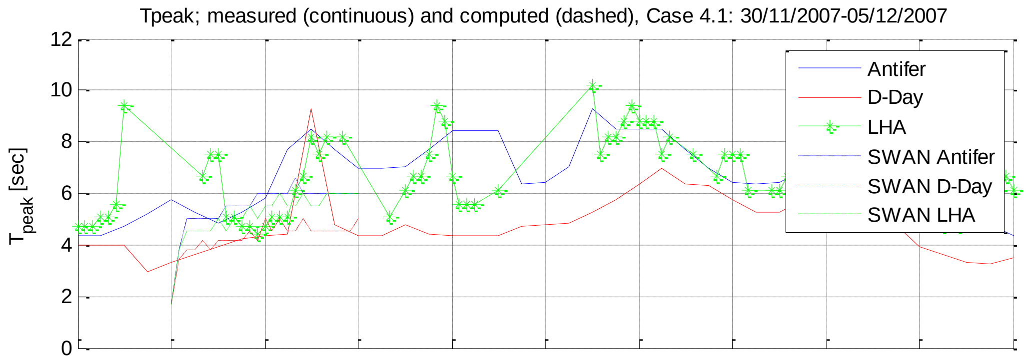
Tpeak; measured (continuous) and computed (dashed), Case 4.1: 30/11/2007-05/12/2007
T_peak [sec]
Antifer
D-Day
LHA
SWAN Antifer
SWAN D-Day
SWAN LHA

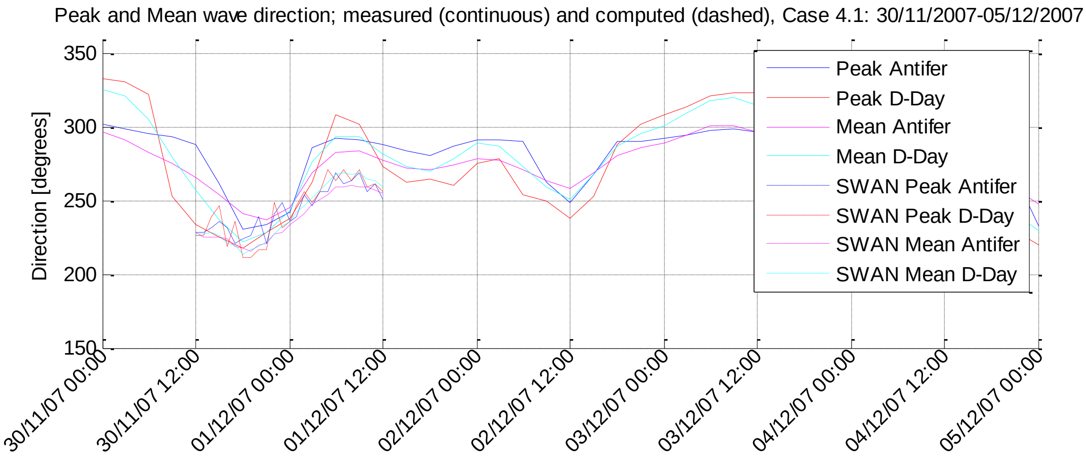
Peak and Mean wave direction; measured (continuous) and computed (dashed), Case 4.1: 30/11/2007-05/12/2007
Direction [degrees]
Peak Antifer
Peak D-Day
Mean Antifer
Mean D-Day
SWAN Peak Antifer
SWAN Peak D-Day
SWAN Mean Antifer
SWAN Mean D-Day
30/11/07 00:00
30/11/07 12:00
01/12/07 00:00
01/12/07 12:00
02/12/07 00:00
02/12/07 12:00
03/12/07 00:00
03/12/07 12:00
04/12/07 00:00
04/12/07 12:00
05/12/07 00:00

Case 4.2

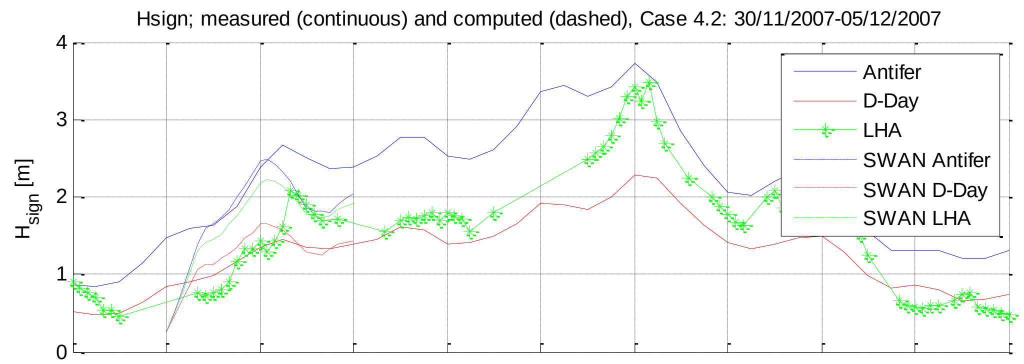

Hsign; measured (continuous) and computed (dashed), Case 4.2: 30/11/2007-05/12/2007
H_{sign} [m]
Antifer
D-Day
LHA
SWAN Antifer
SWAN D-Day
SWAN LHA

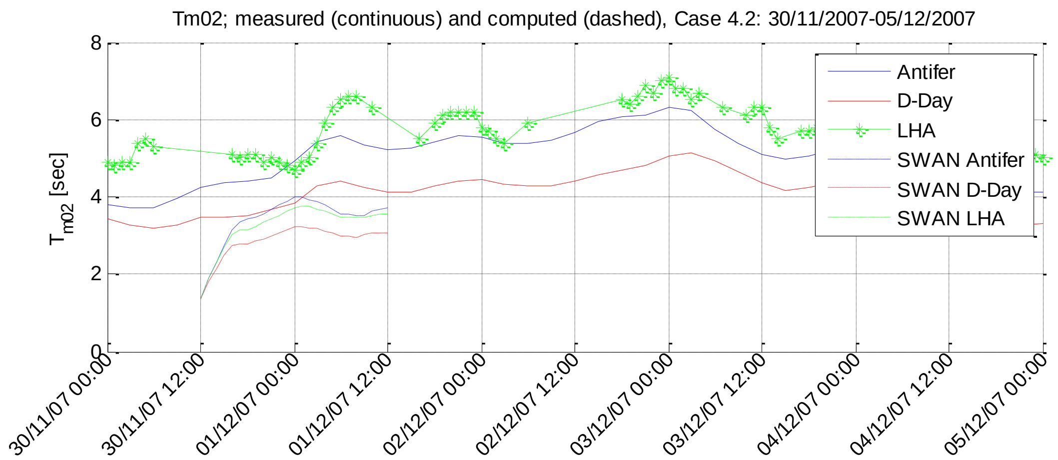

Tm02; measured (continuous) and computed (dashed), Case 4.2: 30/11/2007-05/12/2007
T_{m02} [sec]
Antifer
D-Day
LHA
SWAN Antifer
SWAN D-Day
SWAN LHA
30/11/07 00:00
30/11/07 12:00
01/12/07 00:00
01/12/07 12:00
02/12/07 00:00
02/12/07 12:00
03/12/07 00:00
03/12/07 12:00
04/12/07 00:00
04/12/07 12:00
05/12/07 00:00

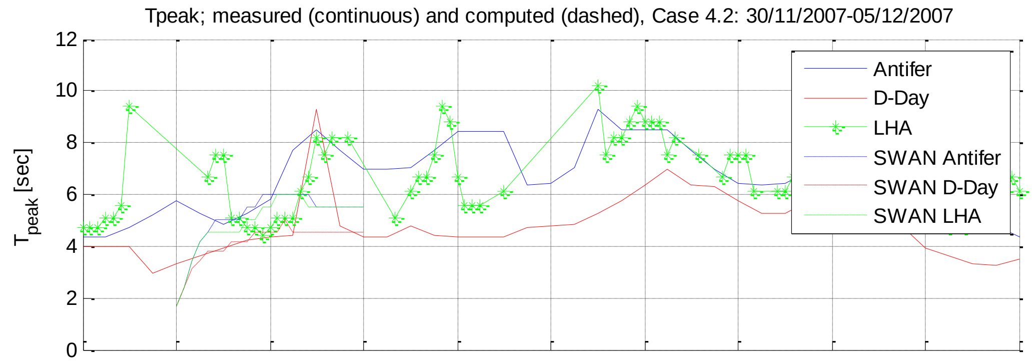

Tpeak; measured (continuous) and computed (dashed), Case 4.2: 30/11/2007-05/12/2007
12
10
8
6
4
2
0
T_{peak} [sec]
Antifer
D-Day
LHA
SWAN Antifer
SWAN D-Day
SWAN LHA

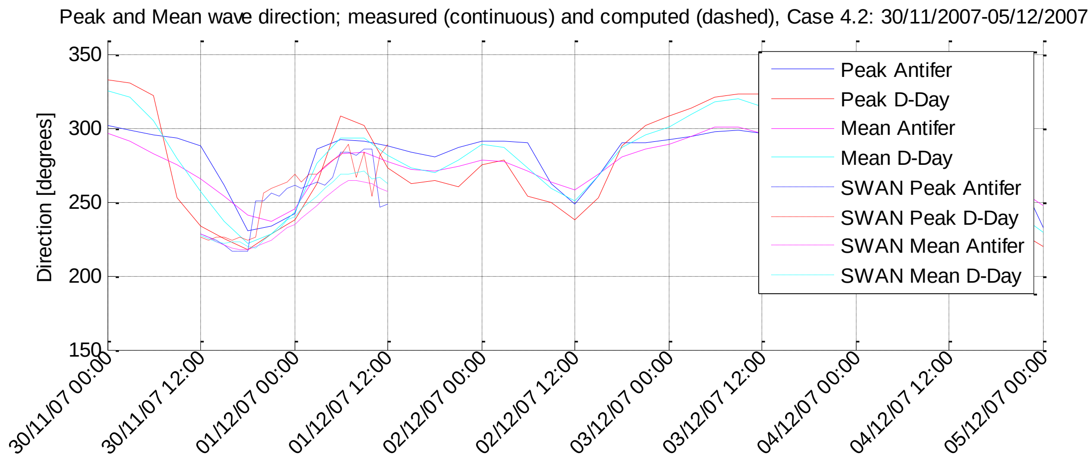

Peak and Mean wave direction; measured (continuous) and computed (dashed), Case 4.2: 30/11/2007-05/12/2007
350
300
250
200
150
Direction [degrees]
Peak Antifer
Peak D-Day
Mean Antifer
Mean D-Day
SWAN Peak Antifer
SWAN Peak D-Day
SWAN Mean Antifer
SWAN Mean D-Day
30/11/07 00:00
30/11/07 12:00
01/12/07 00:00
01/12/07 12:00
02/12/07 00:00
02/12/07 12:00
03/12/07 00:00
03/12/07 12:00
04/12/07 00:00
04/12/07 12:00
05/12/07 00:00

Case 5.1

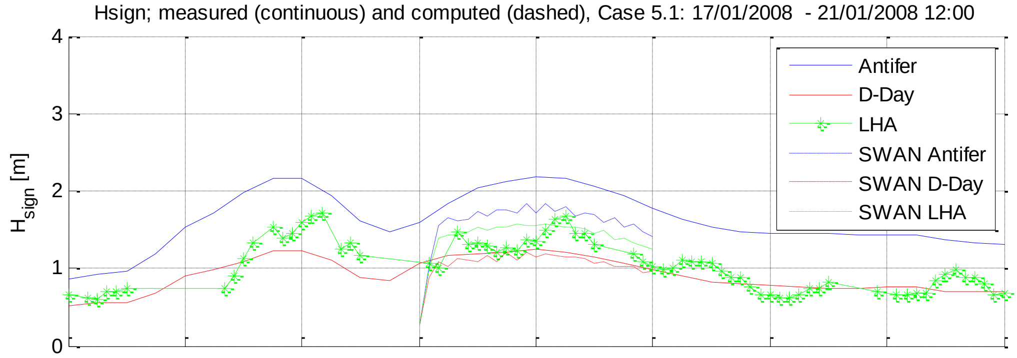

Hsign; measured (continuous) and computed (dashed), Case 5.1: 17/01/2008 - 21/01/2008 12:00
Hsign [m]
Antifer
D-Day
LHA
SWAN Antifer
SWAN D-Day
SWAN LHA

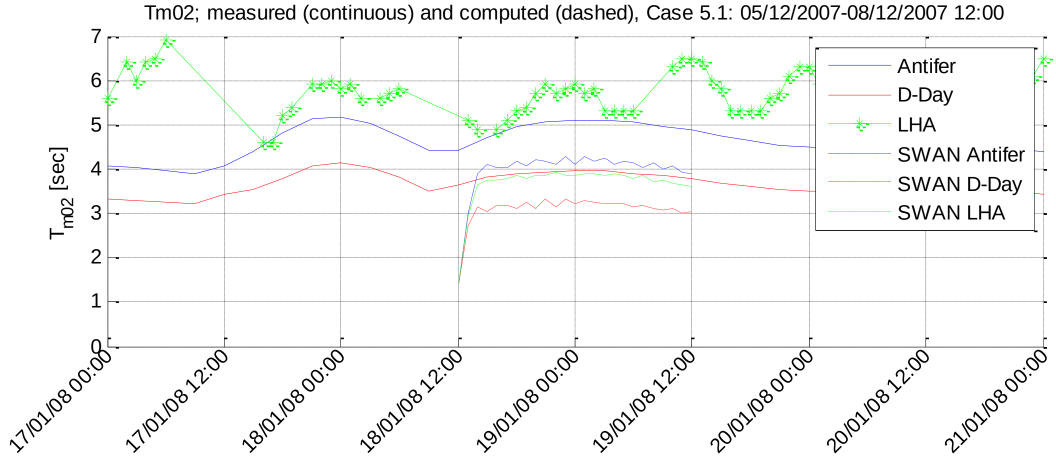

Tm02; measured (continuous) and computed (dashed), Case 5.1: 05/12/2007-08/12/2007 12:00
Tm02 [sec]
Antifer
D-Day
LHA
SWAN Antifer
SWAN D-Day
SWAN LHA
17/01/08 00:00
17/01/08 12:00
18/01/08 00:00
18/01/08 12:00
19/01/08 00:00
19/01/08 12:00
20/01/08 00:00
20/01/08 12:00
21/01/08 00:00

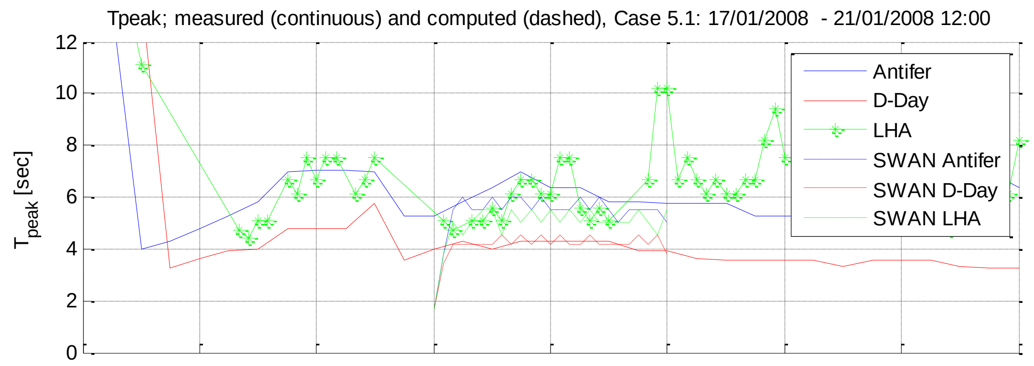

Tpeak; measured (continuous) and computed (dashed), Case 5.1: 17/01/2008 - 21/01/2008 12:00
T_peak [sec]
0
2
4
6
8
10
12
Antifer
D-Day
LHA
SWAN Antifer
SWAN D-Day
SWAN LHA

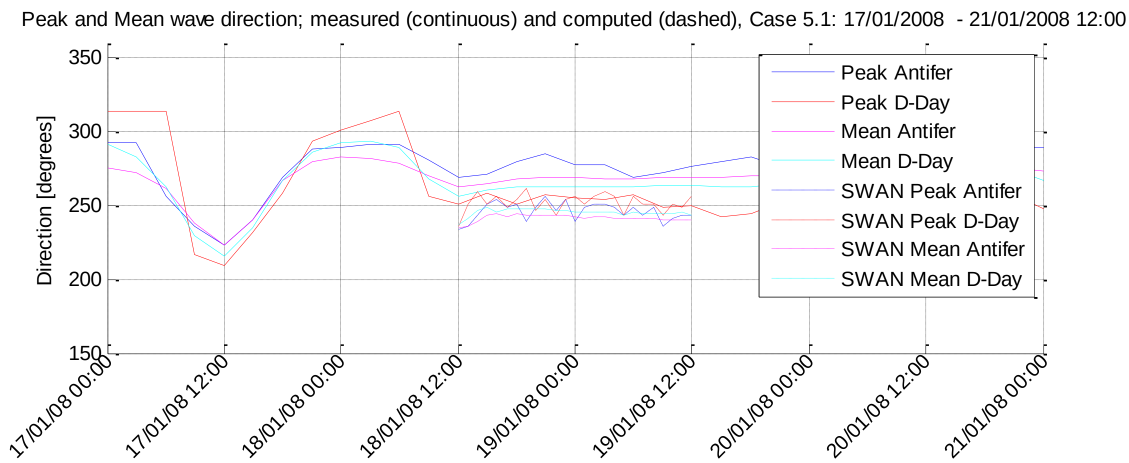

Peak and Mean wave direction; measured (continuous) and computed (dashed), Case 5.1: 17/01/2008 - 21/01/2008 12:00
Direction [degrees]
150
200
250
300
350
Peak Antifer
Peak D-Day
Mean Antifer
Mean D-Day
SWAN Peak Antifer
SWAN Peak D-Day
SWAN Mean Antifer
SWAN Mean D-Day
17/01/08 00:00
17/01/08 12:00
18/01/08 00:00
18/01/08 12:00
19/01/08 00:00
19/01/08 12:00
20/01/08 00:00
20/01/08 12:00
21/01/08 00:00

Case 5.2

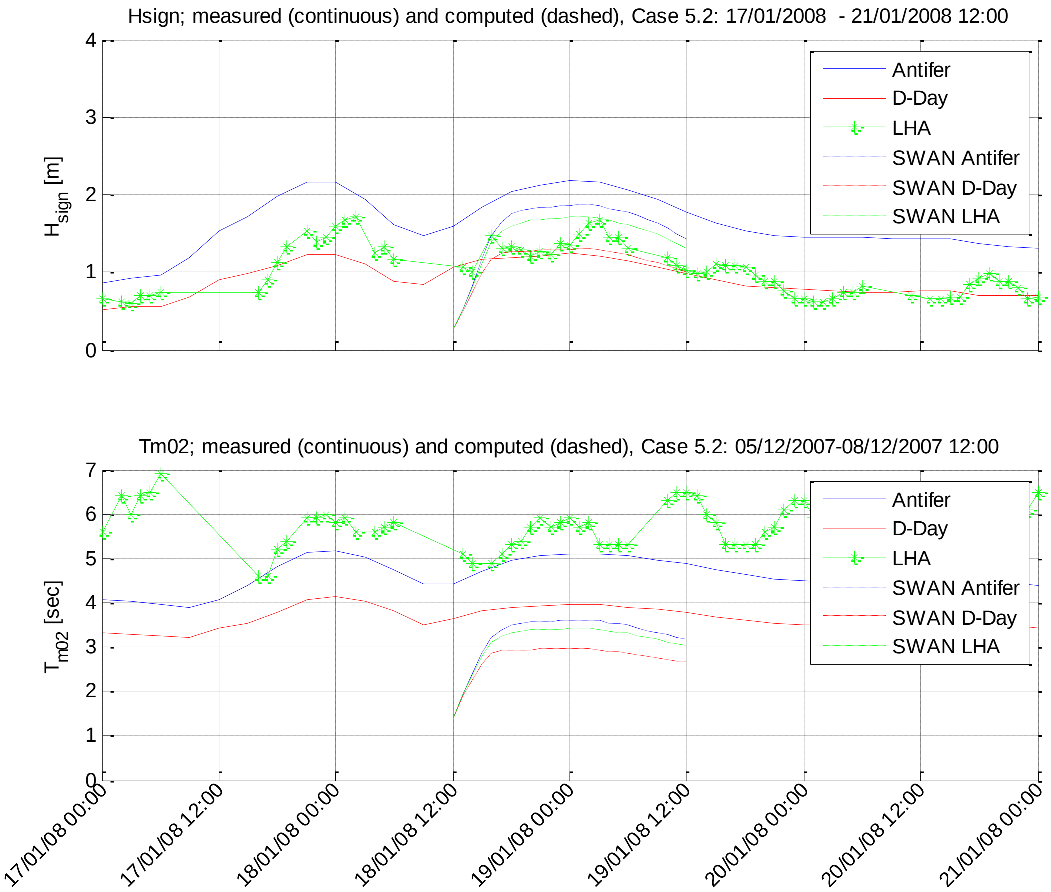

Hsign; measured (continuous) and computed (dashed), Case 5.2: 17/01/2008 - 21/01/2008 12:00
H_sign [m]
Antifer
D-Day
LHA
SWAN Antifer
SWAN D-Day
SWAN LHA
Tm02; measured (continuous) and computed (dashed), Case 5.2: 05/12/2007-08/12/2007 12:00
T_m02 [sec]
17/01/08 00:00
17/01/08 12:00
18/01/08 00:00
18/01/08 12:00
19/01/08 00:00
19/01/08 12:00
20/01/08 00:00
20/01/08 12:00
21/01/08 00:00

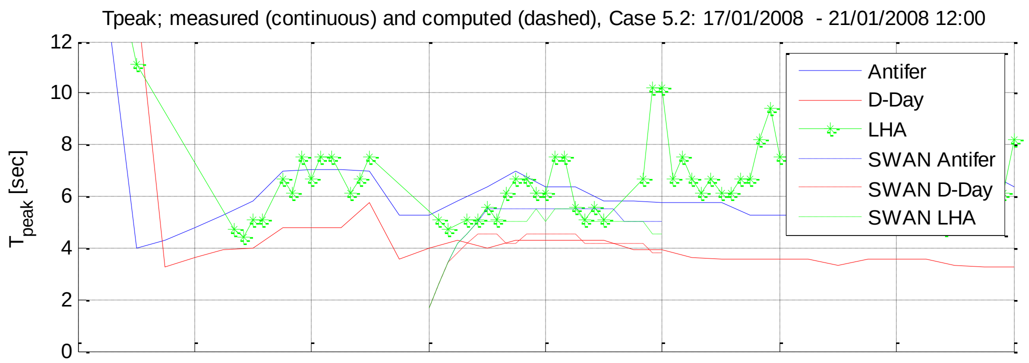

Tpeak; measured (continuous) and computed (dashed), Case 5.2: 17/01/2008 - 21/01/2008 12:00
T_{peak} [sec]
0
2
4
6
8
10
12
Antifer
D-Day
LHA
SWAN Antifer
SWAN D-Day
SWAN LHA

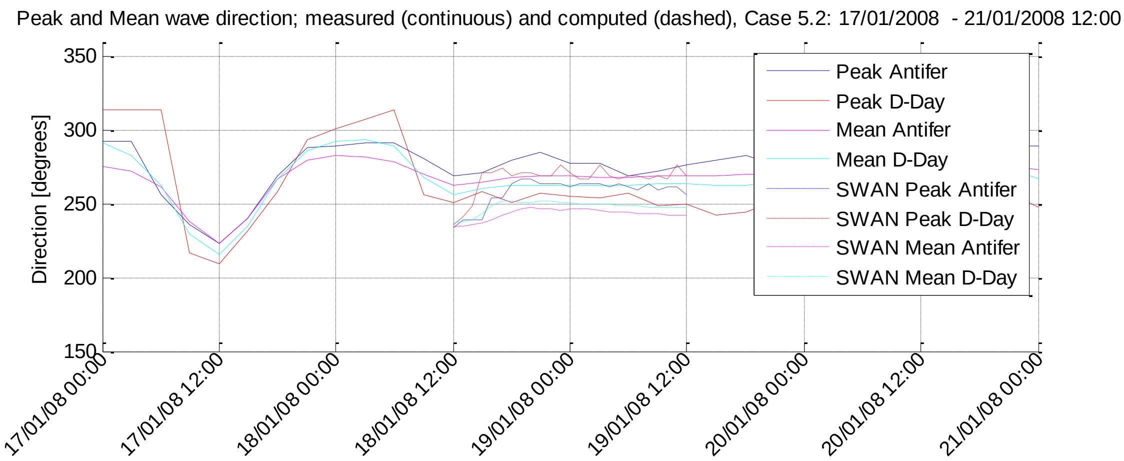

Peak and Mean wave direction; measured (continuous) and computed (dashed), Case 5.2: 17/01/2008 - 21/01/2008 12:00
Direction [degrees]
150
200
250
300
350
Peak Antifer
Peak D-Day
Mean Antifer
Mean D-Day
SWAN Peak Antifer
SWAN Peak D-Day
SWAN Mean Antifer
SWAN Mean D-Day
17/01/08 00:00
17/01/08 12:00
18/01/08 00:00
18/01/08 12:00
19/01/08 00:00
19/01/08 12:00
20/01/08 00:00
20/01/08 12:00
21/01/08 00:00

Appendix E: SWAN results off-shore and near-shore buoys

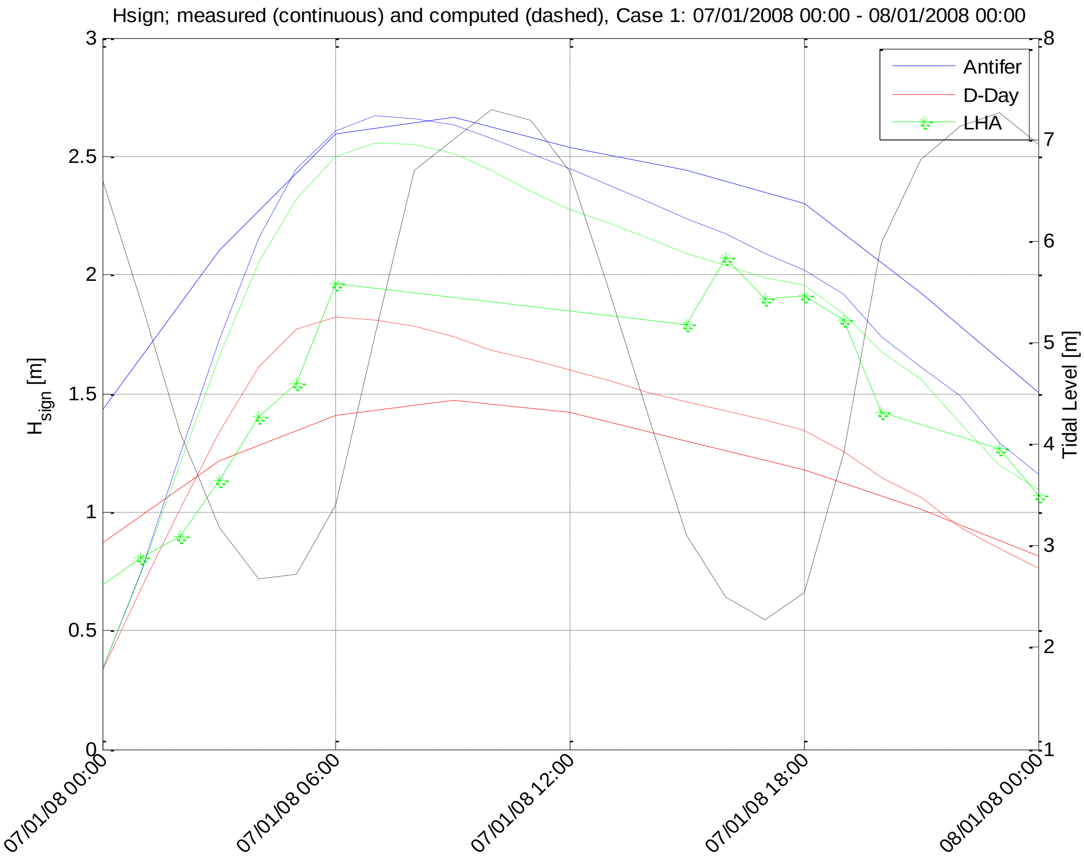

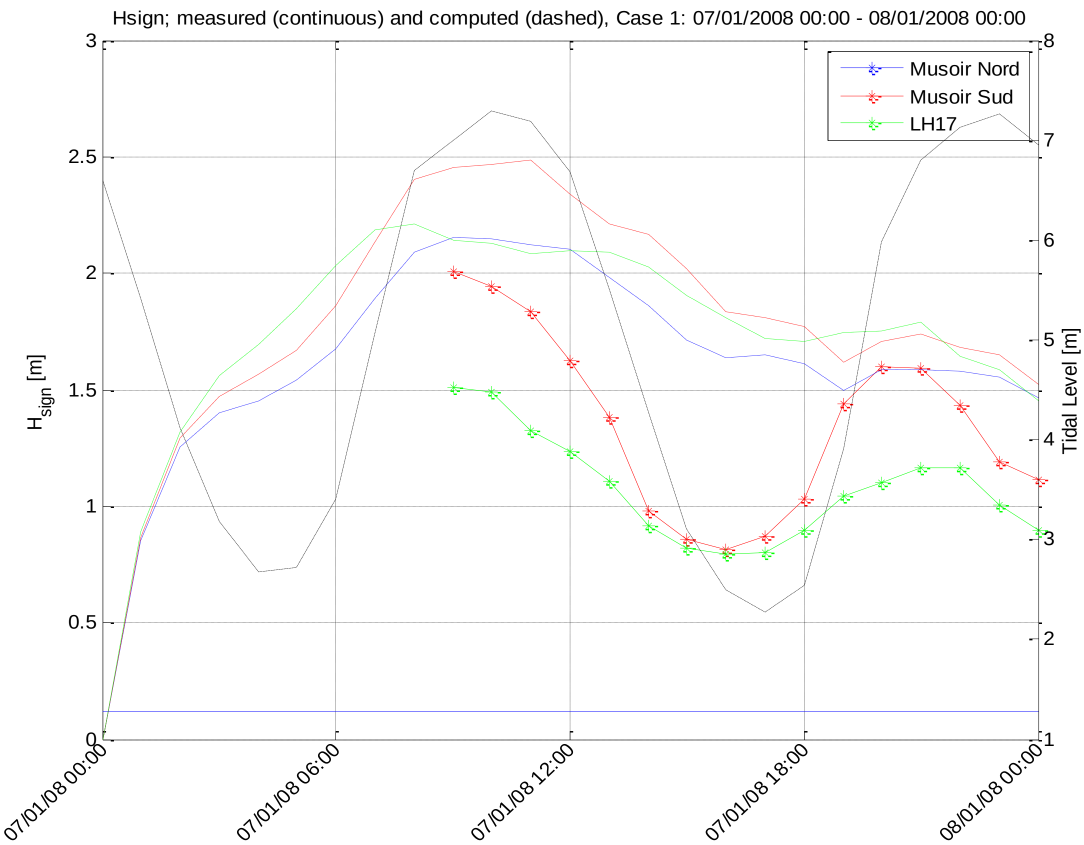

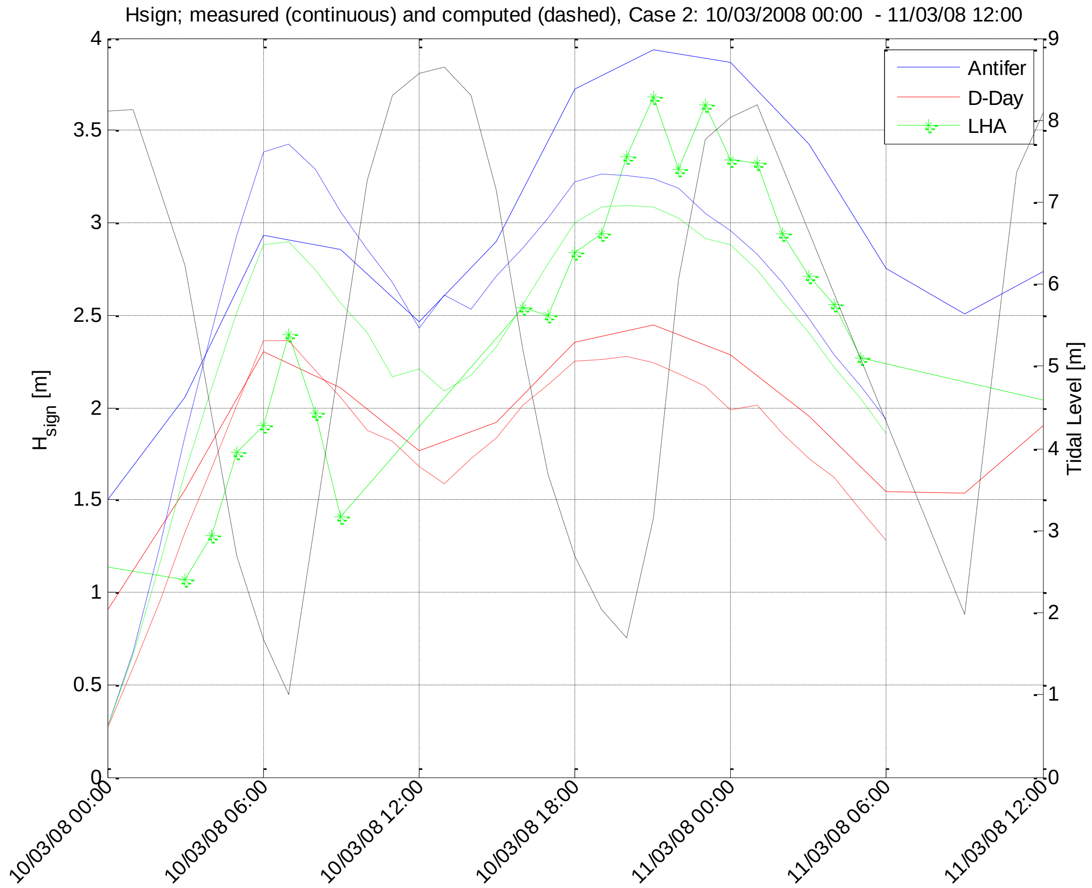
Hsign; measured (continuous) and computed (dashed), Case 2: 10/03/2008 00:00 - 11/03/08 12:00
Antifer
D-Day
LHA
H_{sign} [m]
Tidal Level [m]
10/03/08 00:00
10/03/08 06:00
10/03/08 12:00
10/03/08 18:00
11/03/08 00:00
11/03/08 06:00
11/03/08 12:00

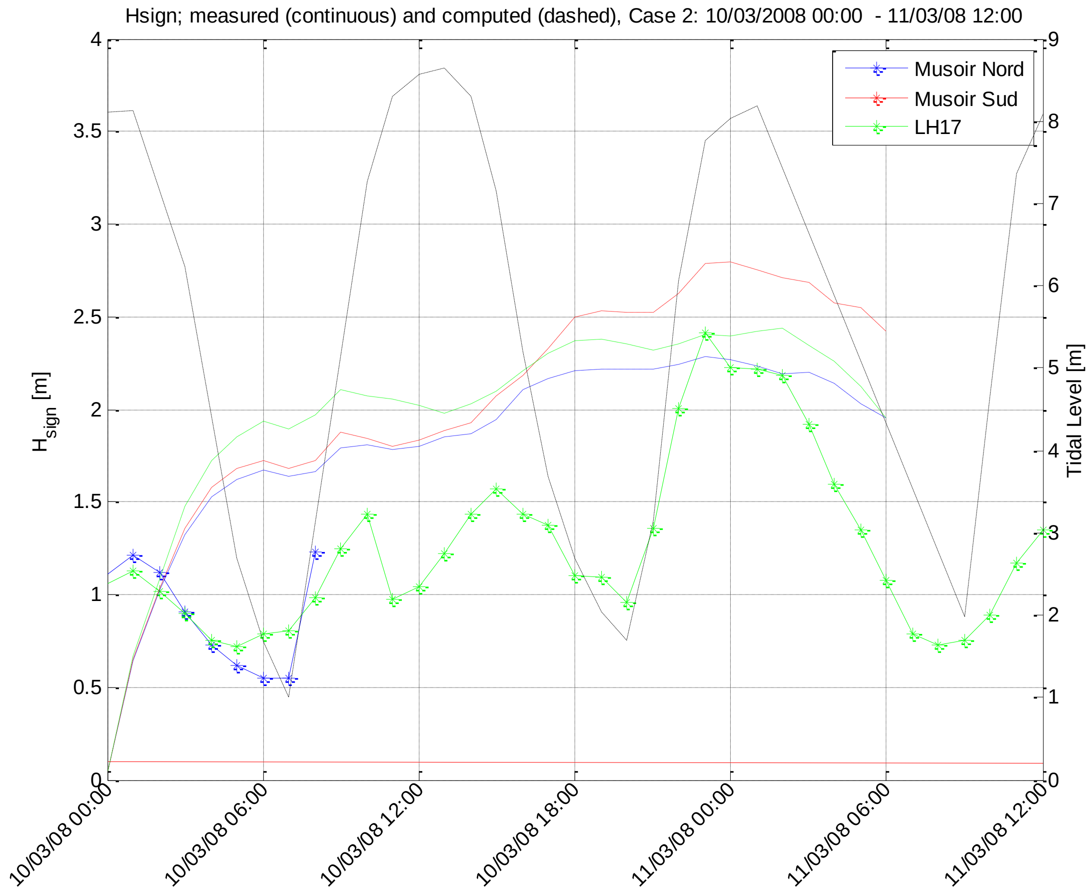
Hsign; measured (continuous) and computed (dashed), Case 2: 10/03/2008 00:00 - 11/03/08 12:00
Musoir Nord
Musoir Sud
LH17
H_{sign} [m]
Tidal Level [m]
10/03/08 00:00
10/03/08 06:00
10/03/08 12:00
10/03/08 18:00
11/03/08 00:00
11/03/08 06:00
11/03/08 12:00

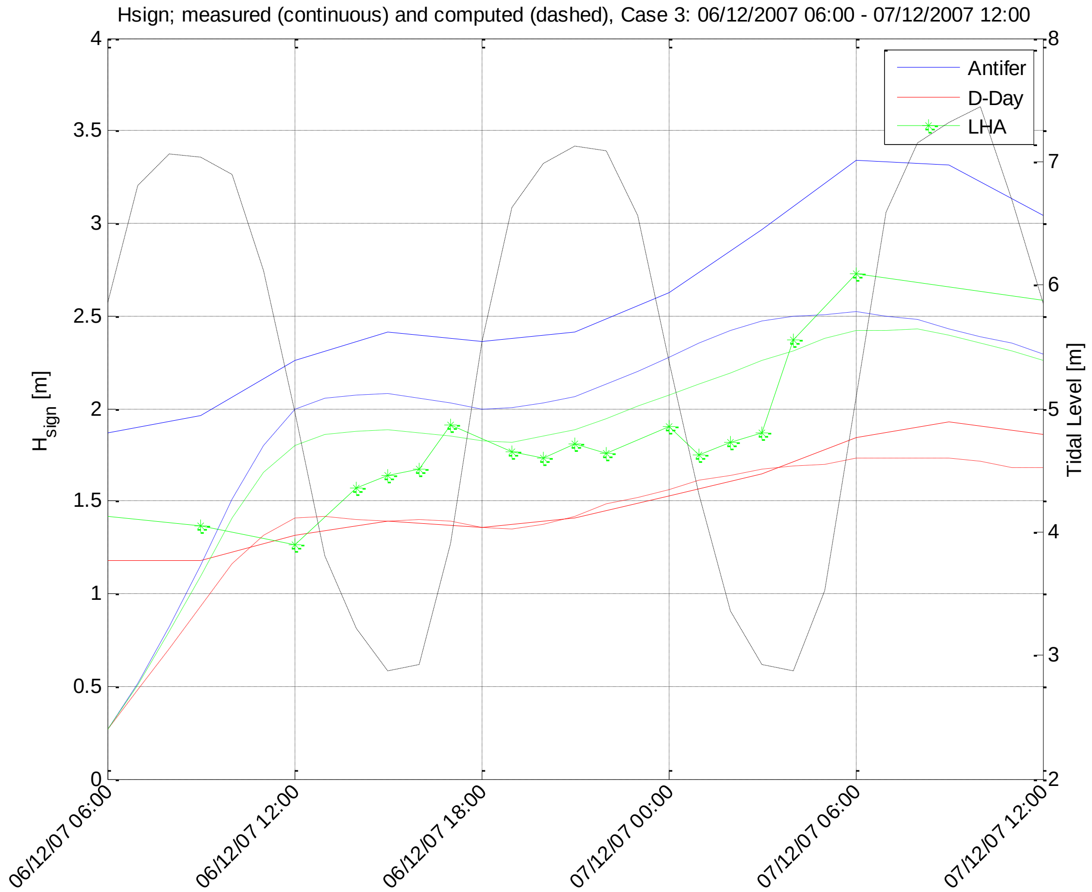

Hsign; measured (continuous) and computed (dashed), Case 3: 06/12/2007 06:00 - 07/12/2007 12:00
Antifer
D-Day
LHA
H_{sign} [m]
Tidal Level [m]
06/12/07 06:00
06/12/07 12:00
06/12/07 18:00
07/12/07 00:00
07/12/07 06:00
07/12/07 12:00

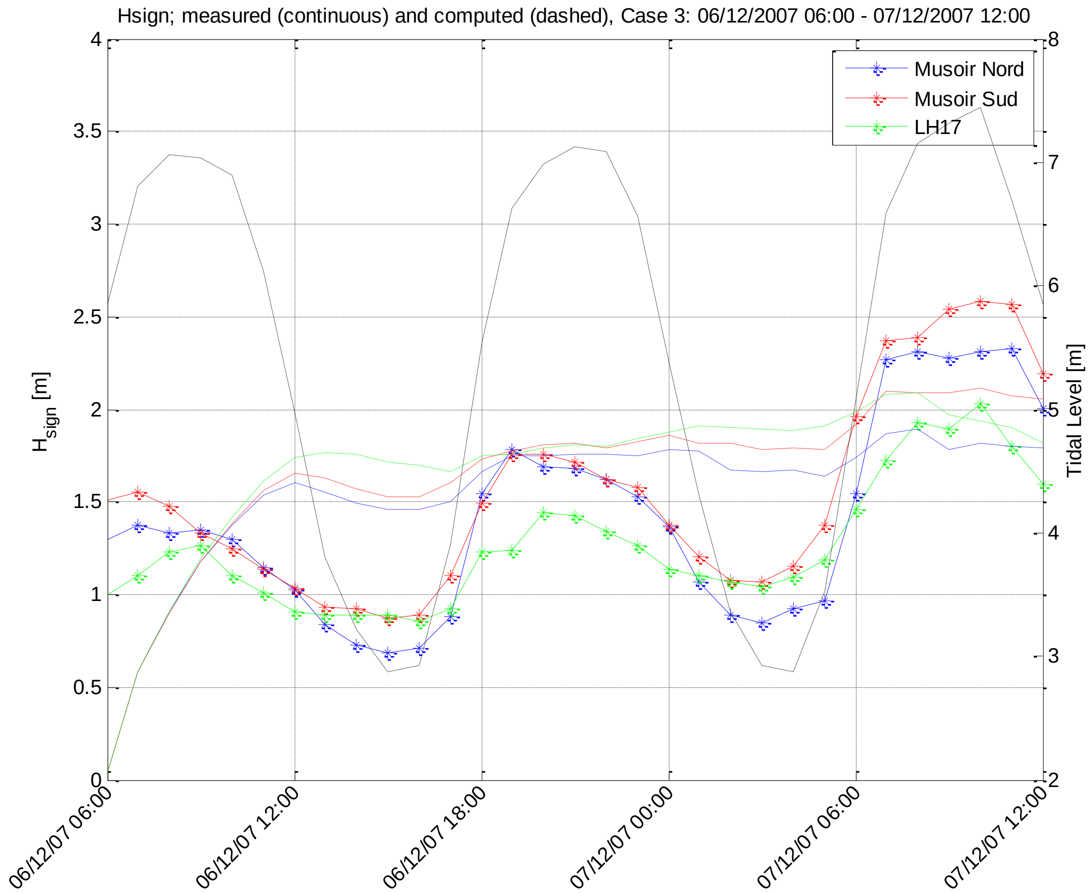

Hsign; measured (continuous) and computed (dashed), Case 3: 06/12/2007 06:00 - 07/12/2007 12:00
Musoir Nord
Musoir Sud
LH17
H_{sign} [m]
Tidal Level [m]
06/12/07 06:00
06/12/07 12:00
06/12/07 18:00
07/12/07 00:00
07/12/07 06:00
07/12/07 12:00

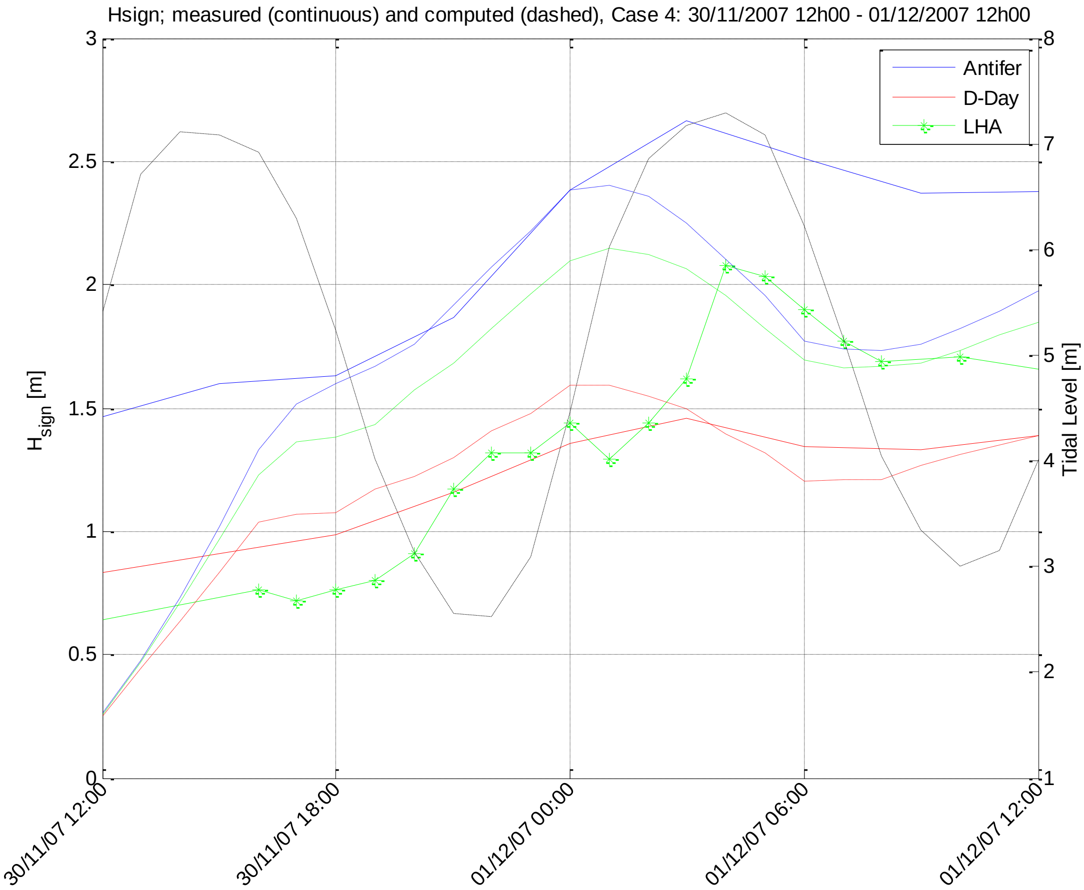
Hsign; measured (continuous) and computed (dashed), Case 4: 30/11/2007 12h00 - 01/12/2007 12h00
Antifer
D-Day
LHA
H_{sign} [m]
Tidal Level [m]
30/11/07 12:00
30/11/07 18:00
01/12/07 00:00
01/12/07 06:00
01/12/07 12:00

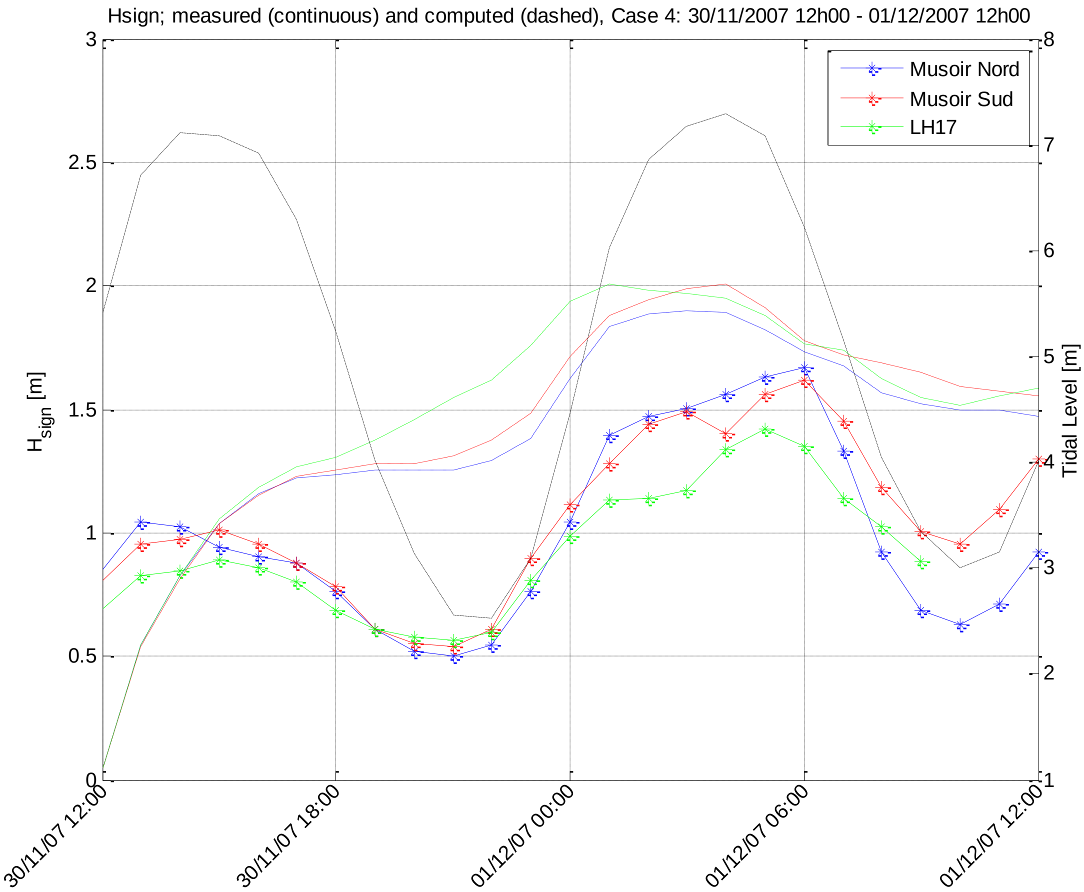
Hsign; measured (continuous) and computed (dashed), Case 4: 30/11/2007 12h00 - 01/12/2007 12h00
Musoir Nord
Musoir Sud
LH17
H_{sign} [m]
Tidal Level [m]
30/11/07 12:00
30/11/07 18:00
01/12/07 00:00
01/12/07 06:00
01/12/07 12:00

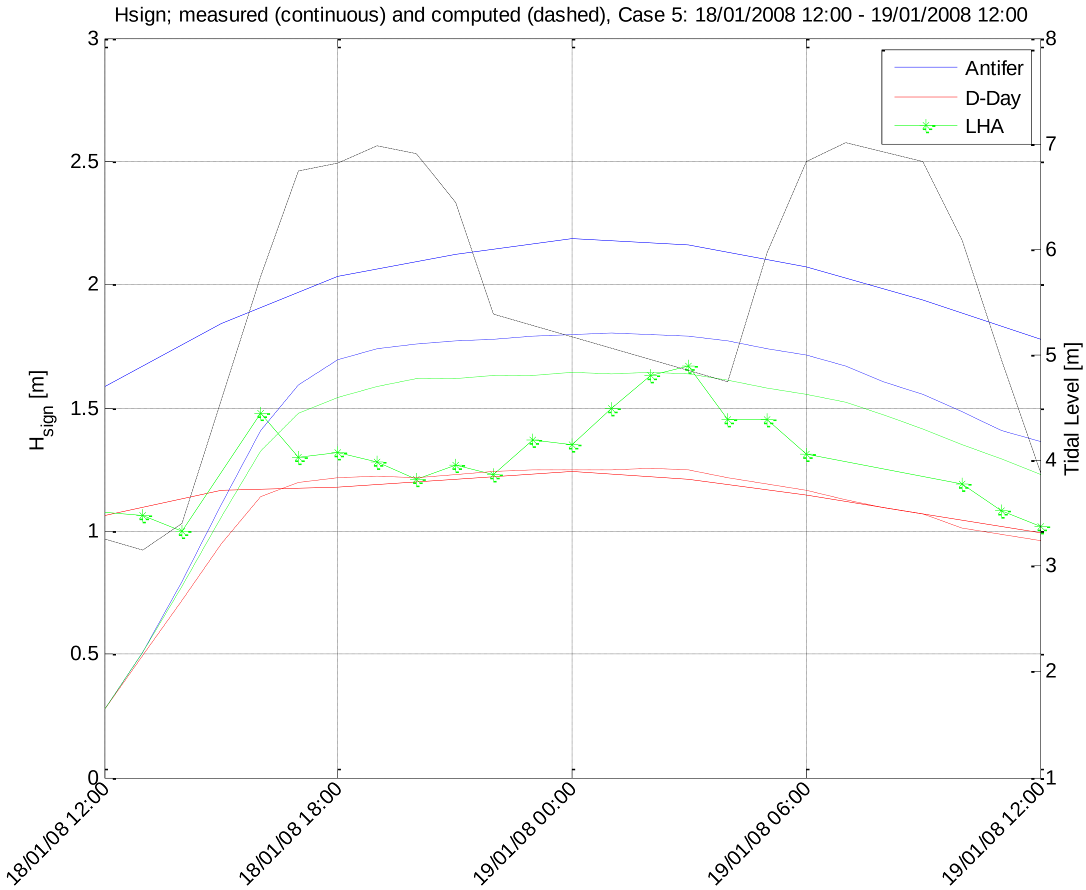

Hsign; measured (continuous) and computed (dashed), Case 5: 18/01/2008 12:00 - 19/01/2008 12:00
Antifer
D-Day
LHA
H_sign [m]
Tidal Level [m]
18/01/08 12:00
18/01/08 18:00
19/01/08 00:00
19/01/08 06:00
19/01/08 12:00

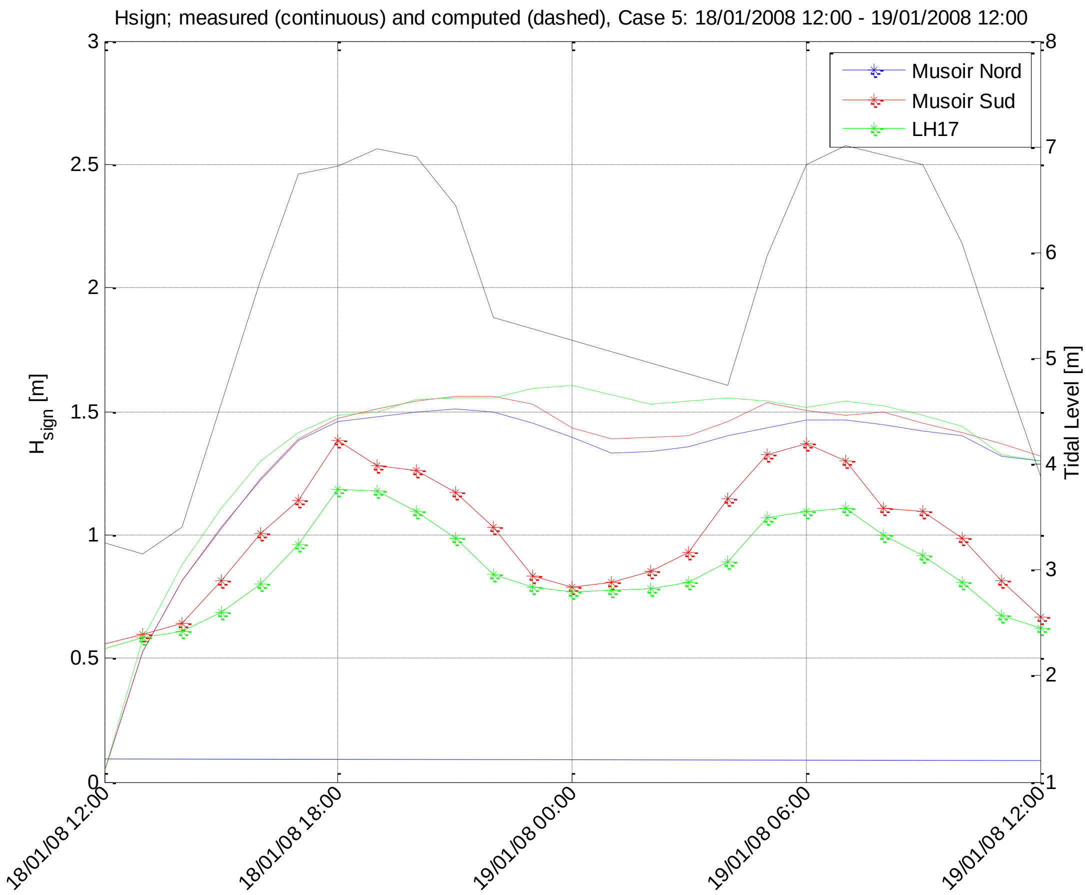

Hsign; measured (continuous) and computed (dashed), Case 5: 18/01/2008 12:00 - 19/01/2008 12:00
Musoir Nord
Musoir Sud
LH17
H_sign [m]
Tidal Level [m]
18/01/08 12:00
18/01/08 18:00
19/01/08 00:00
19/01/08 06:00
19/01/08 12:00

Appendix F: Calculated tidal currents by Telemac

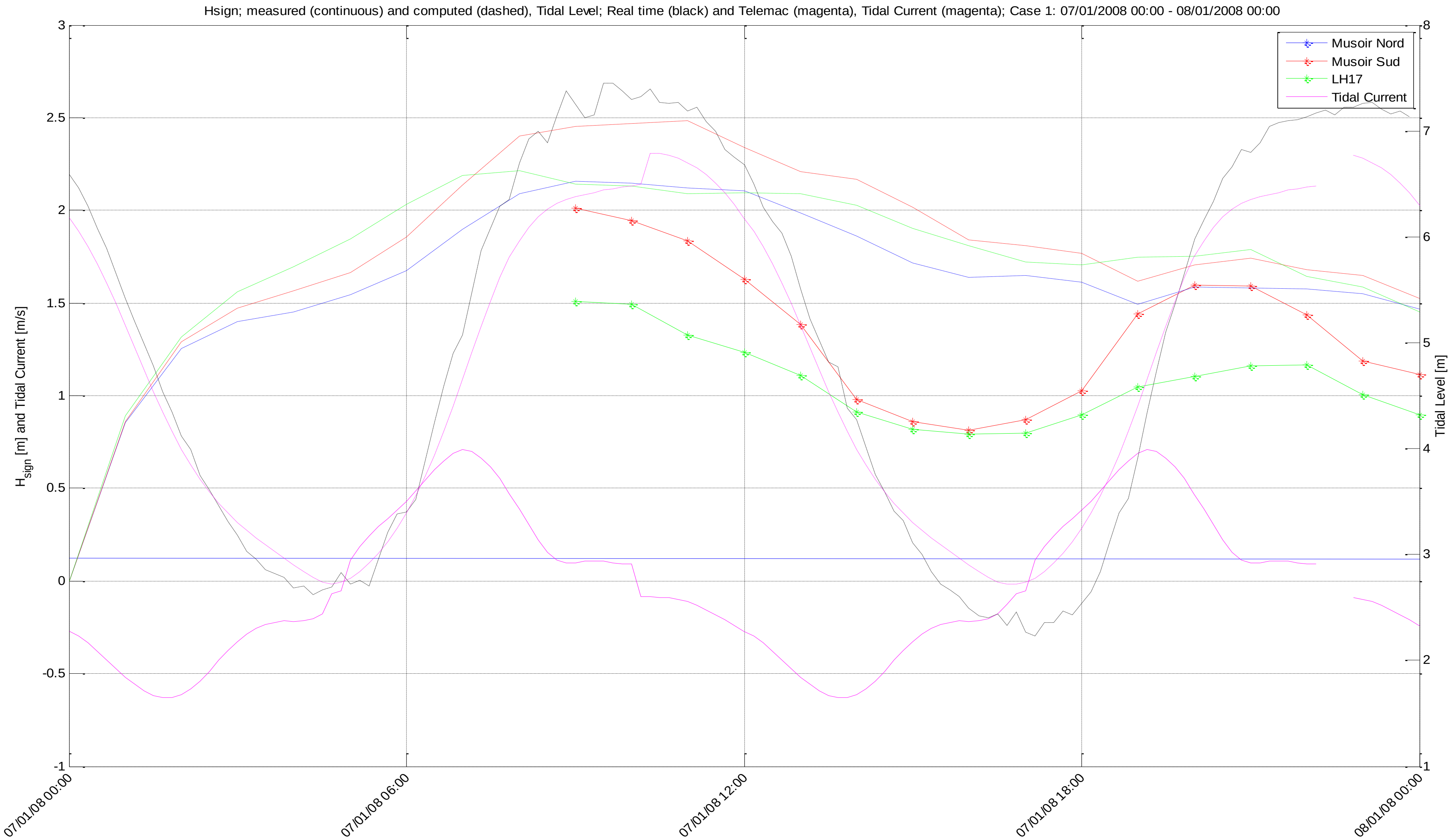

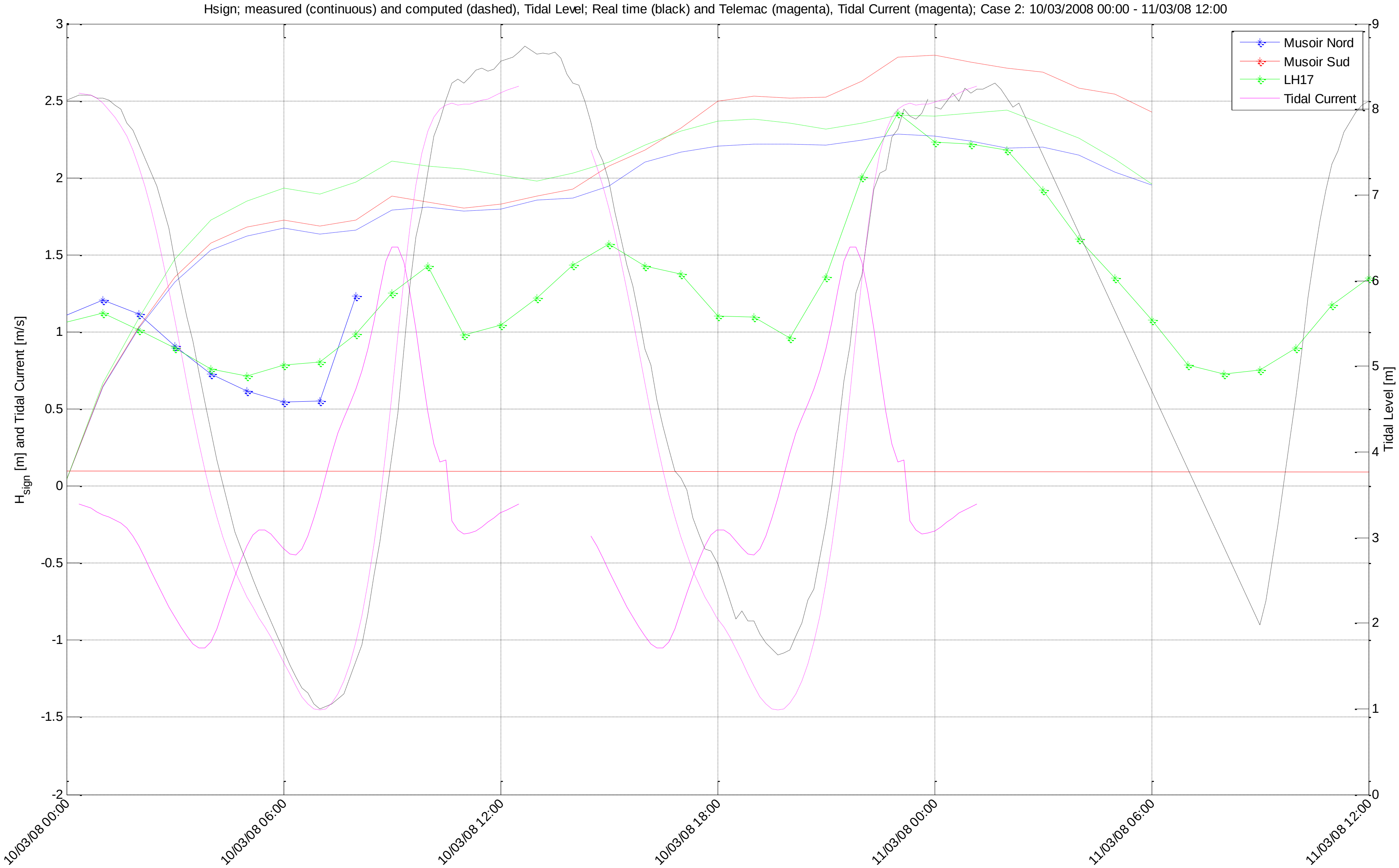
Hsign; measured (continuous) and computed (dashed), Tidal Level; Real time (black) and Telemac (magenta), Tidal Current (magenta); Case 2: 10/03/2008 00:00 - 11/03/08 12:00
Musoir Nord
Musoir Sud
LH17
Tidal Current
H$_{sign}$ [m] and Tidal Current [m/s]
Tidal Level [m]
10/03/08 00:00
10/03/08 06:00
10/03/08 12:00
10/03/08 18:00
11/03/08 00:00
11/03/08 06:00
11/03/08 12:00

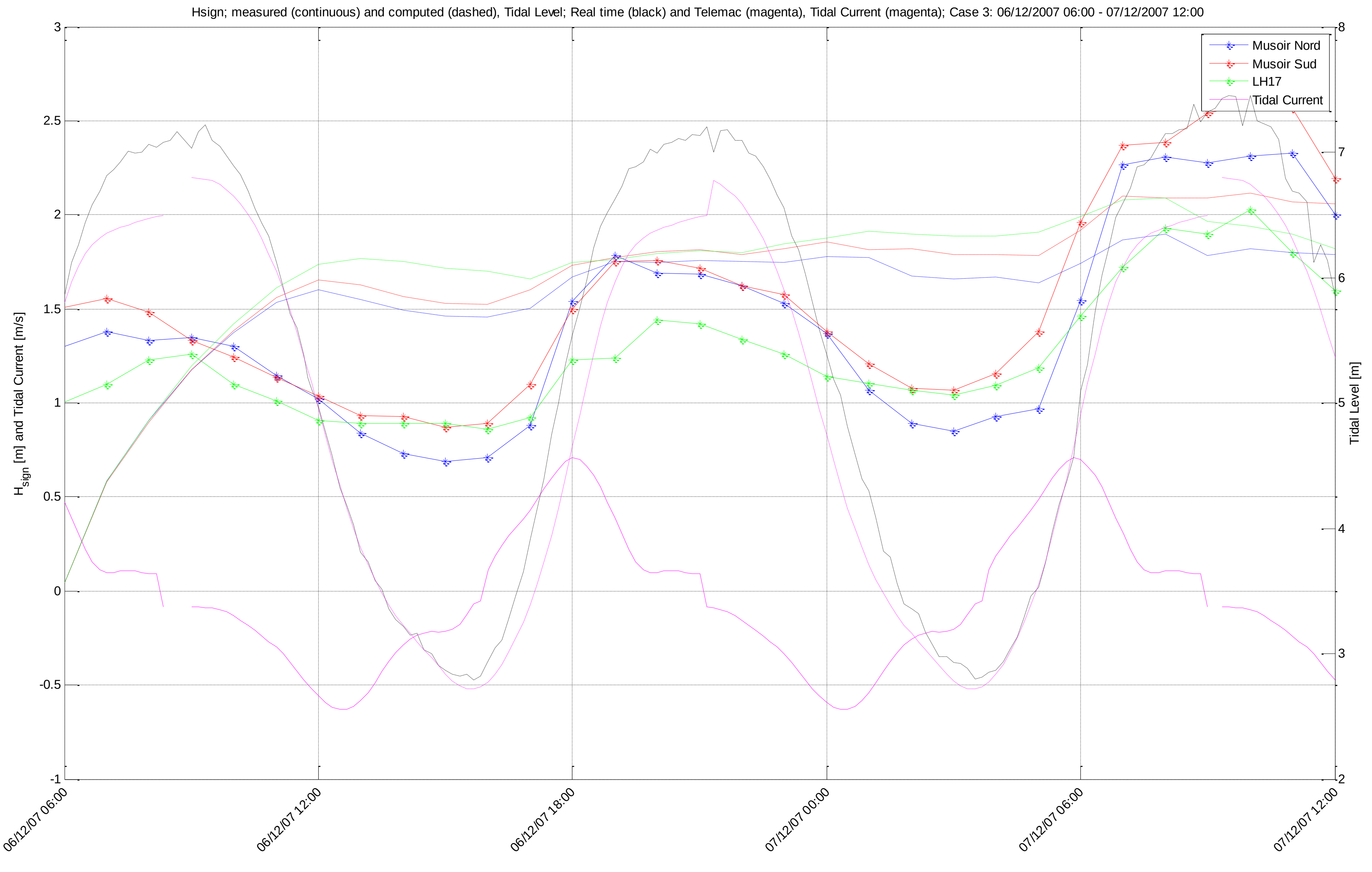
Hsign; measured (continuous) and computed (dashed), Tidal Level; Real time (black) and Telemac (magenta), Tidal Current (magenta); Case 3: 06/12/2007 06:00 - 07/12/2007 12:00
Musoir Nord
Musoir Sud
LH17
Tidal Current
H_sign [m] and Tidal Current [m/s]
Tidal Level [m]
06/12/07 06:00
06/12/07 12:00
06/12/07 18:00
07/12/07 00:00
07/12/07 06:00
07/12/07 12:00
3
2.5
2
1.5
1
0.5
0
-0.5
-1
8
7
6
5
4
3
2

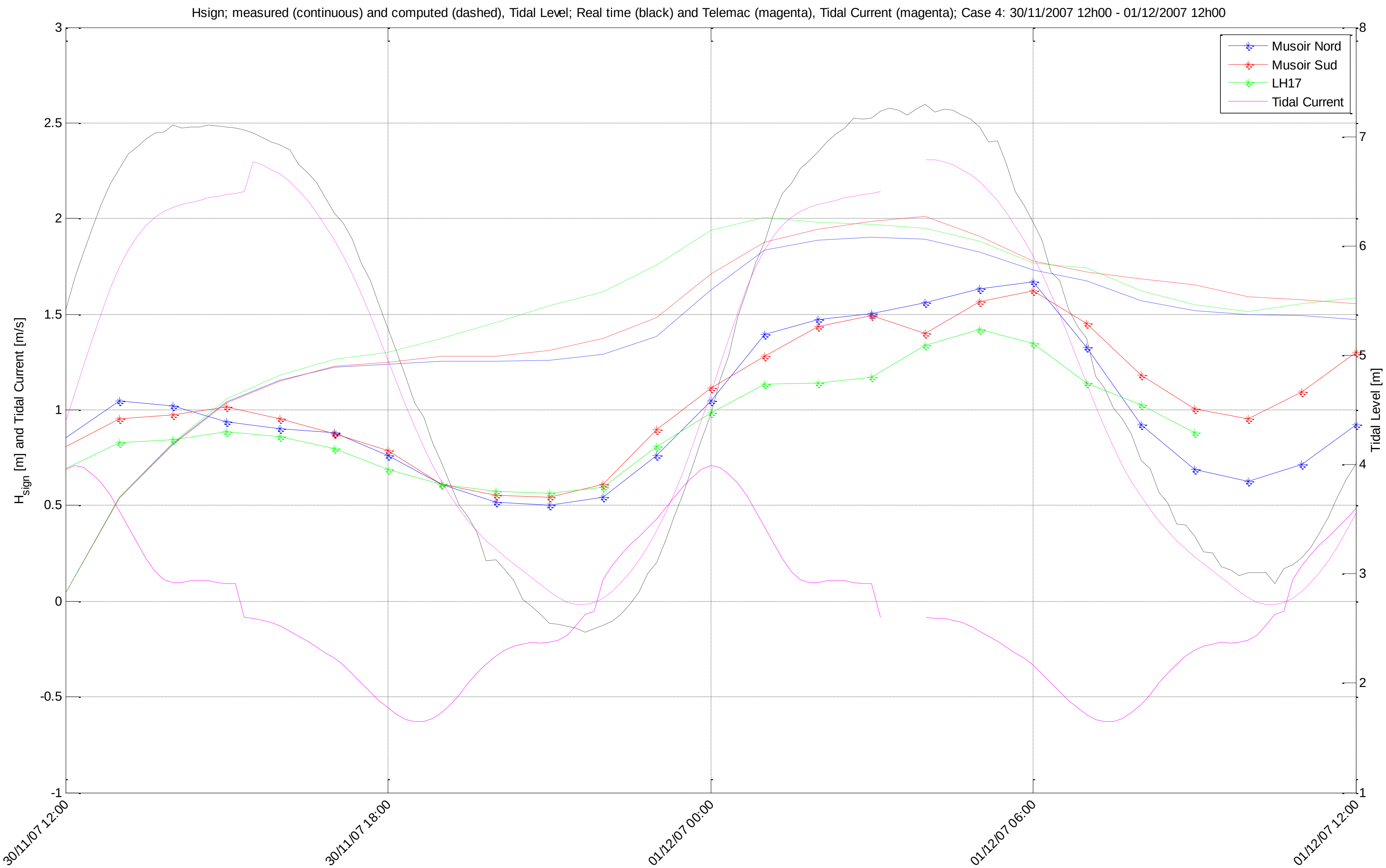
Hsign; measured (continuous) and computed (dashed), Tidal Level; Real time (black) and Telemac (magenta), Tidal Current (magenta); Case 4: 30/11/2007 12h00 - 01/12/2007 12h00
Musoir Nord
Musoir Sud
LH17
Tidal Current
H sign [m] and Tidal Current [m/s]
Tidal Level [m]
30/11/07 12:00
30/11/07 18:00
01/12/07 00:00
01/12/07 06:00
01/12/07 12:00

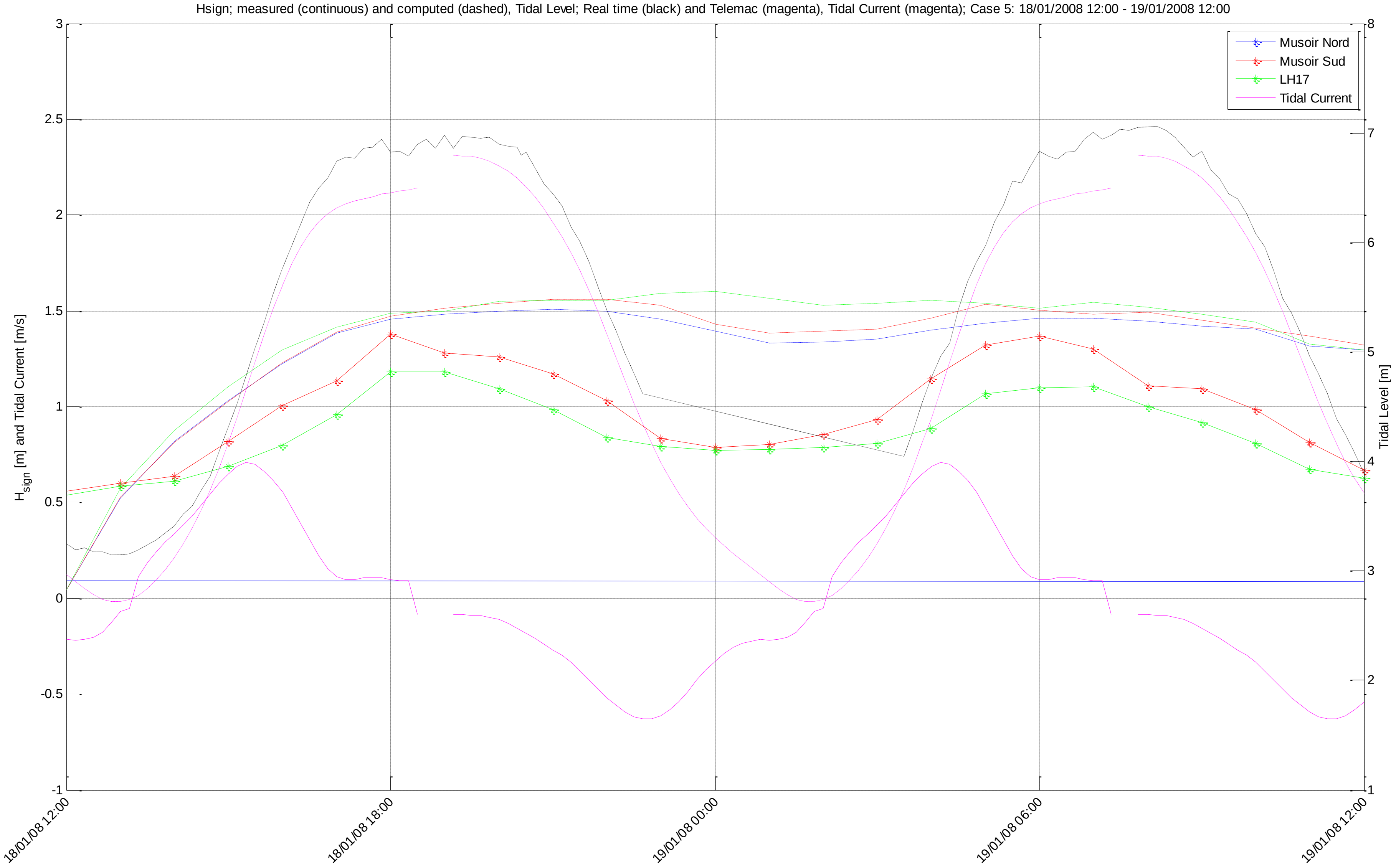

Hsign; measured (continuous) and computed (dashed), Tidal Level; Real time (black) and Telemac (magenta), Tidal Current (magenta); Case 5: 18/01/2008 12:00 - 19/01/2008 12:00
Musoir Nord
Musoir Sud
LH17
Tidal Current
H sign [m] and Tidal Current [m/s]
Tidal Level [m]
18/01/08 12:00
18/01/08 18:00
19/01/08 00:00
19/01/08 06:00
19/01/08 12:00

Appendix G: Direction of waves (SWAN) and current (Telemac) near shore

Direction of waves (SWAN) and direction of current (Telemac); continuous lines; Case 1: 07/01/2008 00:00 - 08/01/2008 00:00

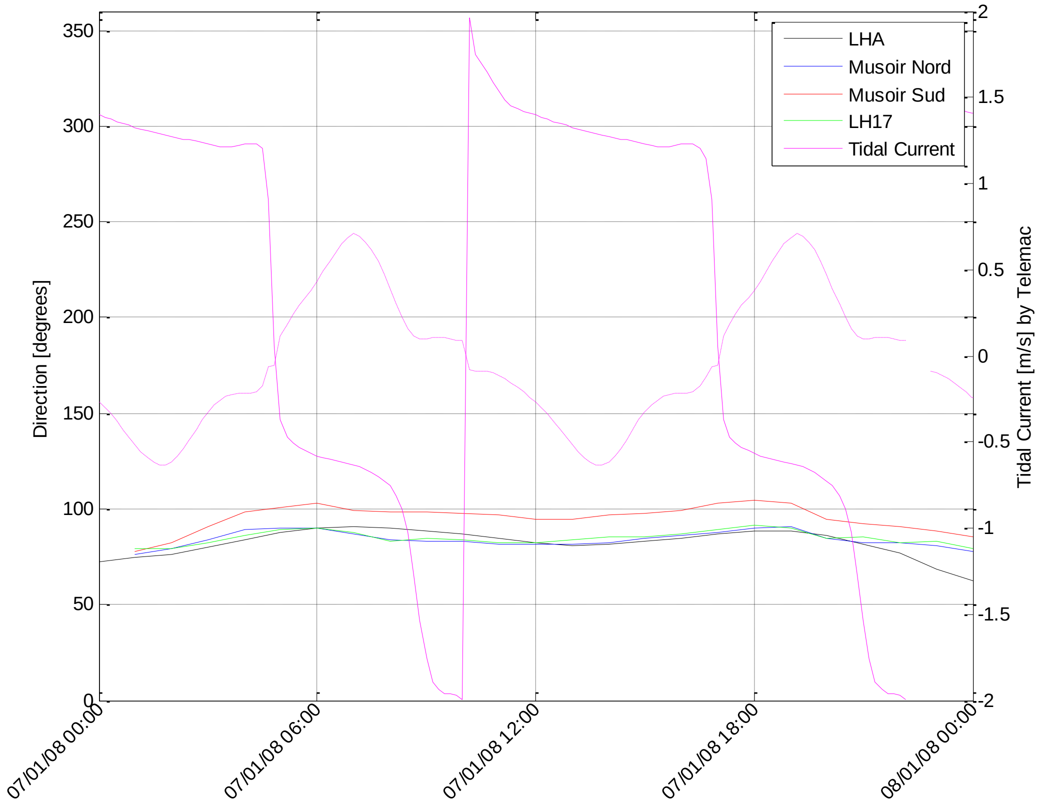

Direction of waves (SWAN) and direction of current (Telemac); continuous lines; Case 2: 10/03/2008 00:00 - 11/03/08 12:00

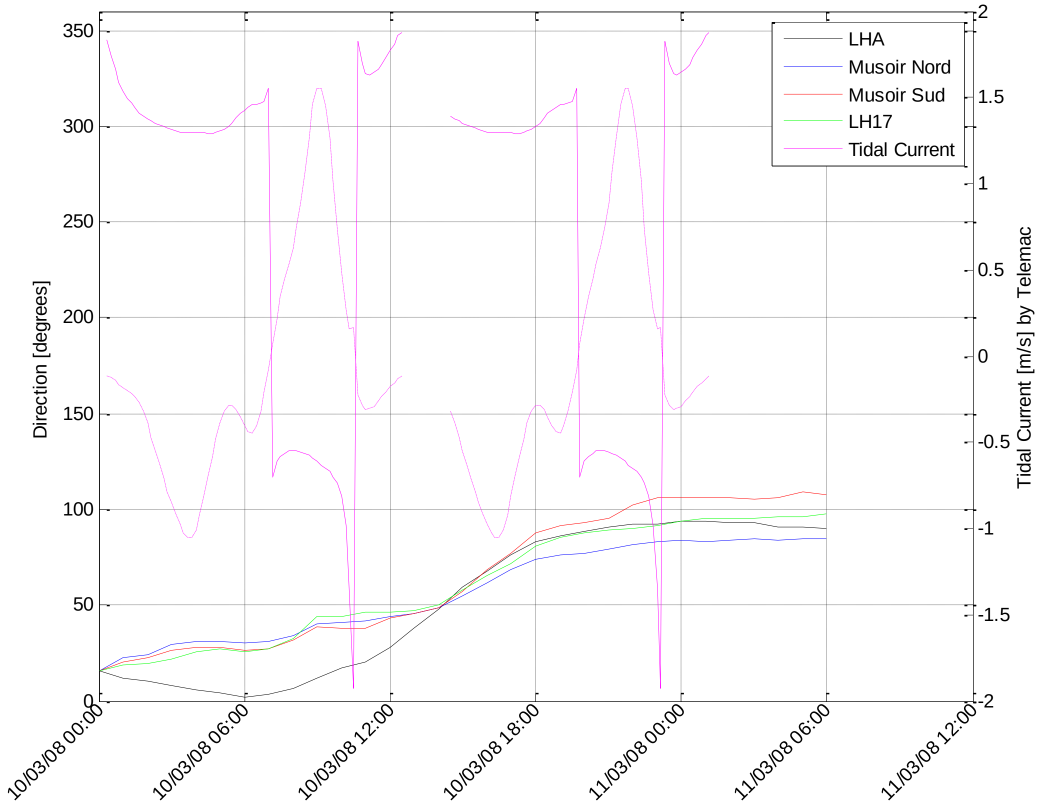

Direction of waves (SWAN) and direction of current (Telemac); continuous lines; Case 3: 06/12/2007 06:00 - 07/12/2007 12:00

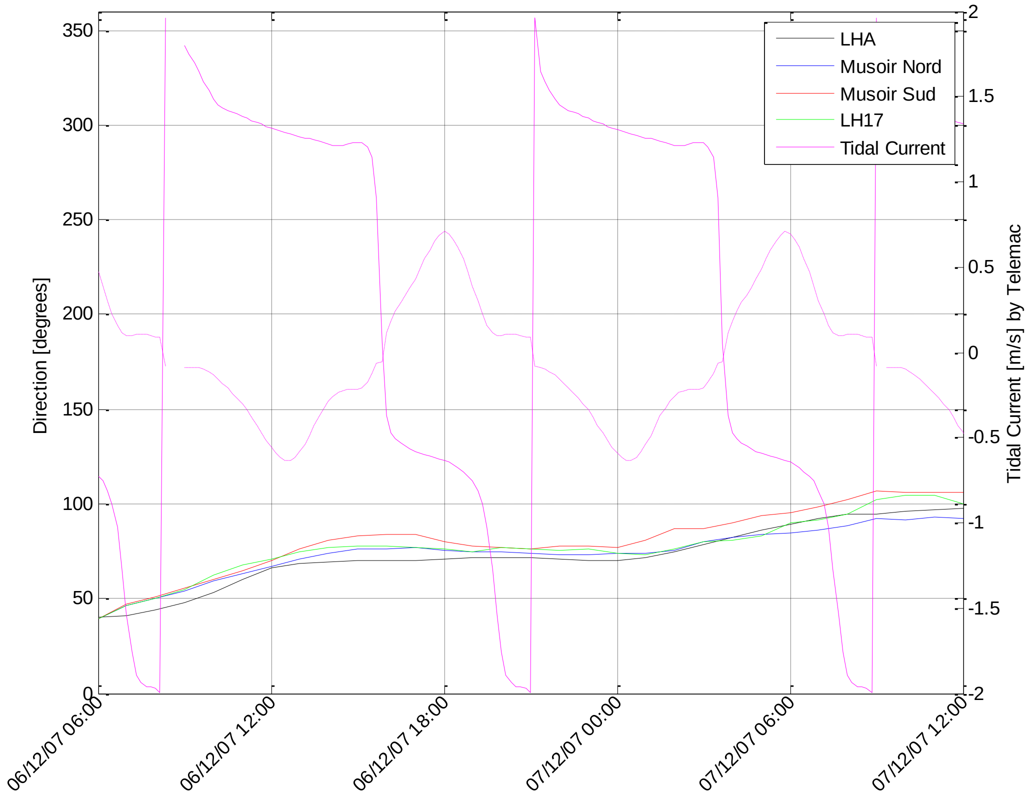

Direction of waves (SWAN) and direction of current (Telemac); continuous lines; Case 4: 30/11/2007 12h00 - 01/12/2007 12h00

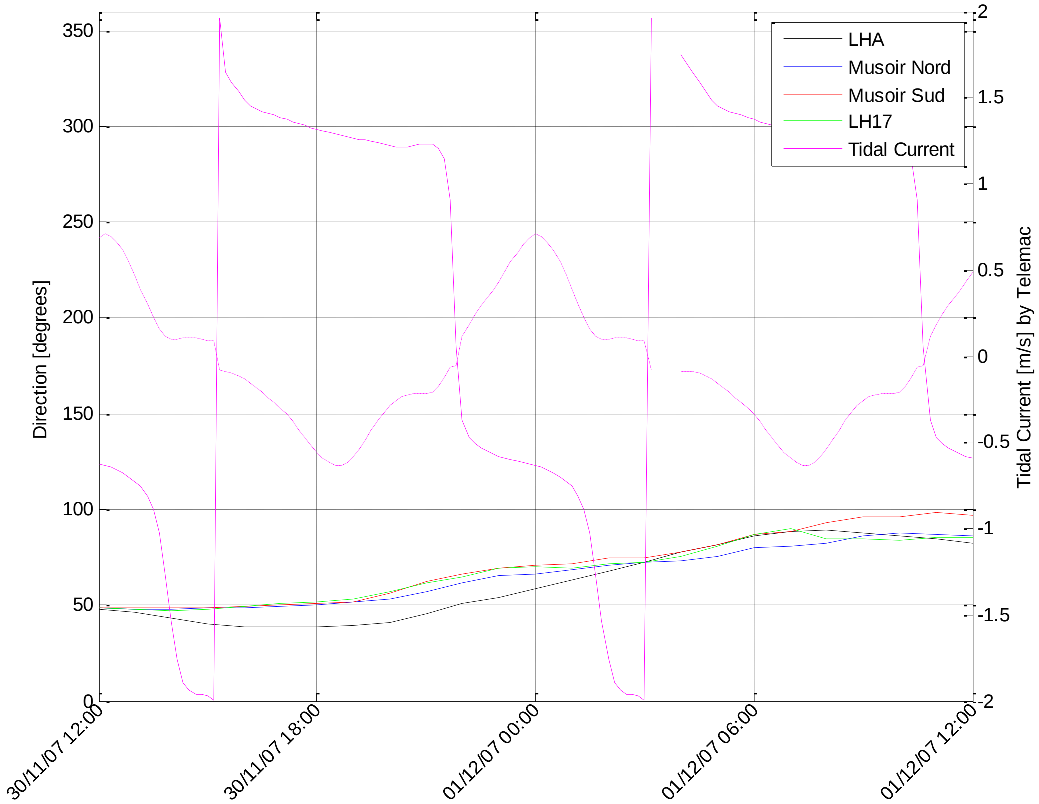

Direction of waves (SWAN) and direction of current (Telemac); continuous lines; Case 5: 18/01/2008 12:00 - 19/01/2008 12:00

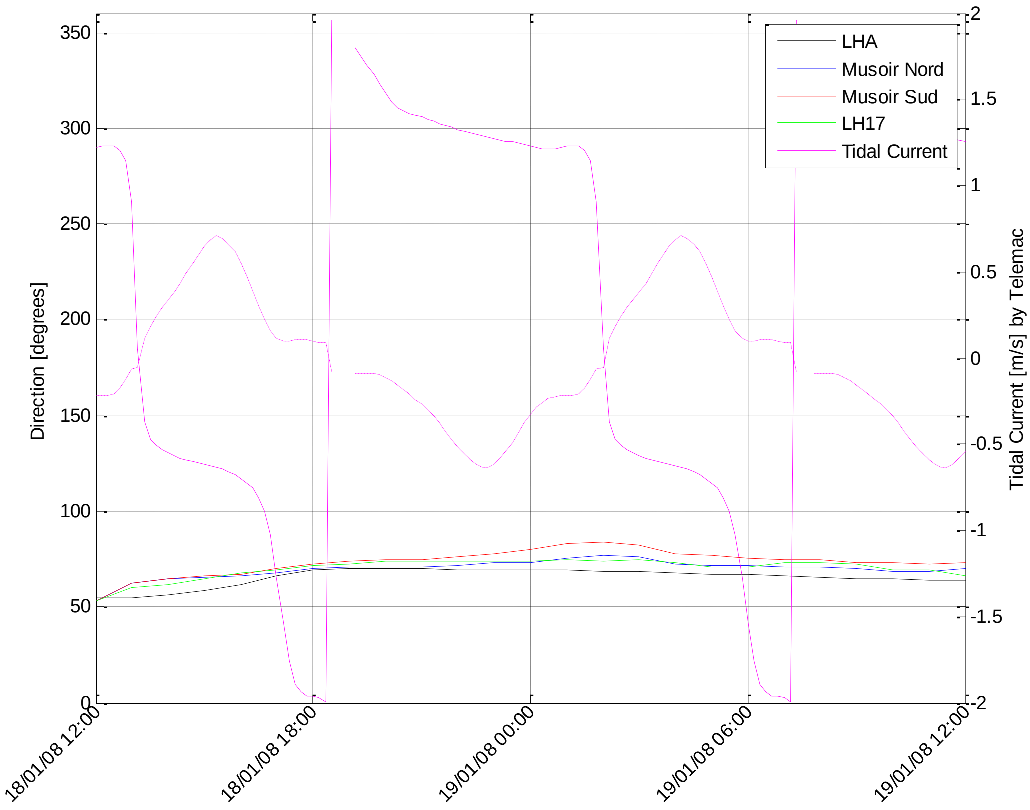

Appendix H: Variance Density Spectra case 3 (1D and 2D)

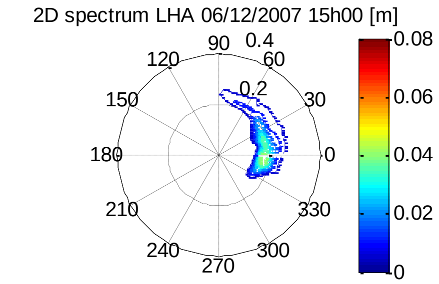

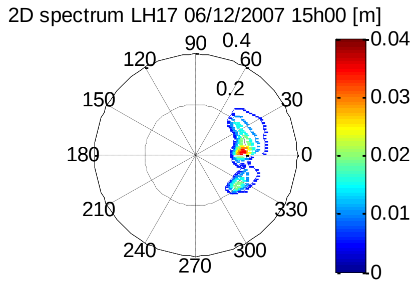

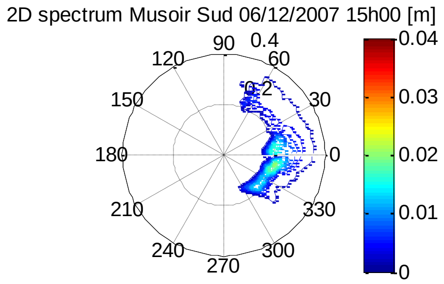

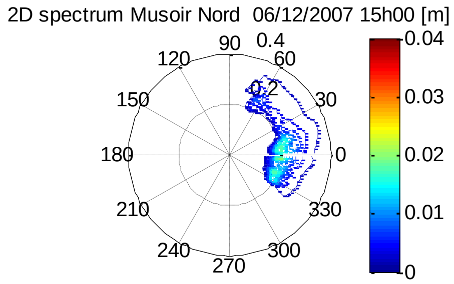

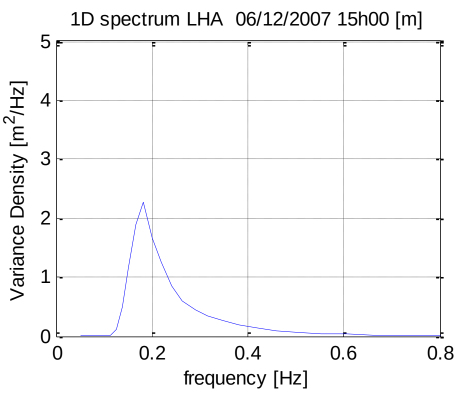

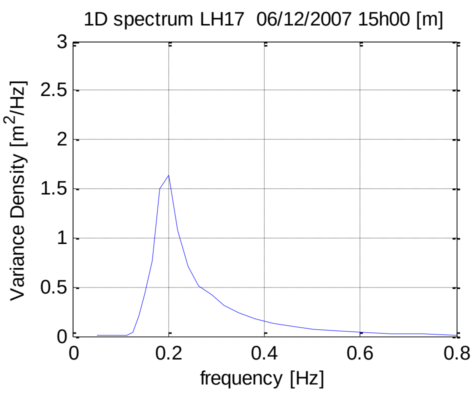

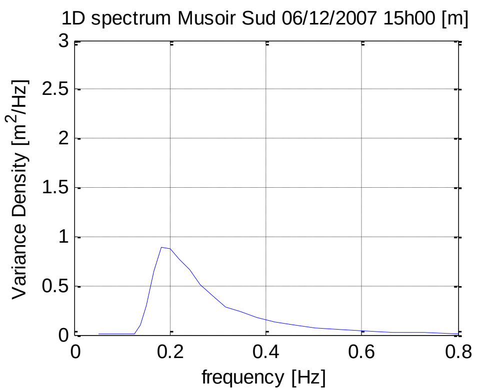

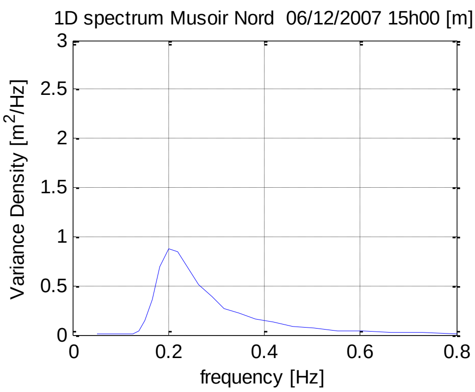

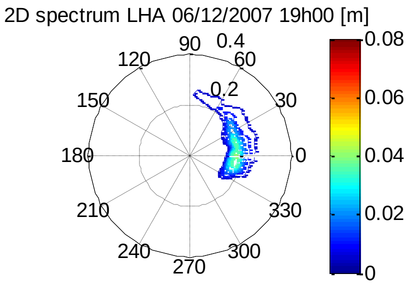
2D spectrum LHA 06/12/2007 19h00 [m]

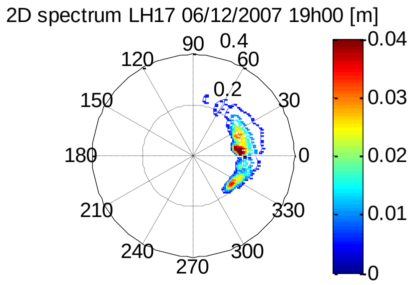
2D spectrum LH17 06/12/2007 19h00 [m]

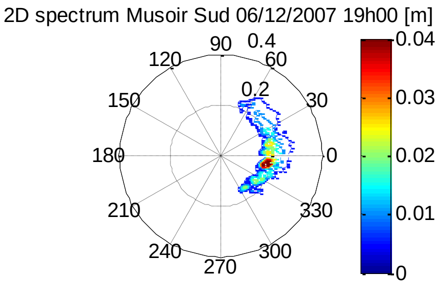
2D spectrum Musoir Sud 06/12/2007 19h00 [m]

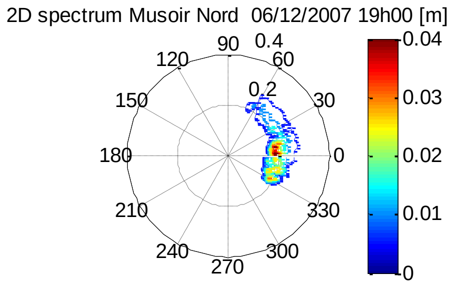
2D spectrum Musoir Nord 06/12/2007 19h00 [m]

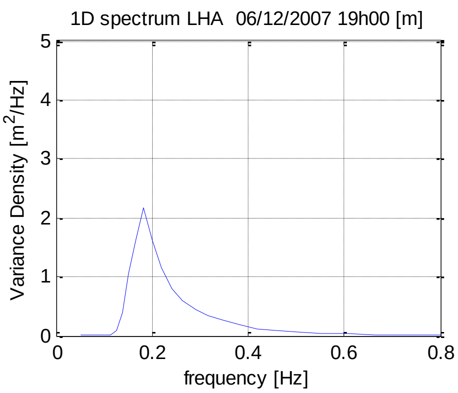
1D spectrum LHA 06/12/2007 19h00 [m]
Variance Density [m^2/Hz]
frequency [Hz]

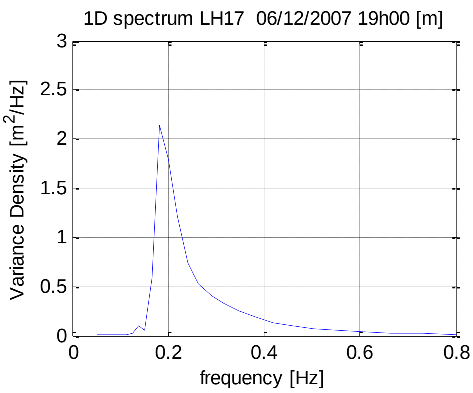
1D spectrum LH17 06/12/2007 19h00 [m]
Variance Density [m^2/Hz]
frequency [Hz]

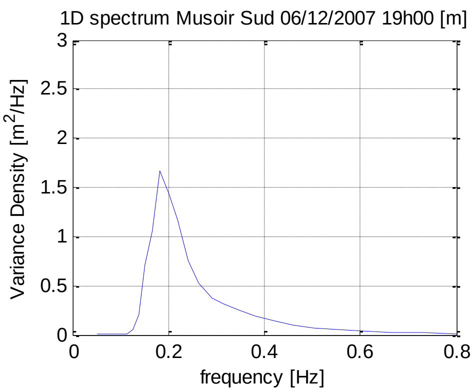
1D spectrum Musoir Sud 06/12/2007 19h00 [m]
Variance Density [m^2/Hz]
frequency [Hz]

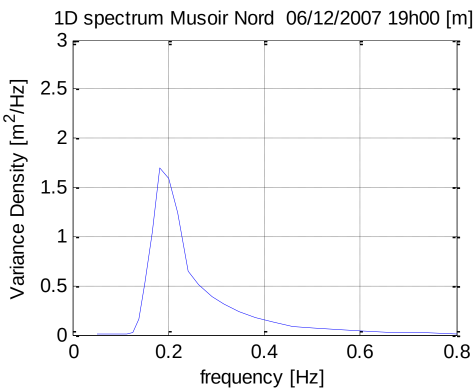
1D spectrum Musoir Nord 06/12/2007 19h00 [m]
Variance Density [m^2/Hz]
frequency [Hz]

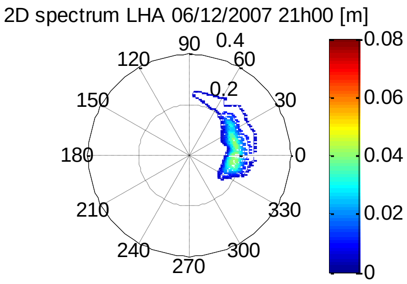
2D spectrum LHA 06/12/2007 21h00 [m]
90
0.4
60
120
0.2
30
150
180
0
210
330
240
300
270
0.08
0.06
0.04
0.02
0

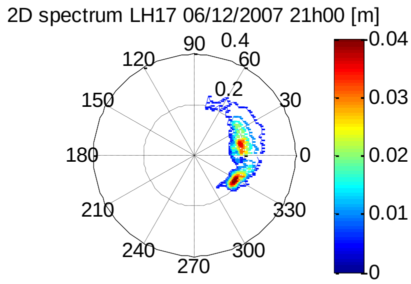
2D spectrum LH17 06/12/2007 21h00 [m]
90
0.4
60
120
0.2
30
150
180
0
210
330
240
300
270
0.04
0.03
0.02
0.01
0

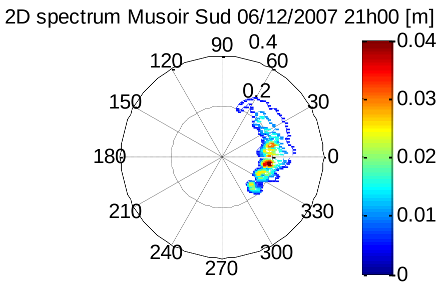
2D spectrum Musoir Sud 06/12/2007 21h00 [m]
90
0.4
60
120
0.2
30
150
180
0
210
330
240
300
270
0.04
0.03
0.02
0.01
0

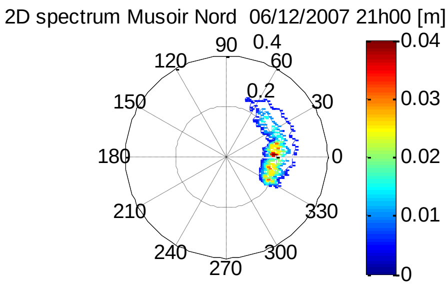
2D spectrum Musoir Nord 06/12/2007 21h00 [m]
90
0.4
60
120
0.2
30
150
180
0
210
330
240
300
270
0.04
0.03
0.02
0.01
0

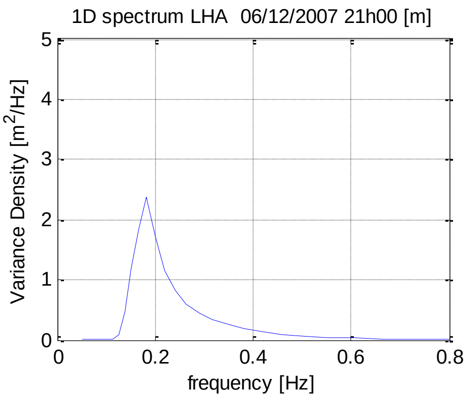
1D spectrum LHA 06/12/2007 21h00 [m]
Variance Density [m2/Hz]
frequency [Hz]
0
1
2
3
4
5
0
0.2
0.4
0.6
0.8

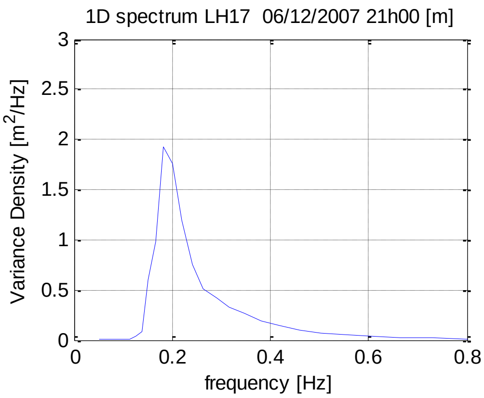
1D spectrum LH17 06/12/2007 21h00 [m]
Variance Density [m2/Hz]
frequency [Hz]
0
0.5
1
1.5
2
2.5
3
0
0.2
0.4
0.6
0.8

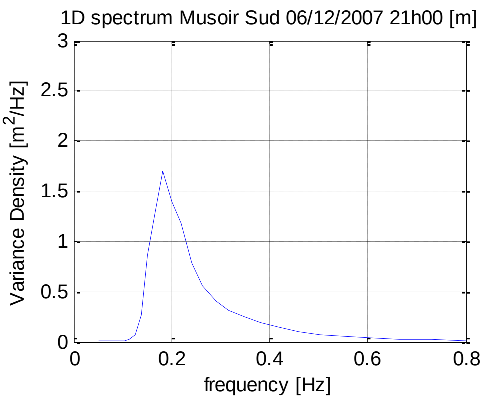
1D spectrum Musoir Sud 06/12/2007 21h00 [m]
Variance Density [m2/Hz]
frequency [Hz]
0
0.5
1
1.5
2
2.5
3
0
0.2
0.4
0.6
0.8

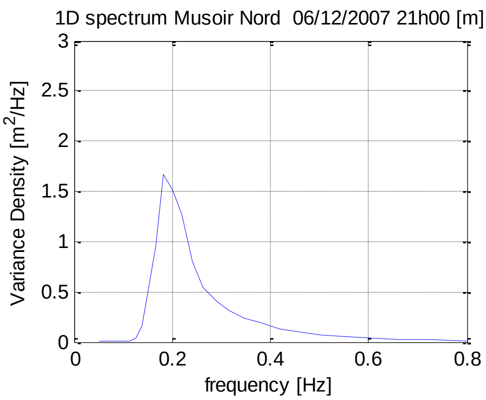
1D spectrum Musoir Nord 06/12/2007 21h00 [m]
Variance Density [m2/Hz]
frequency [Hz]
0
0.5
1
1.5
2
2.5
3
0
0.2
0.4
0.6
0.8

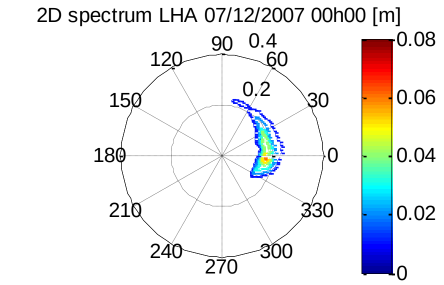
2D spectrum LHA 07/12/2007 00h00 [m]

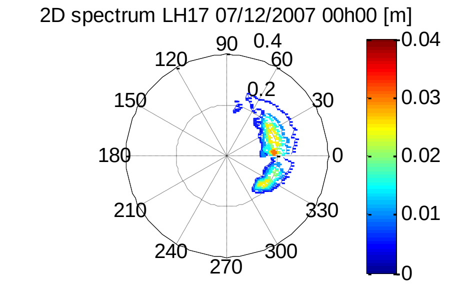
2D spectrum LH17 07/12/2007 00h00 [m]

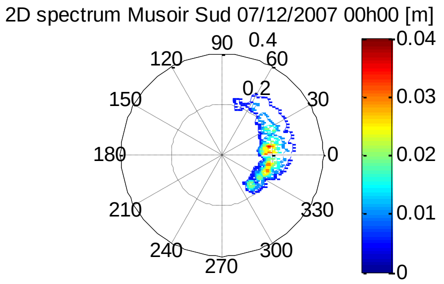
2D spectrum Musoir Sud 07/12/2007 00h00 [m]

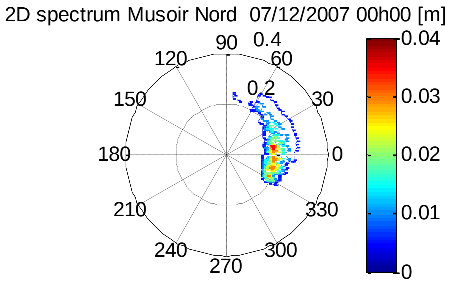
2D spectrum Musoir Nord 07/12/2007 00h00 [m]

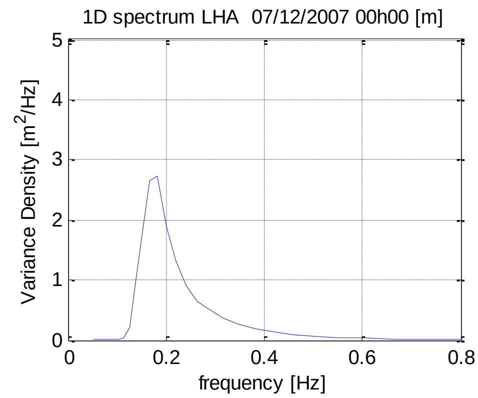
1D spectrum LHA 07/12/2007 00h00 [m]
Variance Density [m2/Hz]
frequency [Hz]

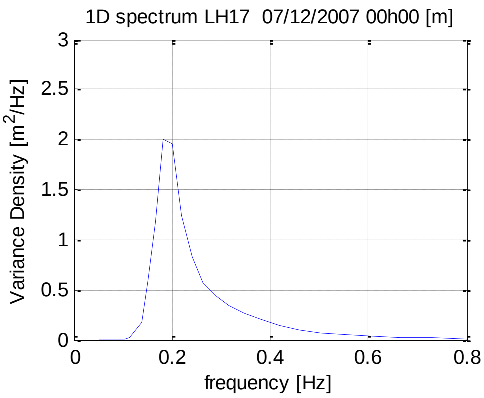
1D spectrum LH17 07/12/2007 00h00 [m]
Variance Density [m2/Hz]
frequency [Hz]

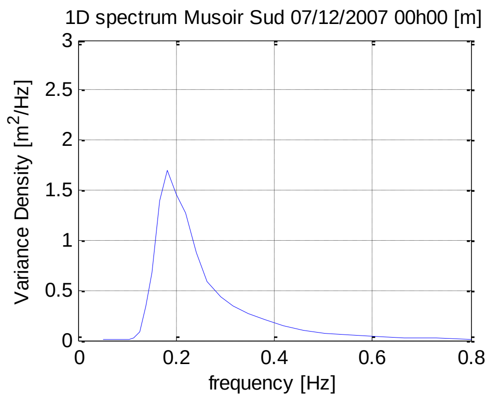
1D spectrum Musoir Sud 07/12/2007 00h00 [m]
Variance Density [m2/Hz]
frequency [Hz]

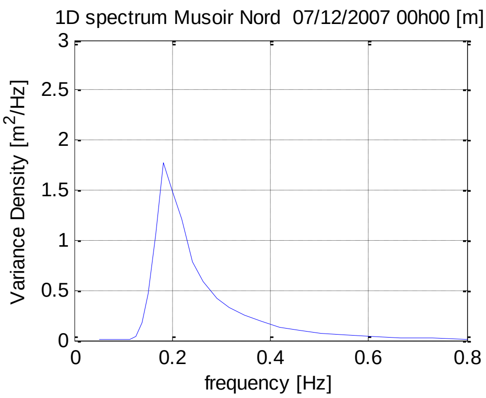
1D spectrum Musoir Nord 07/12/2007 00h00 [m]
Variance Density [m2/Hz]
frequency [Hz]

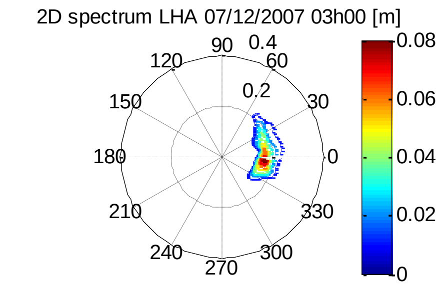
2D spectrum LHA 07/12/2007 03h00 [m]

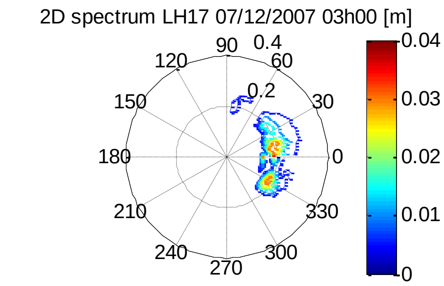
2D spectrum LH17 07/12/2007 03h00 [m]

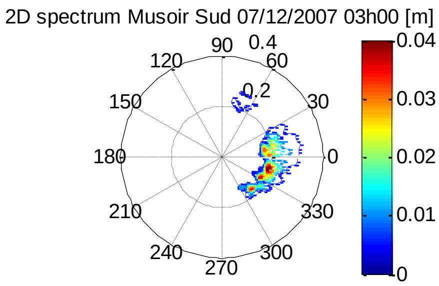
2D spectrum Musoir Sud 07/12/2007 03h00 [m]

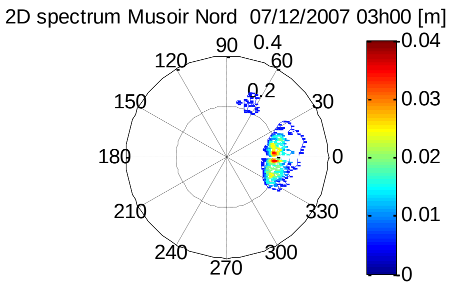
2D spectrum Musoir Nord 07/12/2007 03h00 [m]

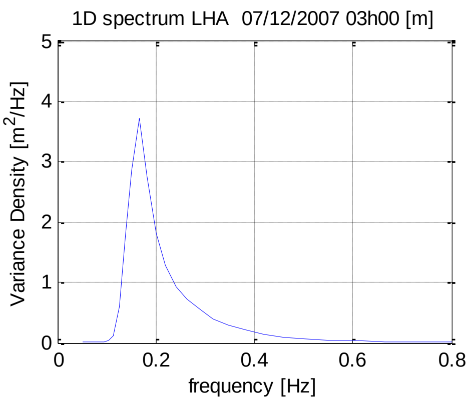
1D spectrum LHA 07/12/2007 03h00 [m]
Variance Density [m2/Hz]
frequency [Hz]

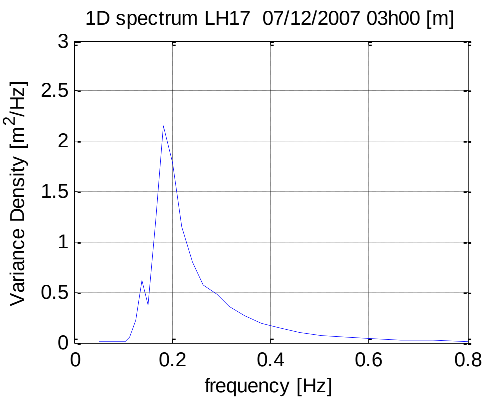
1D spectrum LH17 07/12/2007 03h00 [m]
Variance Density [m2/Hz]
frequency [Hz]

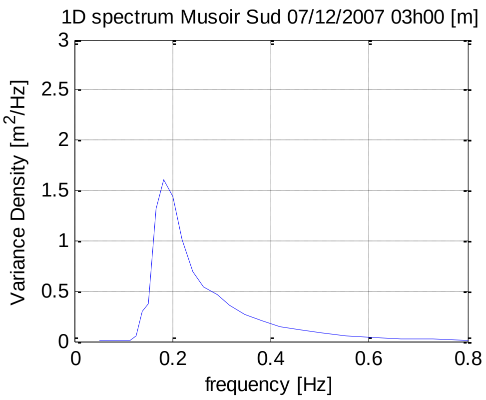
1D spectrum Musoir Sud 07/12/2007 03h00 [m]
Variance Density [m2/Hz]
frequency [Hz]

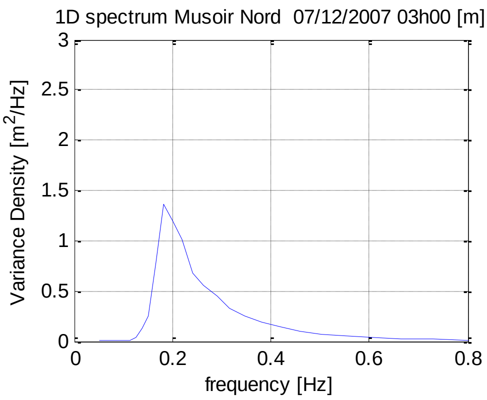
1D spectrum Musoir Nord 07/12/2007 03h00 [m]
Variance Density [m2/Hz]
frequency [Hz]

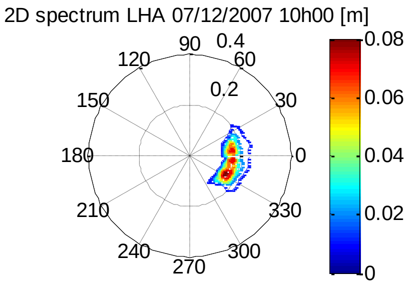
2D spectrum LHA 07/12/2007 10h00 [m]
90 0.4 60 30 0 330 300 270 240 210 180 150 120 0.2
0.08 0.06 0.04 0.02 0

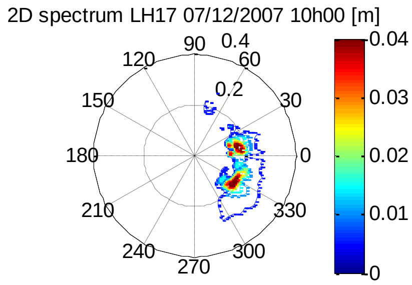
2D spectrum LH17 07/12/2007 10h00 [m]
90 0.4 60 30 0 330 300 270 240 210 180 150 120 0.2
0.04 0.03 0.02 0.01 0

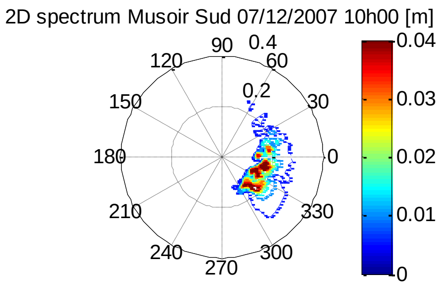
2D spectrum Musoir Sud 07/12/2007 10h00 [m]
90 0.4 60 30 0 330 300 270 240 210 180 150 120 0.2
0.04 0.03 0.02 0.01 0

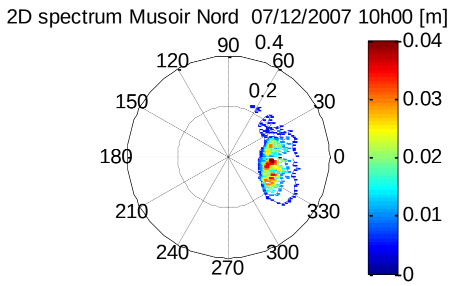
2D spectrum Musoir Nord 07/12/2007 10h00 [m]
90 0.4 60 30 0 330 300 270 240 210 180 150 120 0.2
0.04 0.03 0.02 0.01 0

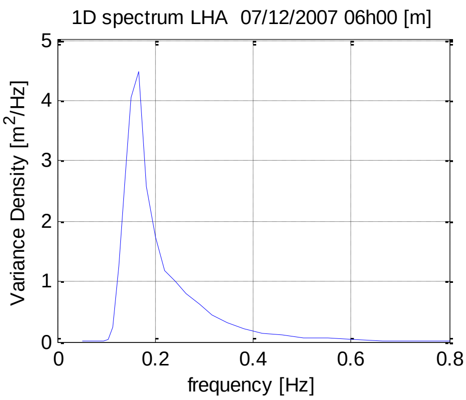
1D spectrum LHA 07/12/2007 06h00 [m]
Variance Density [m²/Hz]
frequency [Hz]

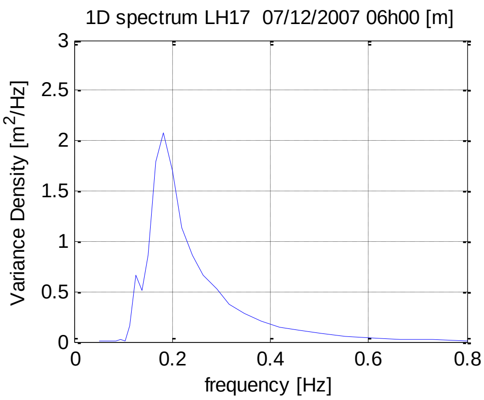
1D spectrum LH17 07/12/2007 06h00 [m]
Variance Density [m²/Hz]
frequency [Hz]

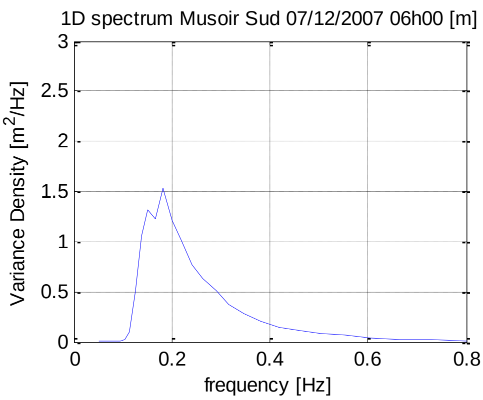
1D spectrum Musoir Sud 07/12/2007 06h00 [m]
Variance Density [m²/Hz]
frequency [Hz]

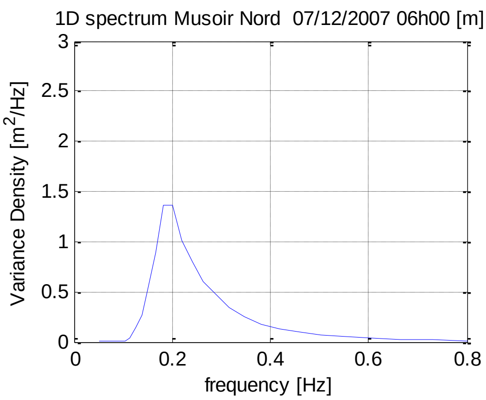
1D spectrum Musoir Nord 07/12/2007 06h00 [m]
Variance Density [m²/Hz]
frequency [Hz]

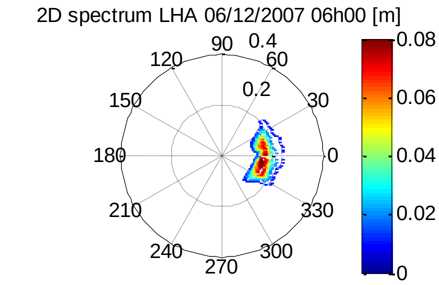
2D spectrum LHA 06/12/2007 06h00 [m]

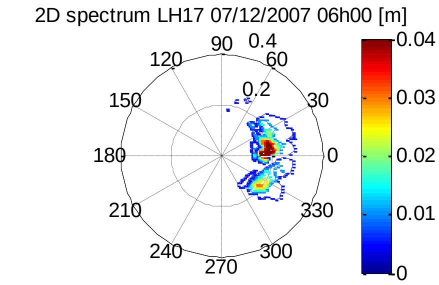
2D spectrum LH17 07/12/2007 06h00 [m]

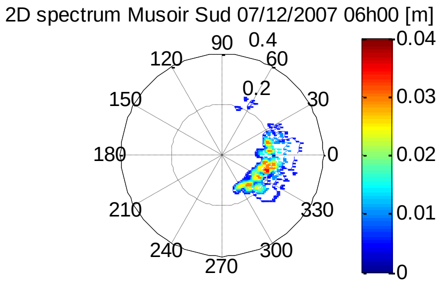
2D spectrum Musoir Sud 07/12/2007 06h00 [m]

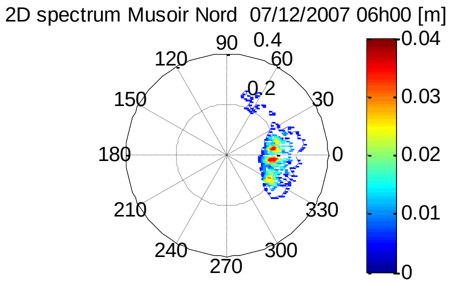
2D spectrum Musoir Nord 07/12/2007 06h00 [m]

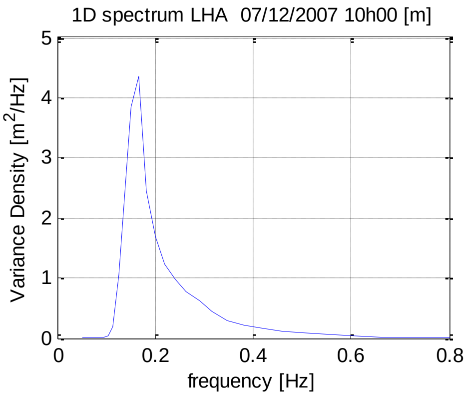
1D spectrum LHA 07/12/2007 10h00 [m]
Variance Density [m2/Hz]
frequency [Hz]

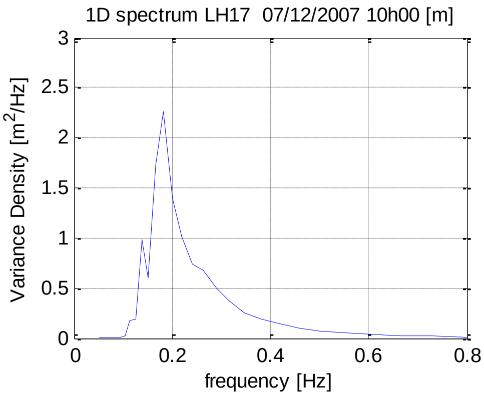
1D spectrum LH17 07/12/2007 10h00 [m]
Variance Density [m2/Hz]
frequency [Hz]

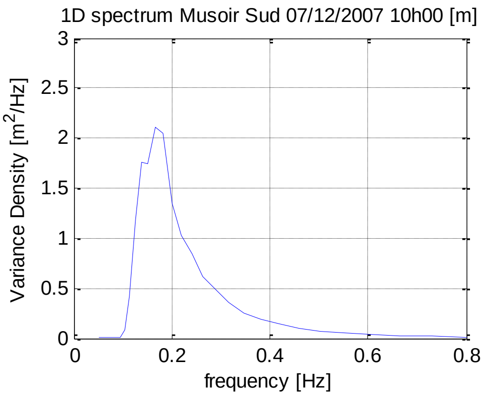
1D spectrum Musoir Sud 07/12/2007 10h00 [m]
Variance Density [m2/Hz]
frequency [Hz]

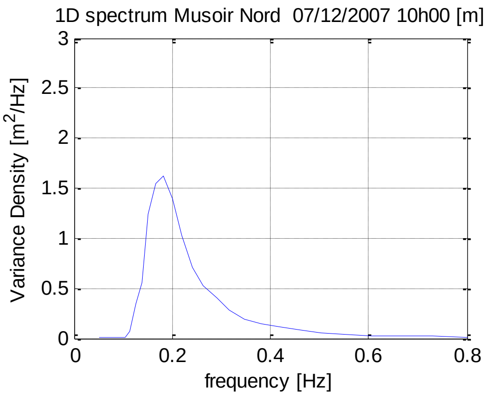
1D spectrum Musoir Nord 07/12/2007 10h00 [m]
Variance Density [m2/Hz]
frequency [Hz]